Department of Mechanical Engineering

Pelletisation of Biomass Oil Palm Kernel Shells for Gasification

Lai Zhenyue

This thesis is presented for the Degree of
Master of Philosophy
of
Curtin University

November 2012

Declaration

To the best of my knowledge and belief this thesis contains no material previously published by any other person except where due acknowledgment has been made.

This thesis contains no material which has been accepted for the award of any other degree or diploma in any university.

Signature: 

Date: 26/11/2012

Acknowledgements

I would like to express my sincere gratitude to:

Professor Aaron Goh Suk Meng, my supervisor

for his guidance, dedication, motivation and enlightening discussions on both scientific and non-scientific matters; and for giving me the opportunity to take on this research project

Associate Professor Chua Han Bing, my co-supervisor

for his support, interest and discussions in my work

Associate Professor Zang Zhuquan, postgraduate studies coordinator

for his advice on HDR matters

Teo Choon Hoong, my husband

for his endless support, encouragement and insightful discussions over my work

Mohd. Izzat Bin Jamil and Wee Yen Seng, my student helpers

for their friendship and experimental assistance

the lab technicians and officers especially Michael, Helda, Vivian, George and Adib

for their technical support on the use of equipment and machine

my friends, especially Amelia, Bridgid and Kimberly

for their companionship

***

Staff Study Support from Curtin University Sarawak, Research funding from Curtin Sarawak Collaborative Research (CSCR), Resources donated by Bintulu Lumber Development (BLD), Technical support and facilities provided by Sarawak Shell Berhad Production Chemistry Lab and Geological Services Department are gratefully acknowledged.

Table of Contents

Abstract

Palm kernel shells are one of the waste products in the palm oil industry. This work was focused on investigating the properties of pellets made from the palm kernel shells for use in syngas generation through gasification. The strength of the pellets increased with compaction pressure but the strength reached a plateau when the pellets achieved no or near-zero porosities, indicating that the maximum strength was achieved. High compaction speeds and short hold time during the compaction process; high humidity conditions and long storage time during post-production were found to result in lower pellet strengths. These effects were mainly related to the porosities of the pellets, and new modifications of the Ryshkewitch-Duckworth model have been proposed to describe the relationships between the strength and the porosity. The strength of binary pellets made of palm kernel shell and HZSM-5 zeolite decreased with increasing zeolite composition. This decrease was associated with higher porosities and elastic rebound of the pellets in the presence of the zeolite particles. Modifications of the Ryshkewitch-Duckworth model have been proposed to predict the strength of the binary mixture pellet, based on strength at zero porosity and the bonding capacity of zeolite and palm kernel shell.

In the gasification studies, the pellets achieved a higher conversion rate from biomass to gaseous products compared to raw palm kernel shells and ground shell powder. The gasification of binary palm kernel shell and HZSM-5 zeolite pellets was proven to be feasible but not as effective in reducing tar from the gaseous products as zeolite added in-situ with raw palm kernel shells. For the same amount of catalyst used, the amount of tar reduced was less when the pelletised form was gasified, compared to that when the raw, ungrounded form was gasified in situ with zeolite. This was probably due to zeolite being trapped within the binary pellet and hence not all the zeolite was available to crack the tar.

List of Publications

1. **Lai Z.Y.**, Chua H.B., Goh S.M. 2012. Influence of process parameters on the strength of oil palm kernel shell pellets. Journal of Materials Science, ISSN 0022-2461, DOI 10.1007/s10853-012-6897-x

2. **Lai Z.Y.**, Chua H.B., Goh S.M. Mechanical strength and effectiveness in gasification gas cleanup of binary oil palm kernel shell and HZSM-5 zeolite pellets – In preparation

Conference and Poster

1. **Lai Z.Y.**, Goh S.M. Factors affecting compressive and tensile strength of oil palm kernel shell pellets. 3rd Regional Materials and Technology Conference, Miri, Sarawak (26 – 27 April 2011) – Poster presentation

List of Symbols

Notation	Description
A	initial contact area
D	diameter of the pellet
E	Young's modulus
F	peak crushing force
L	length of the pellet after ejection
L_0	length of the pellet at maximum compaction pressure
M_i	initial mass of biomass before gasification
M_f	final mass of feedstock remains after gasification
P	compaction pressure
R	rate of conversion
V	volume fraction
V_p	volume of powder
V_{PKS}	volume fraction of palm kernel shell
V_Z	volume fraction of zeolite
V_1	volume fraction of powder component 1
V_2	volume fraction of powder component 2
Z	zeolite
ER	elastic rebound
EFB	empty fruit bunch
HZSM-5	Zeolite Socony Mobil-5 after calcination
LPM	litres per minute
PAH	polyaromatic hydrocarbons
PKS	palm kernel shell
POME	palm oil mill effluent
T1	thermocouple 1
T2	thermocouple 2
ZSM-5	Zeolite Socony Mobil-5
a	fitted constant that is dependent on the composition of the pellet
a_w	water activity
c	a fitted constant that represents the logarithm of reciprocal porosity when compaction pressure is zero

k	bonding constant
k_m	bonding constant of binary pellet
k_{PKS}	bonding constant of palm kernel shell
k_Z	bonding constant of zeolite
k_1	bonding capacity of powder component 1
k_2	bonding capacity of powder component 2
m	mass
m_p	mass of powder
m_T	mass of tar
m_{Tx}	mass of tar from gasification of x% zeolite in pellet
m_{T0}	mass of tar from gasification of 0% zeolite in pellet
n	number of points taken for calculation
r	radius
t	hold time
t_g	time taken for gasification
t_s	storage time
wt	weight
α	a fitted constant that is dependent on the storage condition
β	a fitted constant that represents porosity of the pellet after 1 day of storage
γ	a fitted constant that is dependent on the powder constituents in a binary mixture
δ	interaction factor
ε	porosity during compaction
ε_f	final porosity
ε_m	porosity of binary pellet
ε_0	a fitted constant that represents porosity during compaction when hold time is zero
$\overline{\Delta\varepsilon}$	average change in porosity
φ	a fitted constant that represents final porosity of a binary pellet when the porosity during compaction is zero
λ	a fitted constant that is dependent on particle size
ρ_B	final bulk density
ρ_c	bulk density of the pellet at maximum compaction
ρ_T	true density of the powder

$\rho_{T,m}$	true density of powder mixture
$\rho_{T,1}$	true density of powder component 1
$\rho_{T,2}$	true density of powder component 2
σ	compressive strength
σ_T	tensile strength
σ_0	compressive strength at zero porosity
$\sigma_{0,m}$	compressive strength at zero porosity of the binary mixture
$\sigma_{0,PKS}$	compressive strength at zero porosity of palm kernel shell
$\sigma_{0,Z}$	compressive strength at zero porosity of zeolite
$\sigma_{0,1}$	compressive strength at zero porosity of the powder component 1
$\sigma_{0,2}$	compressive strength at zero porosity of the powder component 2
σ_i	compressive strength at zero storage time
σ_m	compressive strength of binary mixture
$\sigma_{m,exp}$	compressive strength of binary mixture from experimental data
$\overline{\Delta\sigma_m}$	average reduction in strength for binary mixture
ξ_1	mass fraction of powder component 1
ξ_2	mass fraction of powder component 2

Subscript	Description
m	mixture
p	parallel
s	series
exp	experimental
1	component 1
2	component 2

List of Figures

List of Tables

1 Introduction

1.1 Introduction

Malaysia's total energy demand in 2003 was 33.9 Mtoe (million tonnes of oil equivalent) and this energy demand is expected to grow at 5.4% per annum to reach 83.5 Mtoe in 2020 (Ahmad et al., 2011). In order to meet this increasing demand of energy, Malaysia needs to seek an effective and sustainable source of energy. Alternative energy sources that are renewable and sustainable have received extensive public and scientific attention in recent years. Biofuels, such as those gained from energy crops like palm oil, are becoming an important alternative source of energy. Since 2006, Malaysia is the world's second largest palm oil producer and exporter; wastes from the indigenous palm oil industry can be easily acquired (Shuit et al., 2009) and have been identified as one of the biggest renewable energy resource potential (Sumathi et al., 2008). Another advantage associated with using palm oil wastes for energy generation is that the source is obtained without having to compete with the food chain, thus biofuels gained from palm oil crops are considered 'green' and sustainable (Hall and Scrase, 1998).

Palm oil mills in Malaysia use boilers for electricity generation and palm oil extraction processes (Mahlia et al., 2001). Residues from the palm oil crop such as fibre, shell, empty fruit bunch (EFB) and palm oil mill effluent (POME) have been used as fuels for these boilers in palm oil mills. Higher energy conversions are normally obtained from fibre and shell due to their high carbon content and calorific value (Vijaya et al., 2004). EFB needs to be pre-treated by shredding and dehydrating in order to render it more combustible. As such higher pre-treatment costs are incurred. Hence palm fibre and shells are attractive and convenient to use as biofuels compared to EFB.

There are several ways to obtain biofuels from biomass. They include converting the biomass into a bioalcohol, a biogas or a syngas. Syngas is a mixture of carbon monoxide and hydrogen and provides more energy than burning of the biomass itself (Speight, 2008). In addition, the utilisation of syngas is flexible as it may be burned directly in an internal combustion engine or converted into other synthetic fuels. Biomass gasification converts solid fuels to synthesis gas (syngas) using gasification agents such as oxygen, air, steam, or combinations of these oxidising agents. Gasification is considered one of the most promising thermochemical technologies for wide applications such as power generation through gas turbines, production of liquid fuels using Fischer Tropsch synthesis, and production of hydrogen, ethanol and methanol (Belgiorno et al., 2003; Faaij et al., 1997).

The product gas from gasification, which consists of a mixture of carbon monoxide, carbon dioxide, methane, hydrogen and water vapour, is applicable for heat and power generation, production of syngas, and less pollution problems are associated with the downstream applications compared to combustion (McKendry, 2002). For these reasons, gasification of biomass wastes has received worldwide attention as a potential source of biofuels. Typical wastes studied for gasification include pine, olive oil wastes, wood, rice husk, grapevine prunings, sawdust wastes and empty fruit bunch from palm waste (Hernandez et al., 2010; Mohammed et al., 2011a; Velez et al., 2009).

However, there are several difficulties encountered during the gasification of biomass materials. For example, the biomass material may have a highly complex chemical and physical composition and its combustion may take place in an uncontrolled environment (Gil et al., 2010). In addition, the heterogeneity in terms of size and shape of the biomass leads to difficulties in achieving steady-state gasification and transportation processes. Irregular and oversized biomass materials may form bridges which prevent smooth flow of the feed while those that are too fine may clog available air voidage, leading to a high pressure drop and subsequently shutdown of the gasifier (McKendry, 2002). The irregular sizes of the biomass also result in channelling and uneven rates of gasification (Feng et al., 2011; Moghiman et al., 2007). A solution to the heterogeneity in terms of size and shape involves

converting the biomass into a uniform, densified solid via pelletisation. Pelletisation can be achieved by a number of processes, such as extrusion, roll briquetting and compaction under high pressure within a cavity (Tumuluru et al., 2011).

To improve the strength of densified biomass products, process parameters that affect strength and durability need to be studied. Kaliyan and Morey (2009) presented a review on some factors that could affect the strength and durability of densified biomass products and these include the composition of the material, moisture content, particle size of the material, pre-compaction treatment (e.g. heat or steam conditioning), presence of binders, densification equipment variables (e.g. compaction pressure, compaction speed, conditioning time) and post-production conditions such as storage time, post-heat conditioning and storage conditions.

The pelletisation and briquetting of oil palm wastes has previously been performed for animal feed (Dahlan et al., 2000) rather than for converting the wastes into efficient biofuel pellets. In particular, interest in the pelletisation technology of palm wastes has arisen lately due to the potential of palm pellets as a fuel substitute to wood pellets (Daily Express, 2009). An improved understanding of the properties of palm pellets will lead to more efficient recovery of the waste.

Research in the pelletisation of raw oil palm kernel shell is still very limited. Previous studies on the pelletisation of palm oil wastes typically involved binders such as starch, caustic soda and calcium carbonate (Husain et al., 2002; Razuan et al., 2011). The addition of binders does improve agglomeration and strength of the pellets (Razuan et al., 2011). However, the presence of binders may reduce the combustion characteristics of the pellet and increase the pellet's vulnerability to biological decay (Finney et al., 2009). In particular, the combustion efficiency was found to be reduced and high concentrations of alkali metals were found in the ash which could induce slagging or fouling (Finney et al., 2009). As no work has been carried out on the study of pellets made from oil palm kernel shells alone, this research was performed to characterise the mechanical strength of binderless oil palm kernel shell pellets which are compacted under high pressure. The effects of processing parameters such as compaction pressure, compaction speed, hold time,

particle size and binary mixtures on the mechanical properties of oil palm kernel shell pellets were characterised. Storage conditions during post-production of the pellets were also studied for their effects on the strength of palm kernel shell pellets.

Azali et al. (2005) concluded that using palm oil fibres and shells for gasification are feasible but highlighted that the main problem encountered is with cleaning the gas. The syngas from all gasification reactors contain particulates, and organic contaminants (tar) (Anis and Zainal, 2011, Wang et al., 2008) which, if not removed, would damage the engine or gas turbine and incur high maintenance costs. The efficiency of a gas cleaning technology step is therefore fundamental to the successful operation of power plants.

The use of catalysts is the most effective approach in order to reduce the tar content in the syngas (Sutton et al., 2001; Tomishige and Asadullah, 2005). Catalytic processes operate at temperatures similar to those during gasification to remove the tar by converting it to lighter combustible gas components (Anis and Zainal, 2011; Han and Kim, 2008). The catalysts may be applied separately from the biomass fuel stock or are impregnated into the biomass before gasification (Frosch, 1981). So far, no studies have been conducted to investigate the gasification of biomass palm kernel shells pellets. In this project, the effect of different forms of palm kernel shell feedstock, and pellet size on rate of conversion of biomass to gaseous products and amount of tar produced will be studied. Zeolite is chosen as the catalyst in this study because of its potential to eliminate tar from fuel gas (Abu et al., 2004).

An improved understanding of the mechanical properties of palm kernel shell pellets will lead to a more efficient recovery of the waste, stronger and more durable pellets, as well as better gasification characteristics. The focus of the current work is on the compaction of palm kernel shell wastes based on different process conditions and formulation and how these factors affect the resulting mechanical strength and gasification behaviour of the pellets.

This project was divided into two parts. The first part involved the study on the effects of processing parameters such as compaction speed, hold time and

compaction pressure, and post-production conditions such as storage time and humidity level, on the strength of palm kernel shell pellets. Palm kernel shell in different forms namely shells, powder and pellets were gasified to determine the best feedstock form for efficient gasification. In the second part of this work, the strength of palm kernel shell pellets formulated with binary mixtures that incorporate the catalyst was evaluated and gasification studies were carried out to evaluate the effectiveness of the binary pellets in gas cleaning.

1.2 Objectives

The overall aim of this work was focused on investigating the properties of pellets made from the palm kernel shells for use in syngas generation through gasification.

The objectives for the research were as follows:

i) To establish an experimental setup for the production of pellets, measurement of strength and measurement of gasification behaviour and tar amount
ii) To study the effects of compaction pressure, compaction speed, hold time, particle size, porosity, humidity and storage time on the mechanical strength of the pellets
iii) To study the rate of biomass converted to gaseous products during gasification process with respect to the variation in feedstock forms
iv) To study the effects of adding catalysts to the pellets on the mechanical properties and gasification behaviour.

This thesis is organised as follows. In the following chapter, some background information on biomass oil palm kernel shells and their potential will be provided. The mechanisms involved in the compaction of powders or pelletisation as well as empirical model and theories for the evaluation of mechanical strength of pellets will also be presented. Theories related to biomass gasification and literature review on factors affecting pellet strength will be elaborated. Chapter 3 includes detailed descriptions on the production of pellets and compression tests. Descriptions of the experimental setup for gasification will also be introduced.

In Chapter 4, detailed experimental results and discussion pertaining to pellet strength formulated from 100% palm kernel shell and gasification will be presented. The following Chapter 5 will discuss the results obtained from the strength tests and gasification of pellets produced from binary mixtures. Lastly, in Chapter 6, the thesis will conclude with a summary comprising all results obtained from the series of experiments conducted.

2 Background

2.1 Potential of Palm Kernel Shell as Sustainable Energy Source

Increases in prices of fossil fuels and growing environmental concerns regarding their impacts have driven the increased use of biomass worldwide (Dam et al., 2008). In Malaysia, the hot climate encourages oil palm cultivation and this development has made Malaysia a major global oil palm biomass producer (Yusoff, 2006). Under the Tenth Malaysia Plan (2010), the government highlighted palm oil and related products as one of the nation's key economic areas and to attain energy security through the development of alternative sources by 2015. The rapid growth in the palm oil industry is expected to see a corresponding growth in the amount of agricultural waste generated (Ng et al., 2012).

The oil palm (*Elaeis guaineensis*) has become the most important economic plantation crop in Malaysia. The reddish coloured fruits of the oil palm are used for the extraction of edible oil. Figure 2.1a shows the cross-section of an oil palm fruit (Corley and Tinker, 2003). There is a single seed inside each fruit, known as the palm kernel, surrounded by the soft pulp. The oil extracted from the pulp is the edible oil used for cooking while that extracted from the kernel is used mainly in the soap manufacturing industries.

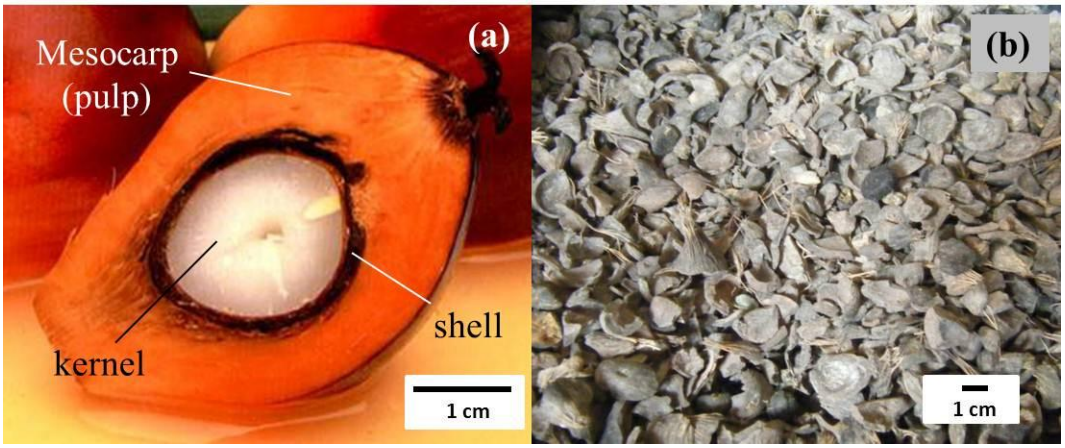

Figure 2.1 (a) Cross-section of an oil palm fruit (source: Corley and Tinker, 2003) (b) Palm kernel shells

The fresh fruit bunch contains 21% palm oil and approximately 27% moisture, while the rest consists of 6-7% palm kernel, 14-15% fibre, 6-7% shell and 23% empty fruit bunch (EFB) are left as biomass residues which can be used as raw materials for value-added industries (Basiron and Simeh, 2005; Umikalsom et al., 1997). During crude palm oil processing, the fresh fruit is melted through a steaming treatment. The residual nuts are further mechanically crashed to extract kernels. The crushed shells are virgin biomass called palm kernel shells (PKS) (Figure 2.1b). One hectare of palm oil plantation produces 50-70 tonnes of palm oil biomass residues annually (Shuit et al., 2009). These palm oil residues include fibre, shell, empty fruit bunches (EFB) and palm oil mill effluent (POME). The proximate and ultimate analysis of fibre, shell, EFB and kernel are shown in Table 2.1 and Table 2.2 (Husain et al., 2002). Table 2.3 (Vijaya et al., 2004; MPOB, 2006) shows the quantity, moisture content and calorific value of some palm oil residues generated in Malaysia.

	Fibre	Shell	EFB
Volatile matter (wt%)	72.8	76.3	75.7
Fixed carbon (wt%)	18.8	20.5	17
Ash (wt%)	8.4	3.2	7.3

Table 2.1 Proximate analysis of some palm oil residues (Husain et al., 2002)

Component (wt%)	Fibre	Shell	EFB
Hydrogen	6	6.3	6.3
Carbon	47.5	52.4	48.8
Sulphur	0.3	0.2	0.2
Nitrogen	1.4	0.6	0.7
Oxygen	36.7	37.3	36.7
Ash	8.4	3.2	2.3

Table 2.2 Ultimate analysis of some palm oil residues (Husain et al., 2002)

	Fibre	Shell	EFB
Quantity (million tonnes)	9.66	5.20	17.08
Moisture content (%)	37.00	12.00	67.00
Calorific value (kJ/kg)	19068	20108	18838

Table 2.3 Amount of palm oil residues generated in year 2005 with their moisture content and calorific values (Vijaya et al., 2004; MPOB, 2006)

Biofuels derived from oil palm wastes are a renewable source of energy that helps reduce the amount of carbon content in the atmosphere through zero carbon emission, thus qualifying for carbon credit under Kyoto Protocol to mitigate global warming (Shuit et al., 2009). Among the palm oil residues, palm shell has the highest carbon content and calorific value which makes it an attractive solution for biofuel. Therefore, palm kernel shell pellet is of great potential as a renewable and sustainable energy source in Malaysia.

2.2 Pelletisation

Pelletisation or the compaction of biomass into pellets is one solution to convert oil palm biomass into solid fuel. The compaction process involves compressing a material under high pressure into a fixed shape and size to increase the bulk density. Before subjecting to compaction, the biomass needs to be ground to a desired particle size and pretreated to reduce moisture level (Cheng, 2010; Kaliyan and Morey, 2009; Rhen et al., 2005). During the compaction process, pressure is applied to the biomass particles within a confined space and when these biomass particles are compressed, bonds are established between particles, thus conferring a certain mechanical strength to the compact (Rhen et al., 2005; Stelte et al., 2011).

The pelletisation of biomass are often done for the benefits of higher energy density, lower transportation and storage costs, and standardised sizes and composition to allow for automatic feeding in domestic and industrial sized boilers (Nasrin et al., 2008; Ng et al., 2012; Shuit et al., 2009). The compaction process is also commonly applied in pharmaceutics to make tablets. In particular, extensive research has been conducted and results on tablet strength and some models and theories proposed will be very relevant to the area of study in this project. These will be further discussed below.

2.2.1 Volume Reduction Mechanisms

When pressure is applied to a powder bed, the bulk volume of the powder is reduced and the amount of air within is decreased. During compaction, particles rearrange themselves and come into closer proximity with each other at lower pressures. As the pressure increases, space becomes more limited thus preventing further rearrangement of particles. At this point, subsequent volume reduction is achieved by plastic and elastic deformation or fragmentation of the particles (Duberg and Nystrom, 1986). Plastic deformation is an irreversible and permanent change in shape or size of the particle while elastic deformation is a reversible process whereby particles resume their original shape after the applied stress is removed. Fragmentation refers to the breakage of particles into smaller units and this normally occurs in particles that are brittle. However, brittle materials are generally undesirable to form pellets as they undergo extensive fragmentation which results in a large number of irregular bonding points that prevent further volume reduction (Maganti and Celik, 1993).

The degree and ease of volume reduction depend on mechanical properties of the powder such as particle shape and size (Bacher et al. 2007; Johansson and Alderborn, 2001; Fell and Newton, 1971) and time dependent factors such as compaction speed and hold time (Armstrong, 1989; Fell and Newton, 1971; Marshall et al., 1993).

2.2.2 Bonding Mechanisms

To a great extent, the strength of the formed pellets depends on physical forces that bind the particles together (Tabil and Sokhansanj, 1996). There are five major groups of binding forces that act between individual particles in densified products (Alderborn, 1996; Bhattacharya et al., 1985; Grover and Mishra, 1996; Li and Liu, 2000). They are solid bridges, interparticulate attraction forces, mechanical interlocking bonds, adhesion and cohesion forces and interfacial forces and capillary pressure. These binding forces have been observed for the densification of pharmaceutical powders (Alderborn, 1996; Nystrom and Karehill, 1996), animal feeds and biomass compacts (Tabil and Sokhansanj, 1996).

Solid bridges form upon particle-particle contact under certain prerequisites based on the chemical and material structure of the particles. If binders or other ingredients are added to the biomass, solid bridges may form due to chemical reaction, hardening of binders or crystallization and solidification of added ingredients (Kaliyan and Morey, 2009; Stelte et al., 2011). Solid bridges are more commonly formed after cooling or drying of the densified product (Kaliyan and Morey, 2009).

Interparticulate attraction forces such as hydrogen bond, van der Waals forces of attraction and electrostatic forces are short-range forces that cause particles to adhere to each other if the particles are brought close enough together (Kaliyan and Morey, 2009). During compaction, fibres and bulky particles can also hook or twist with each other resulting in mechanical interlocking bonds (Kaliyan and Morey, 2009). Mechanical interlocking is possible due to shape irregularities and surface roughness of particles (Fuhrer, 1977). The addition of binders may also contribute to smoothing out surface roughness and increasing the inter-particle contact area or by decreasing the inter-particle distance, thus allowing the interparticulate attraction forces to participate in the bonding mechanism (Stelte et al., 2011).

There are usually three stages during compaction (Holman, 1991). During the first stage, particles rearrange themselves to form a closer packing at lower pressures. At the second stage when pressure is higher, elastic and plastic deformation occurs, allowing particles to flow into smaller void spaces, thus increasing inter-particle

surface contact area (Nystrom and Karehill, 1996). As a result, van der Waals forces of attraction become prominent (Pietsch, 1997). Plastic deformation also causes particles to deform into irregular shapes, which help to promote mechanical interlocking of the particles (Hoag et al., 2008). If the material is brittle, mechanical interlocking then results from the bonding between fragmented particles (Gray, 1968). During the last stage if cooling or chemical reaction is introduced, strong solid bridges are formed (Ghebre-Sellassie, 1989). The rigidity of the compact is thus a result of the formation of new permanent bonds between particles.

2.2.3 Porosity

Powder beds consist of void spaces known as porosity. The compacted powder bed is a heterogeneous system comprising solid particles and air. Typically, porosity decreases during compaction due to the decrease in the amount of air as particles move closer to each other. The value of porosity can range from 0 to 1 or expressed as a percentage from 0% to 100%. The true density and bulk density is determined prior to the calculation of the porosity of a compacted powder bed. The true density (ρ_T) can be calculated using:

$$\rho_T = \frac{m_P}{V_P} \tag{2.1}$$

where m_P is the mass of the powder and V_P is the powder volume. The true density of the powder is commonly measured by the pycnometer (Igathinathane et al., 2010).

The bulk density is defined here as the density of a pellet after the compaction process and the volume of the pellet is based on the shape of the pellet. For a cylindrical pellet, the volume as a whole is calculated by $V = \pi r^2 L$, where r is the radius of the pellet and L is the relaxed or final length of the pellet. The relaxed length is defined as the length of the pellet after ejection from the production die. Compacted bulk density is defined as the bulk density of the pellet during compaction. The compacted bulk density (ρ_c) of a cylindrical pellet can be calculated by the following equation:

$$\rho_c = \frac{m}{\pi r^2 L_0} \tag{2.2}$$

where m is the mass of the pellet and L_0 is the length of the pellet at maximum compaction pressure as illustrated in Figure 2.2a. The final bulk density is defined as the final density of the pellet after ejection from the production die. The relaxed or final length L is used for the calculation of final bulk density. The final bulk density (ρ_B) of a cylindrical pellet can be calculated by the following equation:

$$\rho_B = \frac{m}{\pi r^2 L} \tag{2.3}$$

where L is the relaxed or final length of the pellet after ejection from the production die as illustrated in Figure 2.2b.

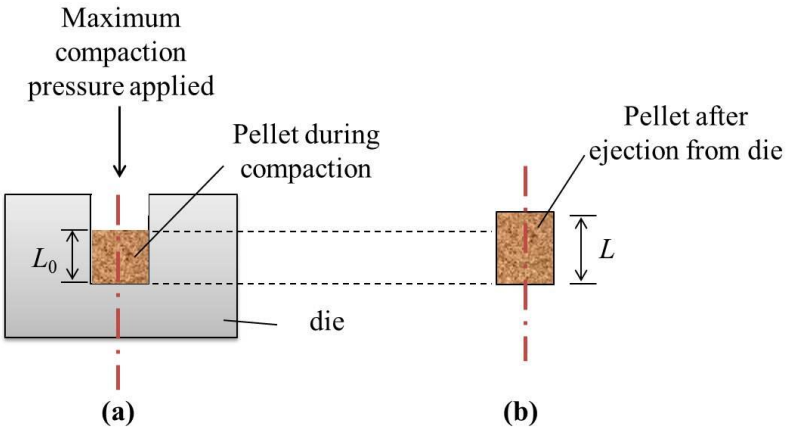

Figure 2.2 Measurement of the length of pellet (a) during compaction, at maximum compaction pressure for the calculation of compacted bulk density (b) after ejection from the die for the calculation of final bulk density

Porosity (ε) of a compacted powder bed during compaction can be determined by the following calculation (Paronen and Ilkka, 1996):

$$\varepsilon = 1 - \frac{\rho_B}{\rho_T} \tag{2.4}$$

where ρ_B is the compacted bulk density of the powder bed and ρ_T is the true density of the solid particles that make up the powder. Equation (2.2) can be substituted into equation (2.4) to determine the porosity of a pellet during compaction. Equation (2.3) can be substituted into the following equation (2.5) to determine the final porosity (ε_f) of the pellet after ejection from the die.

$$\varepsilon_f = 1 - \frac{\rho_B}{\rho_T} \tag{2.5}$$

Since compaction is a process which involves a reduction in the bulk volume of the pellet, the corresponding bulk density of the pellet will increase and hence its porosity is reduced. General studies found that as the porosity of the powder bed reduces, the strength of a pellet increases (Adolfsson and Nystrom, 1996). In addition, it was shown that when the porosity of a powder during compaction approaches almost zero or zero porosity, the strength of the pellet does not show signs of increment and it can be said that maximum strength is achieved (Adolfsson and Nystrom, 1996; Goh et al. 2008).

The porosity of a material also influences its thermal conductivity, thus affecting heat transfer rates (Carson et al., 2005; Francl and Kingery, 1954; Raghavan et al., 1998; Schlichting et al., 2001; Vincent et al., 2012). A decrease in porosity not only improves the mechanical strength of a pellet but also the combustion characteristics (Pabst and Gregorova, 2007). Sugawara and Yoshizawa (1961) concluded that the thermal conductivity of a porous material decreases with increasing porosity. Hamel and Krumm (2008) studied biomass wood chips and reported that a decrease in porosity increased the interstitial airflow velocity and brought about changes in heat and mass transfer conditions which ultimately improved the combustion parameters such as heat conductivity and burning rate, and led to a higher conversion efficiency (Igathinathane et al., 2010).

Carson et al. (2005) distinguished between two basic types of porous material. External porosity materials are defined as particulate materials in which air (for instance) comprises a continuous phase as opposed to internal porosity materials

such as foams or sponges in which air is dispersed within a continuous solid or solid/immobilized-liquid phase (Carson et al., 2005). For external porosity materials, the optimal heat conduction pathway is through the particles and different solid materials vary in terms of thermal conductivities due to non-identical void fractions or porosities (Sugawara and Yoshizawa, 1961; Tavman, 1996). Hence the heat conduction pathways for external porosity materials depend strongly on the contact between neighbouring particles (Carson et al., 2005). The extent of contact between neighbouring particles is material specific and affected by its packing (Felske, 2004). For internal porosity materials, the optimal heat conduction pathway avoids the air voids within the material and travel along the continuous medium. Hence with a lower number of pores within the material, the heat conduction is improved due to increased heat pathways (Carson et al., 2005). So far there have been no reported values on the thermal conductivities of palm kernel shells.

2.2.4 Elastic Recovery

Elastic recovery or porosity expansion is quantified as the increase in pellet height or volume after compaction (Doelker, 1993). Maarschalk et al. (1996a) suggested that elastic recovery is the result of two phenomena namely a decrease in pellet bulk density and an increase in pellet porosity. The increase in pellet porosity occurs during and after the release of compaction pressure from the pellet. The elastic recovery (*ER*) can be calculated according to the following equation (Adolfsson and Nystrom, 1996):

$$ER = \frac{L - L_0}{L_0} \times 100\% \tag{2.6}$$

where L is the relaxed length of the pellet after ejection and L_0 is the length of the pellet at maximum compaction pressure as illustrated in Figure 2.2.

Adolfsson and Nystrom (1996) recorded that an increase in compaction pressure increased the elastic deformation of the particles, which were observed as the elastic recovery of the formed compact. Elastic recovery was thought to be affected by

processing parameters such as die-wall friction during ejection of the pellet from the die due to the rupture of bonds between particles (Adolfsson and Nystrom, 1996). An increase in elastic recovery may lead to a decrease in pellet strength because of the reduction in interparticulate bonding due to bond rupture (Maarschalk et al., 1996b; Rees and Tsardaka, 1994; Zuurman et al., 1999).

2.2.5 Die-Wall Friction

Die-wall friction refers to the friction at the interface between the powder or pellet and the die wall during the compaction process and such die-wall friction hinders pressure transmission, therefore reducing the amount of energy passed on towards the deformation of the particles during compaction (Briscoe and Evans, 1991). This causes non-uniform packing densities within the powder compact which may in turn affect the final strength of the pellet. High wall friction may also create high stress gradients within the powder, causing significant density fluctuations to occur (Briscoe and Rough, 1998).

To overcome the problems associated with die-wall friction, lubricants may be used (Michrafy et al., 2004; Wang et al., 2010). Briscoe and Evans (1991) studied wall friction and lubrication of agglomerated ceramic powder and reported that in an unlubricated die, the changes in wall friction is predominantly affected by the variation in transmitted radial stresses with compaction pressure. However, for a lubricated die, both friction coefficient and transmitted radial stresses are equally important in contributing to wall friction. Train (1956) studied the effects of wall friction and lubrication on density distribution and ejection force of an inorganic powder and found that the lubricated die produced a more uniform density distribution within the compacts compared to the unlubricated die. The ejection force was also found to be significantly reduced due to a reduction in die-wall friction.

Generally, lubrication is used to enhance stress transmission in the axial direction and to minimise the density variation within the compact. However, it is often reported that the increase in axial stress transmission will inadvertently increase the radial stress transmission as well (Dimilia and Reed, 1983; Sixsmith and McCluskey,

1981). Such increase in radial stress transmission may result in an increase in friction force and shear deformation which fractures the tablet during ejection (Hiestand et al., 1977). Wu et al. (2008) pointed out that sufficient bonding and densification during compaction do not guarantee strong pellet products. Both decompression and ejection play a crucial role in deciding whether a compact would retain adequate strength to withstand further handling.

There are a few possible ways to introduce lubrication. One way is to incorporate the lubricants into the powder formulation; another way is to lubricate the die. It was proposed that the powder-lubricant mixture mode of lubrication is more practical at high production rates compared to the die lubrication mode (Michrafy et al., 2004). However, one major disadvantage with the powder-lubricant mixture is that the lubricant reduces the strength of the pellet. It was reported that magnesium stearate, a lubricant used in the pharmaceutics, forms an adsorbed lubricant film around the particles during powder mixing which interferes with the bonding properties of the particles, resulting in low interparticle attraction that resulted in poor tablet strength (Bolhuis and Holzer, 1996; Zuurman et al., 1999). Unlike pharmaceutical tablets, no suitable lubricants have been proposed for incorporation into biomass pellets and knowledge in this area is still very limited. Applying external lubrication on the die is feasible but is not cost-effective as tool surfaces need to be treated and coated to reduce their coefficient of friction (Wang et al., 2010).

2.2.6 Mechanical Properties

Elastic deformation: In general, a material deforms elastically at the initial stage of compaction. A change in shape caused by the applied stress is completely reversible and the material returns to its original shape upon release of the applied stress. During elastic deformation, the stress-strain relationship for the specimen is described by the following equation:

$$stress = E \cdot strain \tag{2.7}$$

where E is the Young's modulus of elasticity.

The elastic deformation region for a specimen is shown graphically in Figure 2.3. Elastic strain results from a change in intermolecular spacing and is reversible for small deformations. Young's modulus of elasticity is calculated by the gradient of the slope in the elastic region.

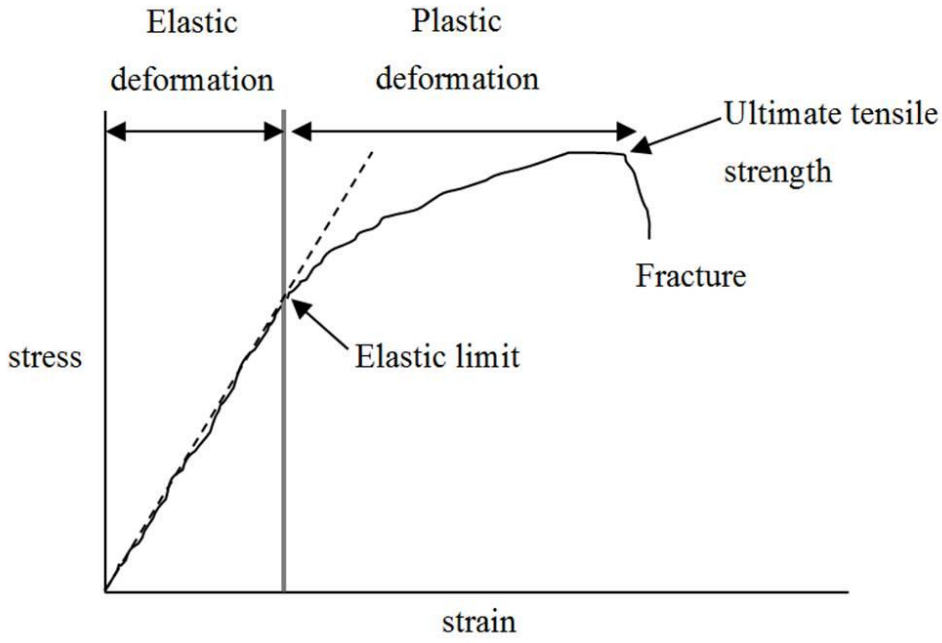

Figure 2.3 Stress-strain curve

Plastic deformation: This relates to the permanent change in shape of the specimen due to the applied stress. The region is denoted by the curved section in Figure 2.3. Plastic deformation is important because it enables powder particles to establish large true contact areas during compaction that can remain after decompression (Hoag et al., 2008; Nystrom and Karehill, 1996).

Brittle and ductile fracture: Materials may either fail in brittle fracture or ductile fracture. Brittle fracture occurs by the rapid propagation of a crack through a specimen whereas in ductile fracture, the specimen will undergo an extensive plastic deformation before reaching the fracture point. Typically, ductile fractures are not observed in pharmaceutical tablets as tablets snap upon hardness testing, which indicates brittle fracture.

Viscoelastic properties: Viscoelasticity reflects the time-dependent nature of stress-strain. During elastic deformation, particles move when stress is applied. With time, particle rearrangements occur. The stress-strain relationship can therefore depend on the time duration over which the test is conducted. Hence processing factors associated with rates such as compaction speed and hold time are noted to have an impact on the mechanical properties of tablets or pellets (Armstrong, 1989; Kaliyan and Morey, 2009).

2.3 Evaluating the Mechanical Strength of Pellets

Mechanical strength tests are carried out to ensure that pellets produced are sufficiently strong to withstand handling procedures as well as to characterise the mechanical properties of pellets. The method of evaluating mechanical strength is usually undertaken by the application of a mechanical stress until the pellet breaks. The value at which the pellet breaks depends on the type of stress applied, direction of application and the shape and dimension of the pellet (Newton et al., 2000).

Uniaxial compression tests are commonly used in pharmaceutics, polymeric structures and biomass applications to determine the strength of a tablet, pellet or material (Fell and Newton, 1970; Jerabek et al., 2010; Mani et al., 2006).

2.3.1 Compressive Strength

Compressive strength or compressive fracture stress can be determined by crushing the pellet in the same direction as during compaction, i.e. parallel to the cylindrical axis, and obtaining the force value. The force obtained is then used to calculate the compressive strength σ (Nystrom et al., 1978) according to the following equation:

$$\sigma = \frac{F}{A} \tag{2.8}$$

where F is the crushing force recorded and A is the initial contact area.

2.3.2 Tensile Strength

The tensile strength (σ_T) or radial tensile strength of a pellet is typically determined by subjecting the pellet to diametrical compression (Fell and Newton, 1970), i.e. perpendicular to the cylindrical axis as illustrated in Figure 2.4 and by the following equation:

$$\sigma_T = \frac{2F}{\pi DL} \tag{2.9}$$

where D is the diameter of the pellet and L is the final length of the pellet.

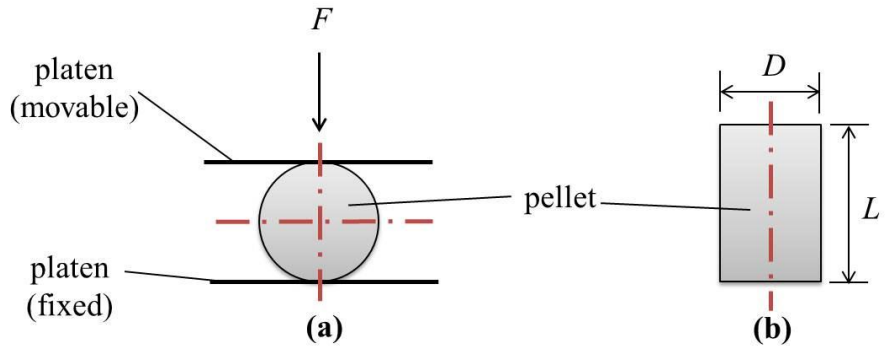

Figure 2.4 View of pellet (a) subjected to diametrical compression (b) dimensions after ejection from production die

To calculate the radial tensile strength, the stress conditions have to be such that the pellet fails in tension. Most pellets are weaker in tension than in compression (Newton et al., 1992). In the radial tensile strength test, the fracture occurs through a diametrical cross section of the pellet hence the measured radial tensile strength reflects an average strength of the pellet.

A pellet that exhibits different mechanical strength values when measured in different orientations is said to be anisotropic (Malamataris et al., 1996; Newton et al., 1993; Nystrom et al., 1978). It has been suggested that mechanical property anisotropy in pellets is important as it contributes to pellet manufacturing failures

(Nystrom et al., 1978). Consequently, an understanding of the compressive and tensile strength of the pellet might lead to improved pelletisation.

2.3.3 Ryshkewitch-Duckworth Equation

There are a few compaction models proposed to describe the strength of particles from the compaction process such as Heckel (1961), Cooper and Eaton (1962) and Kawakita and Ludde (1971). The Heckel and Cooper-Eaton models are still in use to study the compaction mechanism of pharmaceutical and cellulose materials while the Kawakita-Ludde model was proposed for soft and fluffy materials (Kawakita and Ludde 1971).

Ryshkewitch (1953) found that the logarithm of pellet strengths is inversely proportional to the porosity. Since then, the Ryshkewitch-Duckworth (Duckworth, 1953) equation has been commonly used to study the bonding capacity in compacted materials. The Ryshkewitch-Duckworth equation is as follows:

$$\frac{\sigma}{\sigma_0} = \exp(-k\varepsilon) \tag{2.10}$$

where σ is the strength of the pellets, ε the compacted porosity and σ_0 the strength at zero porosity. The constant k represents the bonding capacity and higher values of k correspond to stronger bonding of particles (Maarschalk et al., 1996b; Steendam and Lerk, 1998).

2.4 Factors Affecting Pellet Strength

2.4.1 Particle Size

Particle size has been demonstrated to affect compressibility and compactibility of a material (Bacher et al., 2007; Freitag et al., 2004). Generally, it was found that a decrease in particle size increases a tablet's mechanical strength (Alderborn 1996; Hoag et al., 2008; Patel et al., 2007).

According to Alderborn (1996), the increase in strength with a decrease in particle size is due to a lower probability of defects in the crystal structure of the particle. As particle size decreases, there exists more contact points between adjacent particles for bonding. This facilitates the compressibility or ease of consolidation of a material. A study by Kaerger et al. (2004) on paracetamol and microcrystalline cellulose reveals that smaller particle sizes exhibit higher compressibility than larger particle sizes. This results in an improvement in bulk density and hence pellets with greater strength. For brittle materials, it has been found that compressibility increases with a decrease in particle size whereas for a plastically deforming material, compressibility is independent of particle size (Leuenberger and Jetzer, 1984).

Kaliyan and Morey (2009) defined pellet quality in terms of strength and durability of the pellets. Durability is defined as the abrasive resistance of a densified product (Kaliyan and Morey, 2009). Generally, in the compaction of biomass products, especially on animal feed, finer grind leads to a higher durability of pellet. Furthermore, large particles are fissure points for cracks and fractures in pellets thus affecting pellet quality (Kaliyan and Morey, 2009). Stevens (1987), on the other hand, observed that particle size did not have much impact on the pellet quality of corn grind. Such inconsistencies in observations on how particle size affects the strength of various biomass pellet products indicate a need for characterisation of pellets made from different biomass.

2.4.2 Compaction Speed and Hold Time

Compaction speed refers to the distance moved per unit time for the pellet making machine piston. This speed is then transferable to the plunger during contact with the machine piston. Compaction speed is also known as the punch velocity and can be preset before the compaction process. During compaction, the plunger comes into contact with the particles and there exists a contact time between plunger and particle. Jones (1981) divided the compression event into a series of time periods and proposed a number of definitions:

1. Consolidation time: time required to achieve maximum compaction force.
2. Contact time: time for compression and encompasses the starting time from the application of a pressure to the point when maximum pressure is reached and released immediately.
3. Hold time: time at maximum compaction force.
4. Ejection time: time during which ejection occurs.
5. Residence time: time during which the formed compact is within the die.

Figure 2.5 shows Jones' (1981) definitions in diagrammatic context. For a hold time of 0 s, only a peak is obtained with no plateau. However, if the maximum force is maintained for prolonged periods, a plateau will be observed.

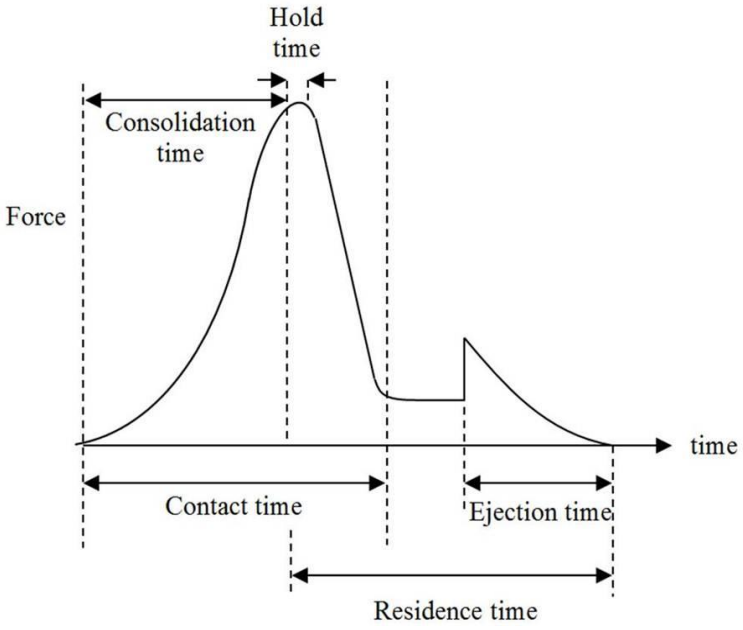

Figure 2.5 Events during the compression process

A longer holding time was found to increase the density and the compressive strength of compacted oak sawdust (Li and Liu, 2000). It was also noted that when holding time was beyond a certain duration, the effect diminished (Li and Liu, 2000) and both the density and the strength no longer changed due to near-zero or zero porosity (Adolfsson and Nystrom, 1996; Maarschalk et al., 1997a).

The effect of compaction speed or punch velocity on the compaction of materials has been commonly studied for pharmaceutical compacts and the relationship differs for different materials. Some researchers (Baba and Nagafuji, 1965; Marshall et al., 1993) found that the strength of the compacts decreased with increasing compaction speed and explained that this was due to a decrease in plastic deformation as a result of a reduction in time available for stress relaxation and thus bond formation (Hiestand et al., 1977). Maarschalk et al. (1996b) pointed out that the fact that compaction speed affects the consolidation mechanism of the compact is indicative of the viscoelastic nature of the material. The elastic recovery was also found to increase with increase in compaction speed due to the decrease in stress relaxation and bond formation, leading to weaker pellets (Akande et al., 1997). Other researchers observed that the strength of perfectly elastic-brittle particles showed no dependence on compaction speed (Rees and Rue, 1978; David and Augsburger, 1977).

Very few studies had been carried out on the effect of compaction speed on the quality of biomass compacts. Li and Liu (2000) studied the effect of compaction speed on the densification of oak sawdust and found that the final density of the compact decreased with increasing compaction speed and levelled off beyond a certain speed. When the compaction speed was further increased beyond this speed, the compaction speed effect became negligible. However, Stevens (1987) reported that compaction speed did not affect the quality of corn and wheat pellets.

2.4.3 Compaction Pressure

Compaction pressure has typically been found to have an impact on the density of a pellet during maximum compaction pressure. Mani et al. (2006) observed that an increase in compaction force or pressure significantly increased the density of biomass pellets from grasses. In addition, Adapa et al. (2009), Li and Liu (2000), Stasiak et al. (2010) and Yusof et al. (2010) all recorded an increase in compact density of the pellet or tablet products as a result of increased compaction pressure. However, the density of a compact does not increase indefinitely with continued increase in compaction pressure. Adapa et al. (2009) reported that application of

pressures beyond a certain value did not lead to further increase in compact density of the biomass pellet as the pellet has approached its true density. This point corresponds to very low or zero porosity and maximum mechanical properties of the compact is said to be achieved (Goh et al., 2008; Maarschalk et al., 1997a).

The relationship between pressure-density has been determined by many researchers. O'Dogherty and Wheeler (1984) suggested that the pressure-density relationship of straw pellets followed a simple power law equation whereas Husain et al. (2002) found an exponential increase in density with increasing pressure for palm fibre and shell briquettes. Razuan et al. (2011) also established an exponential relationship between pressure and density of palm kernel cake pellets. As far as palm kernel shell pellets are concerned, no studies had been conducted before on the effect of compaction pressure on the pellet.

2.4.4 Humidity and Storage Time

Post-production conditions such as the humidity level of the surroundings and the duration of storage may affect the mechanical strength of pellets (Kaliyan and Morey, 2009; Mani et al., 2006; Mollan and Celik, 1995; Rhen et al., 2005). The strength values of wood, alfalfa and hay briquettes were found to decrease after a period of storage, compared to the strength value obtained immediately after production (Mohsenin and Zaske, 1976). During storage, it was also discovered that the briquettes dried and expanded which resulted in a lower strength. Lehtikangas (2000) reported that storage led to negative effects on the durability of pelletised sawdust, logging residues and bark. Water absorption tests showed that the pellets were hygroscopic and had tendencies to attain equilibrium with ambient moisture during storage. It was thus suggested that ambient moisture content or humidity level should be taken into consideration if pellets were to be stored after production.

Li and Liu (2000) studied on wood pellets and observed that when moisture content was higher than 13%, pellets had low densities and easily disintegrated when subjected to small handling forces. Even though high density pellets were achieved at 4% or less moisture content, the pellets could not sustain their good quality after 3

days. Similar to Lehtikangas' (2000) observation, these pellets also had the tendencies to absorb moisture from the air and expand significantly, becoming fragile in a few days. The densities of the pellets were found to decrease with increasing moisture content.

There is a lack of literature on the mechanism behind strength changes particularly for biomass compacts. However, mechanisms for post-compaction changes in mechanical strength of compacts were studied and proposed by researchers in pharmaceutics (Eriksson and Alderborn, 1994; Mollan and Celik, 1995), which may help explain some observations related to biomass compacts. At high humidities, Lordi and Shiromani (1984) discovered that the strength of tablets made from crystalline salts decreased and attributed this phenomenon to the dissolving of interparticulate bonds which resulted in separation of contact points, leading to a decrease in molecular forces of attraction. Such hypothesis may be applicable to powder that adsorb large amount of water at high humidity conditions. On the other hand, Ahlneck and Alderborn (1989) and Eriksson and Alderborn (1994) found that fluctuations in the humidity of the environment can also cause desorption of water which can lead to crystallisation of material dissolved in sorbed water. Consequently, formations of interparticulate bonds occur and increase in compact strength was achieved.

Two mechanisms were proposed for changes in tablet strength with storage time and humidity for non-hygroscopic materials (Nystrom and Karehill, 1986; Rees and Rue, 1978). The first mechanism was associated with the continuing deformation of particles within the tablet during storage time after compaction. This visco-elastic behaviour would lead to formations of new interparticulate bonds that result in increased coherency of the tablet. The second mechanism described formations of new bonds due to the repositioning of amorphous surface material that result in concentration of the material at interparticulate junctions (Ahlneck and Alderborn, 1989). The second mechanism was shown to be related to the relative humidity of the storage environment and the role of the sorbed water at the particle surfaces was to increase mobility of the particles for repositioning.

Thus, various investigators have suggested differing observations and this indicates that the effect of humidity and storage could depend on the nature of the material and its degree of the hygroscopy.

2.5 Binary Mixtures and Binders

Pellets or tablets may sometimes comprise more than one component. The mechanical strength of pellets and tablets then depends not only on processing parameters but also on the formulation. During densification, the compaction properties of the formulation are strongly influenced by the characteristics of the mixture, in particular the particle size fractions of the components (Kasa et al., 2009).

In most cases, the strength of tablets with binary mixtures was lower than the strength calculated from the interpolation of the strength of tablets prepared from pure materials (Adolfsson et al., 1998; Garr and Rubinstein, 1991; Mattsson and Nystrom, 2001). Currently, no single model may be considered as being the best to predict binary behaviour from data of individual powder (Hadzovic et al., 2011; Michrafy et al., 2007).

Binders are materials added to a formulation to improve the mechanical strength of a compact. When binders are added to a powder and compacted, they form a binary mixture comprising more than one component of the formulation. Binders are suggested to be effective because they create large surface areas available for bonding which in turn improves the mechanical strength of a tablet (Mattsson and Nystrom, 2001; Nystrom et al., 1993). However, too much binder may adversely lead to a drop in tablet strength (Veen et al., 2000). Selecting a suitable binder requires knowledge of its functionality and its strength enhancing properties. Furthermore, an understanding of how different materials interact with each other in the mixture is also important in this aspect.

In biomass pelletisation, starch, protein, fibre, fat and lignin are commonly used as binders (Kaliyan and Morey, 2009), but with different results when combined with

different biomass. Previous studies on the pelletisation of palm oil wastes typically involved binders such as starch, caustic soda and calcium carbonate (Husain et al., 2002; Razuan et al., 2011). The addition of binders improved the agglomeration and strength of the pellets (Razuan et al., 2011). However, its downsides include reduced combustion characteristics of the pellet and an increase in the pellet's vulnerability to biological decay (Finney et al., 2009). In particular, the combustion efficiency was found to be reduced and high concentrations of alkali metals were found in the ash which could induce slagging or fouling (Finney et al., 2009).

2.5.1 Model Description for Binary Compacts

Most of the models proposed to predict the mechanical properties for compacts containing two components or binary tablets originate from the field of pharmaceutics. Michrafy et al. (2007) and Wu et al. (2005) investigated the tensile strength of binary tablets comprising silicified microcrystalline cellulose (SMCC) and lactose, and strength of binary tablets comprising microcrystalline cellulose (MCC), hydroxypropylmethyl cellulose (HPMC) and starch respectively using an extended Ryshkewitch-Duckworth model:

$$\ln\left(\frac{\sigma_m}{\sigma_{0,m}}\right) = -k_m \varepsilon_m \tag{2.11}$$

where σ_m is the strength of the binary pellet, $\sigma_{0,m}$ is the strength of the binary pellet at zero porosity, k_m is the bonding capacity of the binary pellet and ε_m is the porosity of the binary pellet. This predictive model (2.11) for the strength of binary pellets is based on the accessible properties of constituent components using the linear mixing rule. The linear mixing rule (Wu and Seville, 2009) assumes that the volumes of the components do not undergo notable changes in a fully densified material and the strength at zero porosity can be approximated as:

$$\sigma_{0,m} = V_1\sigma_{0,1} + V_2\sigma_{0,2} \tag{2.12}$$

where $\sigma_{0,m}$, $\sigma_{0,1}$ and $\sigma_{0,2}$ are the strengths of the binary mixture, constituent powder component 1 and component 2 respectively at zero porosity. V_1 and V_2 are the volume fraction of the powder component 1 and component 2. They are related to the mass fraction ξ_1 of the powder component 1 or mass fraction ξ_2 of component 2, the true densities $\rho_{T,1}$ and $\rho_{T,2}$ of powder component 1 and component 2 respectively, and the true density of the binary mixtures $\rho_{T,m}$ through the following equations:

$$V_1 = \frac{\xi_1 \rho_{T,m}}{\rho_{T,1}} \tag{2.13}$$

$$V_2 = \frac{\xi_2 \rho_{T,m}}{\rho_{T,2}} \tag{2.14}$$

The true densities of the binary mixtures $\rho_{T,m}$ can be determined by using the mixing rule as a function of the true densities of the constituent single component powders, $\rho_{T,1}$ and $\rho_{T,2}$ (Wu and Seville, 2009):

$$\frac{1}{\rho_{T,m}} = \frac{\xi_1}{\rho_{T,1}} + \frac{\xi_2}{\rho_{T,2}} \tag{2.15}$$

Equation (2.16) (Michrafy et al., 2007) can be used to estimate the bonding capacity k_m of the binary pellet:

$$k_m = V_1 k_1 + V_2 k_2 \tag{2.16}$$

where k_1 and k_2 are the bonding capacity of the powder component 1 and 2 respectively.

Michrafy et al. (2007) achieved predictions with the model that were close to the experimental results but concluded that the proposed model had its limitations as it may not be systematically generalized to other powders due to the dependence on the powders used and the range of porosity measurements. Wu et al. (2006) commented

that the proposed model might overestimate the strength of high-density tablet (i.e. ≥0.85) produced at high compaction pressures due to the occurrence of significant plastic deformation of primary particles in the powder bed. Since plastic deformation of a material is non-recoverable, this resulted in the reduction in the volumes of powder particles which contradicted with the assumption that the volumes of the components do not undergo notable changes in a fully densified material. Nevertheless, the proposed model was found to give good predictions of the strength of multi-component tablets based on the properties of the constituent single-component powders since most pharmaceutical tablets have relative densities of 0.7-0.9 (Hancock et al., 2003).

On the other hand, Hadzovic et al. (2011) and Veen et al. (2004) concluded that although the same process parameters (e.g. compaction speed, hold time, compaction pressure) may be used, the strength of some tablets compacted from the binary mixtures may not be predicted from the compaction properties of its individual materials. This phenomenon may be due to the material particles interaction during the compaction process (Veen et al., 2004). Veen et al. (2004) adopted the equivalent box model proposed by Kolarik (1994) that was built upon two possible coupling of two components namely parallel and series for bicontinuous structures. A schematic representation of the structure-dependent fit based on the equivalent box model is shown in Figure 2.6. Each block was presumed to have the mechanical property of the component it represented in relation to its volume fraction.

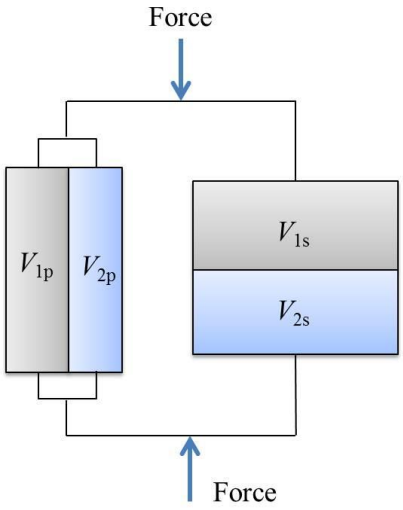

Figure 2.6 Schematic representation of the structure-dependent fit. (Veen et al., 2004)

In the study by Veen et al. (2000), it was found that the tensile strength reduction was related to the percentage of starch incorporated into sodium chloride tablets. The decrease in tensile strength was a result of reduced interparticulate bonding, caused by low adhesive forces or low interfacial interaction between the particles of the components (Hadzovic et al., 2011; Veen et al., 2004). Veen et al. (2004) proposed the following equation based on the structure-dependent fit to predict the strength of binary mixtures:

$$\sigma_m = (\sigma_1 V_{1p} + \sigma_2 V_{2p}) + \delta\sigma_2 V_s \tag{2.17}$$

where σ_m is the strength of the binary mixture, σ_1 and σ_2 are the strengths of components 1 and 2 respectively, V_{1p} and V_{2p} are the volume fractions of components 1 and 2 respectively in parallel coupling, δ is the interaction factor and V_s is the volume fraction in series coupling. δ has a value between 0 and 1 that indicates the adhesive interfacial interaction between the particles of the two components. V_s has the following relationship:

$$V_{1p} + V_{2p} + V_{1s} + V_{2s} = V_p + V_s = V_1 + V_2 = 1 \tag{2.18}$$

At present, no universal model to predict the mechanical properties of binary mixtures exists (Patel and Bansal, 2011).

2.6 Biomass Gasification

Gasification is the main technology for biomass conversion to energy and an attractive alternative for thermal treatment of solid waste (Ayhan, 2005; Belgiorno et al., 2003). The number of different uses of its product gas shows the flexibility of gasification and therefore allows it to be integrated with several industrial processes and power generation systems. In a gasification system, there are three fundamental elements namely (1) the gasifier, for producing the combustible gas (2) the gas cleanup system, to remove harmful compounds from the combustible gas (3) the energy recovery system.

Combustion, gasification and pyrolysis are thermal conversion processes available for thermal treatment of biomass. Pyrolysis is defined as the thermal destruction of organic materials in the absence of oxygen. If pyrolysis is carried out in the presence of small quantity of oxygen, the process is known as gasification. Gasification involves the thermochemical conversion of a solid or liquid carbon-based feedstock into a combustible gas by the supply of a gasification agent (air, oxygen or steam). Figure 2.7 shows a schematic of the gasification process.

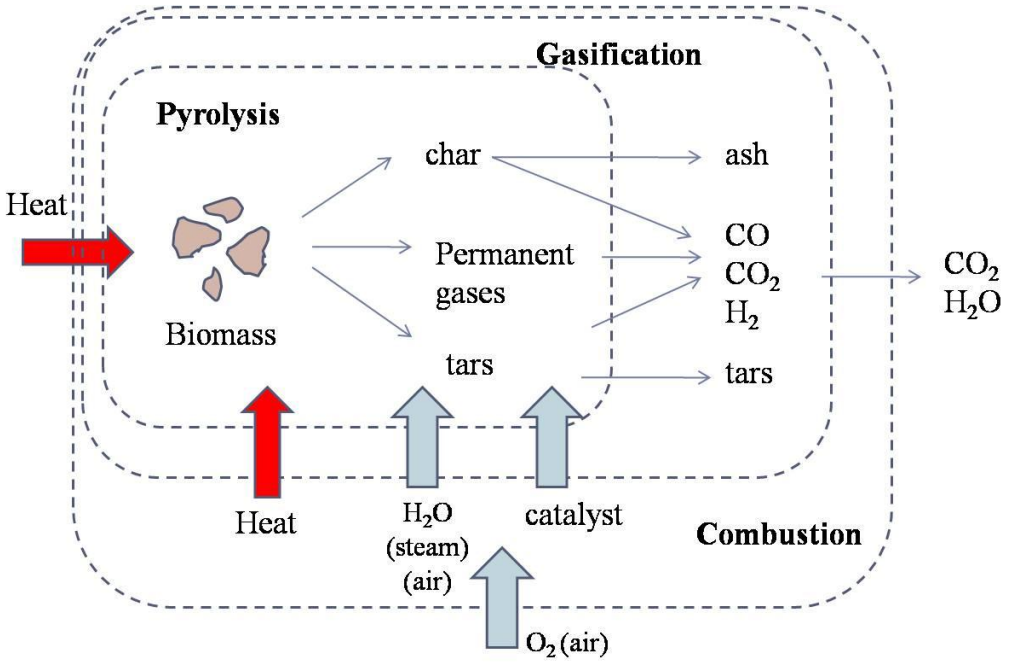

Figure 2.7 Schematic of gasification process (Stassen et al., 2002)

There are two types of gasification: direct and indirect. Direct gasification occurs when an oxidant gasification agent is used to partially oxidise the feedstock. These exothermic reactions supply the energy necessary to keep the temperature of the process up. In contrast, if the process does not occur with an oxidising agent, it is known as indirect gasification and an external energy source will be required (Cheng, 2010).

During the gasification process, a number of exothermic and endothermic reactions take place. Heating and drying are endothermic and require a source of heat to drive them. This heat can be supplied by an external heat source in a process of indirect

gasification and typically happens during the pyrolysis stage. During pyrolysis, char, tar and gases as shown in equation (2.19) (Lv et al., 2007) are produced:

$$\text{Biomass} \rightarrow \text{char} + \text{tar} + \text{gases } (CO_2, CO, H_2O, H_2, CH_4, C_nH_m) \quad (2.19)$$

When gasification agents are introduced, oxidation reaction of biomass pyrolysis products proceed to provide the required heat for the whole gasification process as presented in the following reactions (Higman and Burgt, 2008).

Combustion reaction:

$$C + \frac{1}{2}O_2 \rightarrow CO \quad (2.20)$$

$$CO + \frac{1}{2}O_2 \rightarrow CO_2 \quad (2.21)$$

$$H_2 + \frac{1}{2}O_2 \rightarrow H_2O \quad (2.22)$$

Boudouard reaction:

$$C + CO_2 \leftrightarrow 2CO \quad (2.23)$$

Water gas reaction:

$$C + H_2O \leftrightarrow CO + H_2 \quad (2.24)$$

Methanation reaction:

$$C + 2H_2 \leftrightarrow CH_4 \quad (2.25)$$

Water gas shift reaction:

$$CO + H_2O \leftrightarrow H_2 + CO_2 \quad (2.26)$$

Steam methane reforming reaction:

$$CH_4 + H_2O \leftrightarrow CO + 3H_2 \quad (2.27)$$

The gasification agent allows the feedstock to be converted to gas by means of the above heterogeneous reactions. The combustible gas will contain CO_2, CO, H_2, CH_4, H_2O, trace amounts of higher hydrocarbons, inert gases present in the gasification agent, and various contaminants such as char particles, ash and tars (Bridgwater, 1994).

The resulting product gas from gasification is more versatile than the original biomass feedstock because it can be burnt to produce heat or used in gas turbines to produce electricity (Ayhan, 2005). Introducing steam at high temperatures during gasification will produce synthesis gas or syngas. Syngas comprises carbon monoxide and hydrogen and it may be burned directly in an internal combustion engine or converted into other synthetic fuels. Its heating value is typically 10-18 MJ/Nm^3 via oxygen gasification, which is lower than that of natural gas (35 MJ/Nm^3) (Ayhan, 2005; Bridgwater, 1995). However, biomass gasification has the advantage of creating less pollution problems than the combustion of natural gas, because the carbon dioxide released during biomass utilisation is recycled as an integral part of the carbon cycle (Shuit et al., 2009), thus contributing to the reduction in carbon dioxide emission.

Air is widely used as a gasification agent as it is cheap. However, air contains a large amount of nitrogen which reduces the heating value of the syngas produced (Wang et al., 2008). Using oxygen as gasification agent could produce better syngas with medium heating value but this would mean higher costs as the oxygen supply has to be pure (Ni et al., 2006). If steam is used as the gasification agent, the heating value and hydrogen content in the syngas can be increased but operational costs will simultaneously increase due to the requirement of an external heat source for steam production (Rapagna et al., 2000).

There are some challenges faced in gasification. Wastes such as paper mills waste, forest industry wastes and agricultural residues are directly suitable for gasification, however, their irregularity in shapes, sizes and densities lead to difficulties in achieving efficient, steady-state gasification and transportation processes (FAO, 1986). Moreover, the syngas produced contains harmful compounds which, if not removed, would damage the engine or gas turbine and incur high maintenance costs hence the gas cleanup system is essential. Oil palm wastes such as EFB, fibre and shells has been investigated for gasification but one of the problems highlighted was the cleaning of the product gas (Azali et al., 2005; Mohammed et al., 2011a; Yong et al., 2007). In addition, the gasification of oil palm wastes is still in the early stage of research in Malaysia (Sulaiman et al., 2011). It is therefore vital to look into ways to improve the efficiency of gasification and gas cleaning for the gasification of biomass oil palm kernel shells, which are part of the objectives in this project.

2.6.1 Gasifier

The gasifier is the reactor in which the conversion of a feedstock into fuel gas takes place. Gasifiers can be classified based on the flow pattern between the gas and the biomass, the method of contact between the fuel and gas, and the heating mode used. The major types of gasifiers are fixed bed and fluidised bed.

Fixed bed gasifier has a stationary reaction zone, typically supported by a grate and is usually fed from the top (Cheng, 2010). Fixed bed reactors are subdivided into updraft and downdraft gasifiers. The updraft gasifier has the simplest design and can be constructed of carbon steel shells with a grate at the bottom (McKendry, 2002). An air manifold is used to feed the air through the grates at the bottom. The biomass is introduced at the top of the gasifier and supported on the grate while air is taken in through the grate openings at the bottom and leaves with the syngas at the top (Balat et al., 2009; Zhang et al., 2010). Figure 2.8 shows the various processes taking place in an updraft fixed bed gasifier. Some features of an updraft gasifier include high amounts of tar, low amounts of ash and dust in the gas (Balat et al., 2009; McKendry, 2002). The advantages of updraft gasifier are that the gasifier design is simple and involves low capital costs; the gasifier is also able to handle biomass with

a high moisture and high inorganic content and it is a proven technology (Bridgwater, 1995). The primary disadvantage of updraft gasification is that the syngas contains high amount of tar which requires extensive gas cleanup before utilising for engine, turbine or fuel synthesis (Anis and Zainal, 2011).

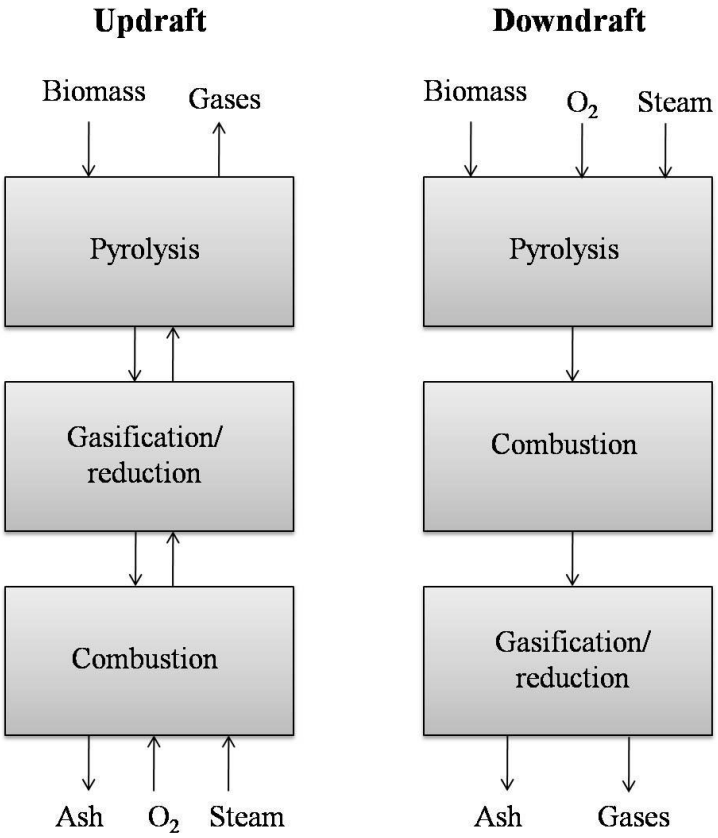

Figure 2.8 Comparison of the zones in an updraft and downdraft gasifier (Cheng, 2010)

Downdraft gasifiers are more complex because it is constructed using two concentric shells (Cheng, 2010). The biomass is fed from the top and the gas leaves at the bottom. The zones of the updraft and downdraft gasifiers are the same but in different orders as shown in Figure 2.8 (Cheng, 2010). The gas contains low amount of tar because the long-chained molecules are broken down when the gas is vented through the combustion zone; however, high amounts of ash and dust can still be found, in contrast with updraft gasifier (McKendry, 2002; Zhang et al., 2010). Owing to the low tar content in the gas, minimal gas cleanup is required; hence this gasifier is generally favoured for small-scale electricity generation with an internal

combustion engine (Bridgwater, 1995). To perform biomass gasification in a downdraft gasifier, the moisture content in the biomass should be less than 25% and the size of the biomass should be uniformly sized between 4 and 10 mm, a more stringent fuel requirement compared to updraft gasifier and this has become one of the disadvantages associated with downdraft gasification due to higher pre-treatment costs (Cheng, 2010; Quaak et al., 1999). In addition, the gas exit temperatures are also significantly higher than that from an updraft gasifier, therefore a secondary heat recovery system and flue gas cleanup will be required (Quaak et al., 1999).

2.6.2 Biomass Pellets for Gasification

In order to maximise energy conversion from biomass, it is important to utilise the biomass efficiently. Gil et al. (2010) highlighted that combustion processes of biomass materials are complicated for three main reasons. Firstly, the fuel may have a highly complex chemical and physical composition. Secondly, its combustion may take place in an uncontrolled environment and thirdly, the moisture content, density and heterogeneity of the biomass have a negative effect on the efficiency of combustion. Densification of biomass materials would contribute to improving their behaviour as a fuel by increasing their homogeneity. The fabrication of biomass pellets has attracted increasing interest and pelletised biofuel is rapidly becoming an important renewable source of energy production (Larsson et al., 2008).

The use of any biomass for conversion to energy will be affected by its characteristics such as (1) moisture content, (2) proximate analysis, (3) ultimate analysis, (4) heating value, (5) bulk density and (6) alkali metal content (Kirubakaran et al., 2009). Moisture content in the biomass has a significant impact on the conversion process. High moisture content will reduce the temperature achieved in the oxidation zone, resulting in incomplete cracking of the hydrocarbons released from the pyrolysis zone (Demirbas, 2007; Zhang et al., 2010). Increasing the moisture from 0% to 40% was found to decrease the heating value in MJ/kg by about 66% (Cheng, 2010). In gasification, some moisture is desirable for the production of hydrogen which will increase with higher moisture content in the biomass (McKendry, 2002). However, decreasing the moisture content beyond 30% gives

only marginal improvements in overall efficiency (McKendry, 2002). Oil palm residues have moisture content on a wet basis of about 15% to 63% (Quaak et al., 1999). The proximate and ultimate analyses of oil palm residues are summarised in Table 2.1 and Table 2.2.

The bulk density and uniformity of a biomass is an important characteristic that affects transportation costs, size of fuel storage and handling equipment (Gil et al., 2010). Irregularity in biomass sizes can lead to technical challenges in gasification as oversized biomass materials may prevent the feed from moving down smoothly and fine biomass materials may clog and damage the gasification equipment (McKendry, 2002).

It is therefore vital to understand the characteristics of palm kernel shells for the optimum design of pellets that can maximise energy conversion in biomass gasification. Using palm kernel shells as feedstock for pyrolysis to increase bio-oil yield (Islam et al., 1999; Kim et al., 2010; Li et al., 2007) had been studied before but these investigations were based on fluidised bed gasification with palm kernel shells as wholes rather than in pelletised form.

2.6.3 Gas Cleanup

Before using the syngas for other applications, it has to be cleaned to remove contaminants. Typical contaminants in syngas and their potential problems are summarised in Table 2.4 (Bridgwater, 1995).

Contaminant	Problems	Cleanup method
Tars	Deposits on pipes, clogging of equipment, hinders removal of particulates	Tar cracking, tar removal
Particulates	Accumulation on engine parts, erosion of equipment	Filtration, scrubbing
Alkali metals	Corrosion of filters, turbine blades, catalyst deactivation	Cooling, condensation, filtration, adsorption
Nitrogen compounds	Environmental emissions	Scrubbing, selective catalytic reduction
Sulphur, chlorine compounds	Environmental emissions, corrosion	Lime or dolomite scrubbing or absorption

Table 2.4 Typical contaminants in syngas, problems and cleanup processes (Bridgwater, 1995)

One of the main problems in utilising syngas is the high amount of tar in the gas which require removal if engines, turbines or compressors are to be used to process the gas (Bridgwater, 1994). Biomass volatises as it thermally decomposes and the volatised materials can undergo further decomposition to permanent gases (CO, CO_2, H_2, light hydrocarbons), or it can undergo dehydration, condensation and polymerisation reactions to form tar. Tar is a complex mixture of condensable hydrocarbons, which includes single ring to 5-ring aromatic compounds along with other oxygen-containing hydrocarbons and complex polyaromatic hydrocarbons (PAH) (Devi et al., 2002). It has a molecular weight greater than benzene and its actual composition is complex and dependent on the gasifier operating conditions (Cheng, 2010). The continual build-up of tar present in the syngas can cause blockage and corrosion in downstream equipment, and reduce overall efficiency of the gas yield (Anis and Zainal, 2011). Internal combustion gas engines can tolerate tar content up to 50-100 mg/Nm^3 while gas turbines work better when tar content is less than 5 mg/Nm^3 (Milne et al., 1998).

Tars can be removed by physical or chemical methods. Physical methods involve cooling the syngas in a condenser on the outside which causes the tar to condense on the inside and drained out from the bottom. Tar can also be removed by cooling the gas by spraying water into the gas stream with a venturi scrubber which causes the tar to condense into water droplets. The resulting wastewater stream then requires treatment before disposal. However, these methods were reported to be poorly efficient and treatment may be too costly (Bridgwater, 1995).

Another way to remove tars is through thermal cracking. Biomass tars are refractory to cracking via thermal treatment with high temperatures of 1000-1300°C (Bridgwater, 1994; Depner and Jess, 1999; Quaak et al., 1999). This can be done by high temperatures in the hearth zone of a fixed bed gasifier and/or increase the gas residence time. Thermal cracking is simple to control and involves low cost. However, thermal cracking alone is lowly efficient and subjected to lower heating value (LHV) losses (Belgiorno et al., 2003).

Catalytic cracking is a form of chemical method for tar removal by converting the tar into light combustible gases in a bed of catalyst, such as dolomite or nickel at high temperatures, usually around 800-900°C (Belgiorno et al., 2003; Bridgwater, 1995). Catalytic processes can operate at much lower temperatures compared to thermal processes, alleviating the need for expensive alloys for reactor construction (Belgiorno et al., 2003). The biggest advantage of this method is that no waste streams are produced that require treatment before disposal and the LHV remains unchanged. However, costs are involved to construct the catalytic cracking unit for the system and cracking process may be difficult to control (Belgiorno et al., 2003).

To remove other contaminants such as dust and particulates from syngas, physical methods such as cyclones, barrier filters and electrostatic precipitators can be used (Anis and Zainal, 2011). However, tars still pose the greatest challenge to gas cleanup due to its impact on downstream equipment and syngas utilisation hence it is worth looking into efficient methods that reduce tar. Moreover, elimination of tar by a suitable and cheap method will enhance the economic viability of biomass gasification.

2.6.4 Catalytic Cracking

There are several methods to remove tar: (1) scrubber, (2) thermal cracking and (3) catalytic cracking. The interest on the catalytic cracking in biomass gasification has grown over the past three decades (Mohammed et al., 2011b; Xu et al., 2010).

Catalysts are used in two main ways in a gasification system: (1) to improve the quality of the product gas by cracking tars that result from the incomplete gasification of pyrolysis products and (2) to improve the quality of the product gas in terms of composition to allow for more efficient and cost effective synthesis of higher value products, for example changing the ratio of carbon monoxide to hydrogen (Lv et al., 2007; Xu et al., 2010). The selection criteria for the catalyst should preferably fulfil the following points (Sutton et al., 2001): (1) effective in removing tar, (2) capable of reforming methane if the desired product is syngas, (3) provide a suitable syngas ratio for the intended process, (4) inexpensive, (5) strong, (6) easily regenerated and (7) resistant to deactivation.

The catalysts may be incorporated in the gasification reactor (primary catalysts) or added as a secondary process (secondary catalysts). Primary catalysts can be added directly into the gasifier with the biomass prior to gasification via wet impregnation of the biomass or dry mixing with it. Primary catalysts have the main purpose of reducing tar content but little effect on the conversion of methane and C_{2-3} hydrocarbons in the product gas (Sutton et al., 2001). They operate at the same conditions as the gasifier and are usually non-renewable. Hence primary catalysts that are selected should consist of cheap disposable material. Secondary catalysts are placed in secondary reactors downstream from the gasifier; therefore they can operate at conditions different from the gasifier. When the raw gas passes over the catalyst, hydrocarbons may be reformed on the catalyst surface with either steam or carbon dioxide to produce additional carbon monoxide and hydrogen. Secondary catalysts thus have the advantage of synthesising more valuable products in the downstream catalytic process. Figure 2.9 shows the catalytic processes in a gasification system (Bridgwater, 1994).

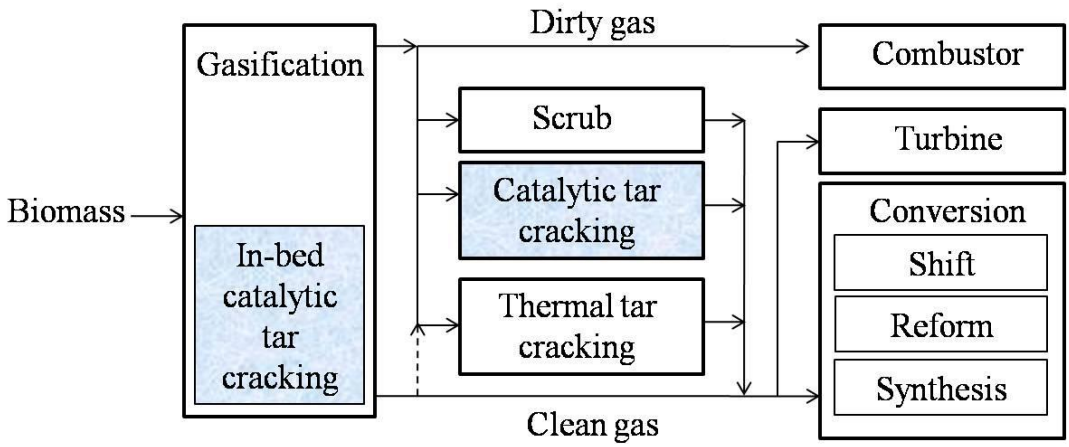

Figure 2.9 Catalytic processes in gasification (Bridgwater, 1994)

There are three main groups of catalysts used in catalytic cracking to reduce tar in syngas: (1) naturally occurring catalysts, (2) alkali metals and (3) nickel-based catalysts. Table 2.5 summarises some common catalysts used (Wang et al., 2008).

Catalyst group	Examples	Main advantages	Technical challenges
Naturally occurring catalyst	Dolomite, olivine, clay, zeolite	Cheap	Moderate reforming efficiency, easily eroded and broken
Alkali metal	KOH, $KHCO_3$, K_2CO_3, $NaCO_3$	Highly reforming efficiency, increased hydrogen in syngas	Increased plugging and deactivation of other metal catalysts at high temperatures
Nickel-based catalyst	NiO/Al_2O_3, $Ni/CeO_2/Al_2O_3$	Highly reforming efficiency, increased hydrogen in syngas	Expensive, metals are easily deactivated by coke, poisoned at high temperatures, require hot-water-resistant support materials

Table 2.5 Common catalysts for tar reduction in syngas (Wang et al., 2008)

Natural dolomite is the most popular catalyst used for tar elimination (Delgado et al., 1997; Perez et al., 1997; Rapagna et al., 2000). Apart from being a cheap disposable catalyst, it is successful in significantly reducing the tar content in syngas. According to Delgado et al. (1997), dolomite used in fixed bed biomass gasification at a reaction temperature of 910°C could convert 98% of tar. When catalysts Ni/zeolite were used in fixed bed biomass gasification at a reaction temperature of 750°C, tar conversion was 99% (Buchireddy et al., 2010).

2.6.5 Zeolite

Although dolomites are cheap, they are not active for reforming the methane present in the product gas; hence dolomites are not suitable catalysts if syngas is required (Sutton et al., 2001). The main function of dolomite is to act as a guard bed for the removal of heavy hydrocarbons prior to the reforming of the lighter hydrocarbons to produce a product gas of syngas quality. As such, another common and naturally occurring catalyst, zeolite, was selected as the catalyst for gas cleanup in this project. Currently, the research on using zeolite as a catalyst for gasification of oil palm kernel shells is still very limited.

Zeolites are crystalline silicates and aluminosilicates linked through oxygen atoms, producing a three-dimensional network containing channels and cavities of molecular dimensions (Corma, 2003) as shown in Figure 2.10 (Weitkamp, 2000). Figure 2.11 shows the physical appearance of white zeolite powder. Zeolite have particle sizes ranging between 0.1 to 1.1 μm (Martinez and Lopez, 2005; Ren et al., 2010). Zeolites are acidic catalysts and available in various natural or synthetic forms. They are classified according to their compositions and structure. The advantages of zeolites are related to their acidity, better thermal/hydrothermal stability, better resistance to nitrogen and sulphur compounds, tendency toward low coke formation, and easy regenerability (Buchireddy et al., 2010). In addition, zeolites had been successfully applied in fluid catalytic cracking (FCC) units (Al-Khattaf, 2002). However, the main disadvantage is their rapid deactivation due to coke formation (Anis and Zainal, 2011).

Figure 2.10 Structure of HZSM-5 zeolite from (a) top view (b) side view (Weitkamp, 2000)

Figure 2.11 Physical appearance of HZSM-5 zeolite powder

In the case of tar reduction, various commercially available zeolites were tested by some researchers (Buchireddy et al., 2010; Horne and Williams, 1995; Olazar et al., 2008; Radwan et al., 2000; Vitolo et al., 2001). Olazar et al. (2008) investigated the effect of HZSM-5, H-Y and H-beta zeolites on scrap tyre pyrolysis under fast heating conditions and found that HZSM-5 was more efficient for gas formation and increasing the yield of gases. Buchireddy et al. (2010) investigated the catalytic activity of ZY, Zβ and ZSM-5 zeolites on tar removal and found that zeolites with larger pore size and higher acidity had better catalytic activity. Chin et al. (2010) studied the effect of HZSM-5 zeolite on tar reduction for palm shell gasification and achieved 75% reduction in tar compared to the non-catalytic process.

HZSM-5 zeolite can be obtained from the thermal decomposition of the NH_4-exchanged form of ZSM-5 via calcination (Koningsveld and Koegler, 1997; Nayak and Choudhary, 1983). HZSM-5 was used in the pyrolysis of biomass and helped increased the aromatic fraction in the bio-oil (Carlson et al., 2009). The acid sites of HZSM-5 promote a series of dehydration, decarbonylation, decarboxylation, isomerisation and dehydrogenation reactions, converting the oxygenated products generated in the pyrolysis process into more stable aromatic compounds (Perego et al., 2011). The effect of HZSM-5 on tar reduction for palm shell gasification had been investigated by Chin et al. (2010). The catalyst was added into the gasifier with the palm shells.

2.7 Conclusion

The biomass palm kernel shell is of great potential as a renewable and sustainable energy source in Malaysia due to its abundance, high carbon content and ability to reduce carbon emissions into the atmosphere. Biomass palm kernel shells can be converted to useful energy via biomass gasification. However, the shape and size heterogeneity of raw palm kernel shells often leads to difficulties in gasification and transportation processes (Chok et al., 2010; Lu et al., 2010). To resolve this problem, pelletised palm kernel shells has been proposed to solve the challenges in gasification. Characterisation of its mechanical properties is a major focus of this thesis.

In addition, a major problem associated with biomass gasification is the presence of contaminants such as tar in the gaseous products which, if not removed, would damage the engine or gas turbine and incur high maintenance costs. The use of catalysts is the most effective approach in order to reduce the tar content in the syngas (Sutton et al., 2001; Tomishige and Asadullah, 2005). Thus the incorporation of catalyst into the pellets has also been studied.

3 Experimental Procedures

3.1 Introduction

In this section, the preparation of powder from raw palm kernel shells and the production of pellets based on varying processing parameters using the universal testing machine; followed by crush test procedures will be outlined and explained. The experimental setup for gasification and descriptions on data collection steps will be presented.

3.2 Preparation of Materials

Raw oil palm kernel shells were donated by Bintulu Lumber Development Sdn. Bhd., Malaysia. The shells were milled (Disk mill FFC-23, China) at a rotational speed of 5800 rpm into powder form. The resulting powder was passed through a 1.2 mm sieve screen and only particles with sizes lower than 1.2 mm were collected. Binders will not be added to the palm kernel shell powder in this project so as not to compromise the combustion characteristics of the pellet and conflict with the objective on gasification studies.

The powder was sieved using a sieve shaker (Endecotts Sieve Shaker EFL2000, UK) and woven wire mesh sieves of nominal aperture sizes 75 μm, 150 μm, 300 μm and 425 μm. Sizes of oil palm kernel shell powder – 75-150 μm, 150-300 μm and 300-425 μm were used for the experiments.

The powder was dried in an oven (Memmert Universal Drying Oven UNB 500, Germany) at a temperature of 120°C for 5 hours until the water activity level of 0.3 as measured using a water activity meter (Decagon Aqualab Lite, US) was achieved. The powder was then transferred to an enclosed chamber for at least 24 hours prior to any testing. A relative humidity of 11% in the chamber was achieved by using

saturated lithium chloride solution (Greenspan, 1977). These steps were taken to ensure that the initial conditions of the powder were consistent in all experiments.

3.2.1 Measurement of True Density of Powder

The true densities of each powder size were determined using a 100 ml pycnometer (Technico, England). Water was found not to be suitable as the working liquid because the powder tended to agglomerate and float on water. Instead, kerosene was used as the floating tendency was reduced. The powder was added into the pycnometer and its mass was recorded. Kerosene was then added into the pycnometer and the volume occupied by the powder was calculated. The density of kerosene was separately determined by a hydrometer (Zeal, England). Finally, the true density of the powder was calculated.

3.2.2 Microscopy and Particle Size Analysis of Powder

Slide samples of the powders were viewed using Leica, EZ4D stereo microscope with a zoom magnification of 35×. Micrographs of the samples were captured using a camera attached with the microscope.

750 g of powders were sieved using the sieve shaker for 15 to 20 minutes and the weight of each powder size range was measured using a weighing balance. This procedure was repeated for three batches of powders to obtain data for weight analysis.

Figure 3.1 shows the overall weight distribution of the various particle sizes obtained after sieving. The highest weight fraction was for particle size >425 μm. However, palm kernel shell powder with size >425 μm was found to be unsuitable for compaction as the particles were too coarse and hard to be compressed into pellets. Particle size <75 μm had the lowest weight fraction and the amount was insufficient for experimental use. Particle sizes 75-150 μm, 150-300 μm and 300-425 μm were therefore selected for further experiments due to their ease of compaction and abundance.

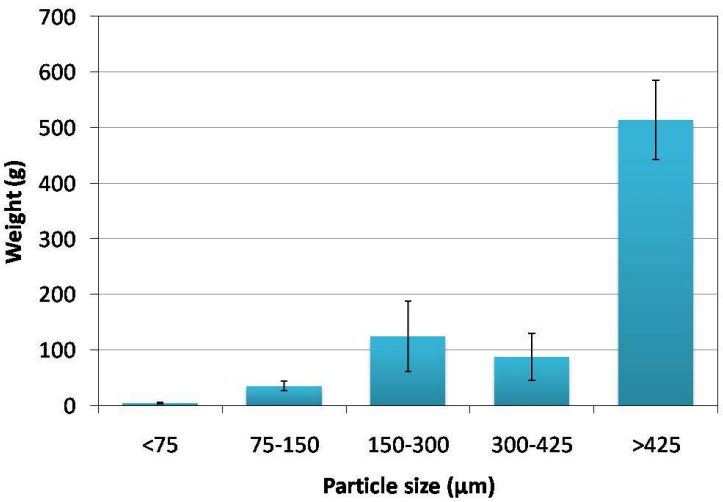

Figure 3.1 Overall weight distribution of various particle size range after sieving

3.3 Production of Pellets

The individual pellet produced was cylindrical in shape with a nominal diameter of 6 mm, length of 6 mm and a nominal weight of 0.19 g. Each pellet was produced using a universal testing machine (Lloyd LR10K, UK) with a load cell of 10 kN. The compaction process was performed using a set of custom-made stainless steel die. The die comprised a detachable base, a die case and a plunger. The die case had an outer diameter of 50 mm and a cylindrical cavity of a 6 mm diameter. The cylindrical plunger was 20 mm in length and 6 mm in diameter. The die assembly and components are shown in Figure 3.2. The compaction speed, compaction pressure and hold time were independently set by the machine's control unit.

The same universal testing machine was used to eject the pellet. The detachable base was removed and the remaining assembly was placed on the ejector base, which collect the pellet after the ejection.

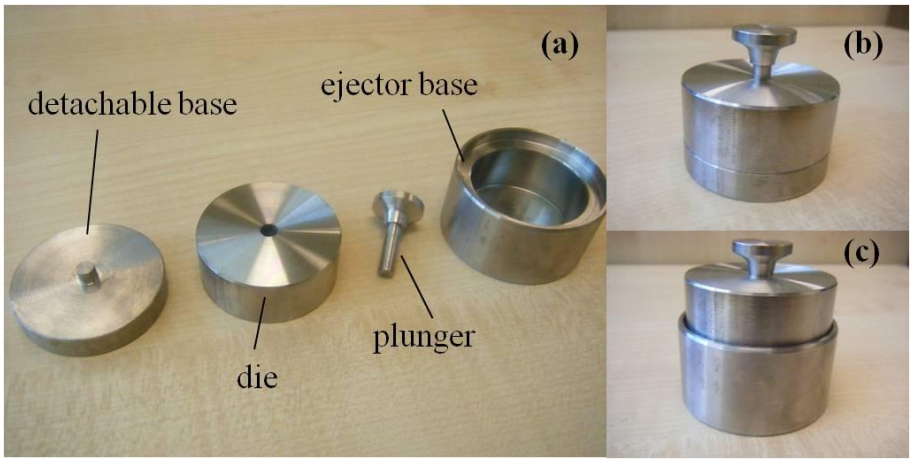

Figure 3.2 (a) Components of die assembly (b) Compaction die assembly (c) Ejection die assembly

The weight of each pellet was measured after ejection on an analytical balance (Ohaus SPS202F, US). In addition, the final length of the pellet *L* was also measured using a vernier calliper immediately after the pellet was ejected.

3.3.1 Water activity

To ensure that the palm kernel shell powder remained at the same level of moisture before tests were conducted, a preliminary drying test was carried out. Two batches of powder were dried in separate ovens (Memmert Universal Drying Oven UNB 500, Germany) for 10 hours; one at 60°C and the other at 120°C. The temperatures selected were less than 140°C such that the melting point of lignin (140°C) was not exceeded (Mani et al., 2006). Lignin is present in biomass materials and when the biomass is heated, lignin becomes soft and melts. Since the powder was required to make the pellets, the melting of lignin was not desirable at this stage.

The water activity a_w of the powder was measured using a water activity meter (Decagon, Aqualab Lite). The meter with an accuracy of ±0.015 and a range from 0 to 1.000 was calibrated with 0.5M of sodium chloride (NaCl) solution before measurement. Water activity of the powder was measured every 1 hour interval during drying in the oven. Three samples of 1 g powder were extracted from each batch for every water activity measurement.

Figure 3.3 shows the water activity in the powder at different time intervals during the drying process. It is noted that the water activity of the powder at both drying temperatures reached a plateau at ~0.3 after 10 hours. As the temperature doubled, the time taken to dry the powder to the required water activity was halved. This preliminary study shows that a period of 5 hours and drying temperature of 120°C was sufficient to dry the powder for subsequent experimental tests.

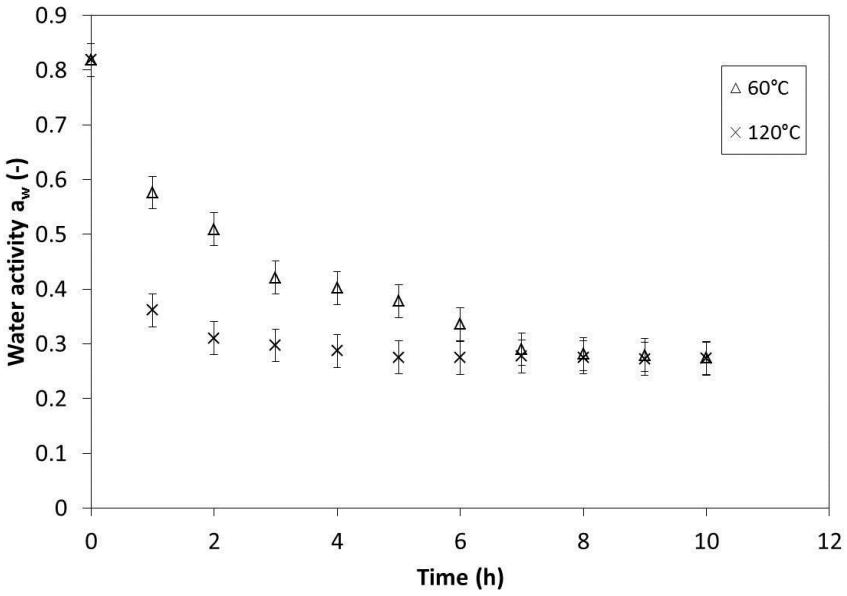

Figure 3.3 Level of water activity in powder at different drying time intervals

3.3.2 Compaction Pressure

The compaction of the pellets was carried out at 25±2 °C and in an environment with relative humidity of 60%. The three powder size ranges (75-150 µm, 150-300µm and 300-425 µm) were used to study the effect of compaction pressure. Each powder size was compacted using the universal testing machine at pressures ranging from 130 to 200 MPa in the absence of lubrication. The universal testing machine was preset to compaction forces ranging from 3800 to 5800 N to achieve this range of compaction pressures. Equation (2.8) was applied to translate the compaction forces to compaction pressures. The compaction speed and hold time were preset at 100 mm/min and 3 s respectively. After the pellet was formed, it was ejected from the die at a speed of 10 mm/min and subjected to either compressive or diametrical compression tests at a speed of 10 mm/min. Force-displacement data were recorded

by the testing machine itself. The relaxed or final length of the ejected pellet was measured with a pair of vernier callipers in order to determine the elastic recovery according to equation (2.6) and the mass of the ejected pellet was measured on an analytical balance. Equation (2.4) was used to calculate the porosity of the pellet. The strengths of the pellets compacted with different compaction pressures were plotted against their corresponding porosities to observe if the trend followed the Ryshkewitch-Duckworth empirical model. Each compact was prepared in five replicates for each pressure value.

3.3.3 Compaction Speed and Hold Time

The effect of compaction speed was studied using the three different particle sizes to make pellets at a compaction pressure 164 MPa with zero holding time. The compaction speed was varied from 1 mm/min to 100 mm/min. Thereafter, the formed pellet was ejected at a speed of 10 mm/min and subjected to compression tests to measure the strength. The speed of the piston was set at 10 mm/min for the compression test. Three replicates were taken for each set of test.

The effect of hold time during compaction was studied at a compaction pressure of 164 MPa and compaction speed of 100 mm/min at different holding times ranging from 0 to 300 s.

3.3.4 Humidity and Storage Time

The initial storage condition of the powder was at a relative humidity of 11%. Pellets produced under the same process conditions (compaction pressure 188 MPa, compaction speed 100 mm/min and hold time 3 s) were stored at humidity levels 11%, 43% and 57% for a period of 30 days. 43% and 57% humidity levels were achieved using saturated potassium carbonate and sodium bromide solutions (Greenspan, 1977). Pellet strength was tested immediately after production and after 1, 5, 15 and 30 days of storage at a piston speed of 10 mm/min and 5 mm displacement. The length of each pellet was also measured with vernier calipers to

determine the degree of elastic recovery. Three replicates for each crush test were conducted.

3.4 Mechanical Strength Test

The same universal testing machine (Lloyd LR10K, UK) was used to perform the compression tests. Polished steel plates (Figure 3.4a) were used as the compression platens. The tests were conducted at a constant speed of 10 mm/min. The compressive strength was determined in the axial direction, i.e. parallel to the cylindrical axis (Figure 3.4b). The tensile strength was determined by subjecting the pellet to diametrical compression (Figure 3.4c), i.e. perpendicular to the cylindrical axis. Figure 3.5 shows the orientation of a pellet during axial compression and diametrical compression tests. Figure 3.6 shows a detailed view of the outcomes from the compression tests.

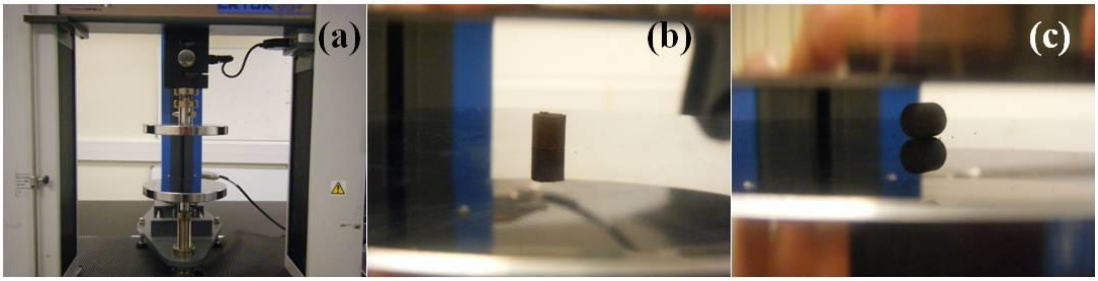

Figure 3.4 (a) Uniaxial press and experimental assembly (b) Axial compression test (c) Diametrical compression test

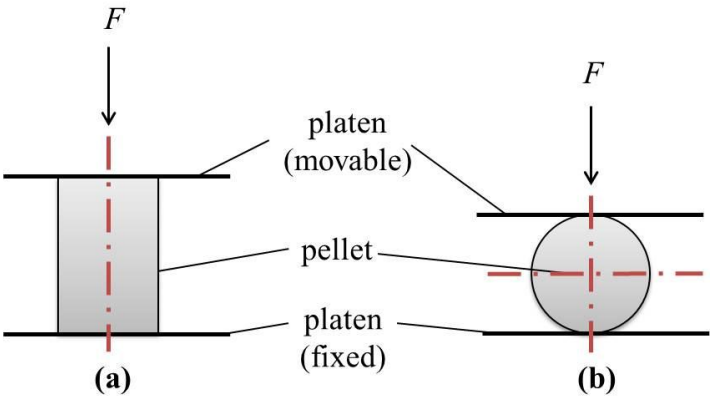

Figure 3.5 Orientation of the pellet during (a) axial compression test and (b) diametrical compression test

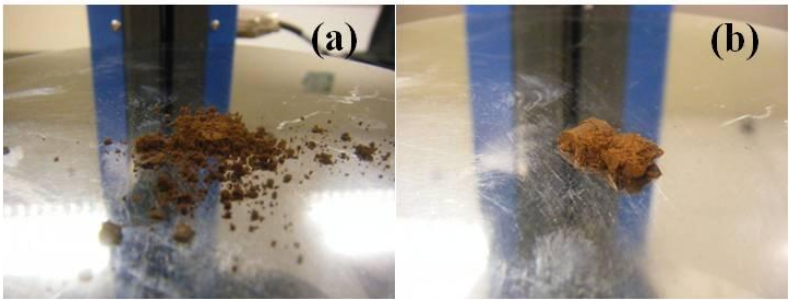

Figure 3.6 Views of pellet after breakage (a) axial compression (b) diametrical compression

The compressive strength was calculated by equation (2.8) and the radial tensile strength was determined by equation (2.9).

3.5 Binary Pellets Compaction

ZSM-5 (Zeolite Socony Mobil-5) zeolite was selected as the catalyst for catalytic cracking of tar in the gasification of oil palm kernel shell pellets. ZSM-5 is a high-silica synthetic zeolite catalyst that is widely used in the petroleum industry as a heterogeneous catalyst for hydrocarbon isomerisation reactions. It has a pore size of 5.1-5.6 Å (Sadeghbeigi, 2000). The shape selectivity of ZSM-5 allows preferential cracking of long-chain, low octane normal paraffin, as well as some olefins, in the gasoline fraction (Sadeghbeigi, 2000). Due to its low cost, using ZSM-5 is claimed to be the cheapest way to achieve octane enhancement with the additional advantage of the formation of C_3-C_5 alkenes for alkylate feed and oxygenate formation and widely used in industries (Olah and Molnar, 2003).

The binary mixtures of zeolite and palm kernel shell (PKS) powder (size 150-300 μm) were mixed in varying weight percentages. The zeolite used was ZSM-5 (CBV 3024E, supplied by Zeolyst International, USA). It has a SiO_2/Al_2O_3 mole ratio of 30 and its nominal cation form is ammonium. HZSM-5 zeolite was obtained from the calcination of ZSM-5 zeolite at a temperature of 600°C for 4 hours in a furnace. This was done to activate the catalytic properties of zeolite (Kunkeler et al., 1998). After calcination, the zeolite was stored in a humidity chamber at a humidity level of 11% for at least 24 hours prior to mixing.

The weight percentage of zeolite in each binary mixture was varied between 5-50% (i.e. 5% Zeolite + 95% PKS, 10% Zeolite + 90% PKS, 15% Zeolite + 85% PKS, 25% Zeolite + 75% PKS and 50% Zeolite + 50% PKS). The percentage of zeolite incorporated in the binary mixture in this study was selected to be below 50% because it was not desired to include high amounts of catalyst during gasification due to high costs. The true densities of binary mixtures palm kernel shell and zeolite were measured using a 100 ml pycnometer (Technico, England).

10 g of each formulation was prepared and mixing was performed with a kitchen blender (Pensonic blender, PEN-PB330). The binary mixtures were stored in a humidity chamber with humidity level of 11% for at least 24 hours prior to pelletisation. The pellets with varying formulations were compacted at different compaction pressures ranging from 135 to 198 MPa. Pellets with 100% zeolite composition were also compacted at different compaction pressures ranging from 135 to 198 MPa. The individual pellet produced was cylindrical in shape with a nominal diameter of 6 mm, length of 6 mm and a nominal weight of 0.19 g. Each pellet was produced using a universal testing machine (Lloyd LR10K, UK) with a load cell of 10 kN. The compaction was made at the speed of 100 mm/min with a 3 s hold time at an ambient temperature of 25±2°C. The same universal testing machine was used to eject the pellet at a speed of 10 mm/min. The weight of each pellet was measured after ejection on an analytical balance (Ohaus SPS202F, US). In addition, the final length of the pellet L was also measured using a vernier calliper immediately after the ejection. The compact was prepared in three replicates for each formulation. The compression test was conducted immediately after the production of each pellet.

The same universal testing machine (Lloyd LR10K, UK) was used to perform compression tests on the pellets. The tests were done at a constant speed of 10 mm/min. Only axial compression tests were performed to determine the compressive strength of the pellets. The strengths and corresponding porosities were calculated according to equation (2.8) and equation (2.4) respectively to determine the Ryshkewitch-Duckworth relation between the strength and porosity for each binary mixture.

3.6 Gasification

3.6.1 Experimental Setup

Gasification studies were conducted in a laboratory-scale updraft fixed bed reactor (Chin et al., 2010). A laboratory-scale updraft fixed bed reactor was used due to its simple design and fabrication on small-scale. The experimental setup consisted of two parts: (1) gasifier and (2) tar collection section. Figure 3.7 shows a schematic of the overall experimental setup for gasification. The gasifier was designed for operation under atmospheric or pressurized conditions. The test facility consists of the gasifier and the liquid trap for the condensation and collection of tar. The fixed bed gasifier with an internal diameter of 60 mm and height of 280 mm was made of stainless steel 304 and an external heat source was located at the dense bed zone. The gasifier was insulated with ceramic fiber insulation (supplied by Progresif Kukuh Sdn. Bhd., Malaysia) to minimise heat loss from the reactor. Two K-type thermocouples (T1 and T2) were installed across the reactor: the probe T1 in the dense bed zone, defined as the gasification reaction zone (at a height of 20 mm above the distributor) and probe T2 in the freeboard zone (at a height of 140 mm above the distributor). The pelletised feedstock was added manually. Air and nitrogen were supplied by a compressor. Air was chosen as the gasification agent in this project due to its low cost and availability. As the gasification system did not have a steam reforming component, the production of syngas with high hydrogen content was not looked into. Rather, the focus was on the gas cleaning stage (reducing tar from the gas) and the gasification efficiency of the pellets.

The gaseous products from the gasification were channeled to the liquid trap to separate the condensed tar from the gas. For tar sampling, the method developed by Hasler and Nussbaumer (2000) was adopted because this method is applicable to atmospheric fixed bed gasifiers and allows for a longer duration of sampling for gas contaminants. The tar collection section comprised 4 condenser or absorption traps (250 ml each) filled with 200 ml of distilled water. The four condenser traps were immersed in a water bath at room temperature.

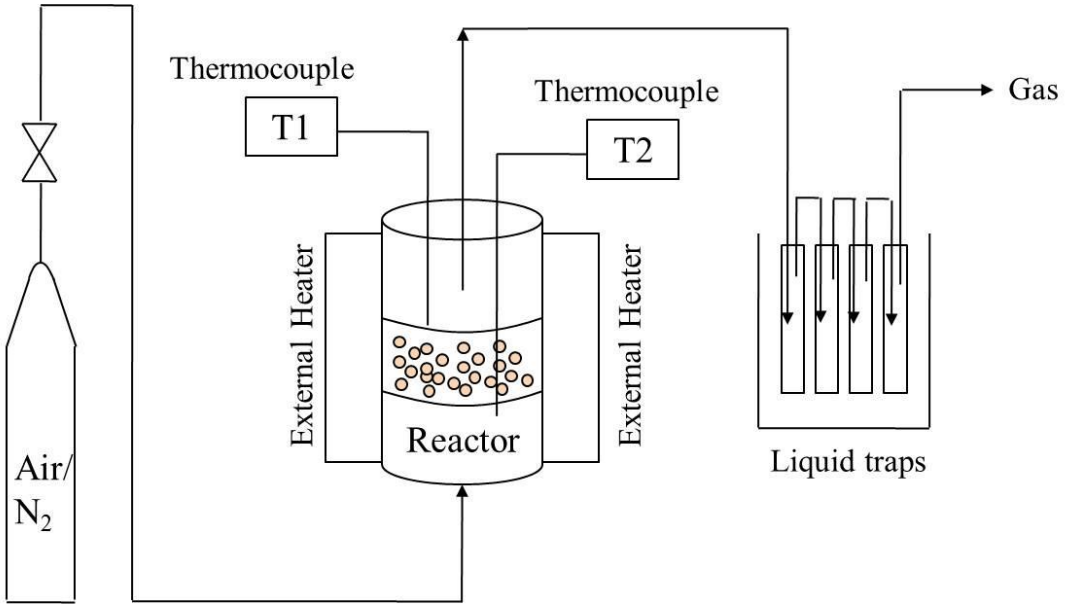

Figure 3.7 Schematic diagram of the experimental setup for gasification

3.6.2 Preparation of Feedstock

The feedstocks for the gasification experiments were oil palm kernel shells, powder and pellets. Oil palm kernel shells powder was prepared and stored according to the method described in Section 3.2. The powder size selected for use was 150-300 μm. To prepare the palm kernel shells as the feedstock, the shells were first sieved into the following size range 2.36-4.75 mm, dried and stored according to the method described in Section 3.2.

A 25-ton XLP-series hydraulic press (Enerpac, USA) was used to produce palm kernel shell pellets as feedstock. The powder was compacted at 195 MPa and each pellet had an aspect ratio of 1. The pellets were stored in fixed humidity chambers with a humidity level of 11% for at least 24 hours prior to gasification.

The bulk density of each feedstock was measured by pouring the feedstock into a 50 ml or 50 cm^3 measuring cylinder. The mass of the feedstock that occupies the volume of 50 cm^3 was then weighed by an analytical balance (Ohaus SPS202F, US). The bulk density was calculated by dividing the mass of the feedstock by the

occupied volume of 50 cm^3. 5 replicates were performed for each feedstock to determine the bulk densities.

3.6.3 Experimental Procedures

At the start of each experimental run, the pellets were fed manually into the gasifier and the reactor was heated up by the external heat source. At a temperature of 250°C, the palm kernel shell biomass started to decompose to volatile gases and solid char. At this point, the air and nitrogen compressors were turned on to force the air and nitrogen through the distributor into the reactor. Air and nitrogen were introduced at a gas flow rate of 5 and 3 LPM respectively, which is equivalent to 13% oxygen. The gaseous products leaving the gasifier were channeled to the 4 liquid traps whereby the tar product was trapped. The experiment was stopped five minutes after the first drop in temperature was observed. This drop in temperature corresponded to the cessation of reaction between the volatile gases and the gasification agents. The five minutes rule was observed to confirm that the drop in temperature was indeed due to the cessation of reaction between the volatile gases and gasification agents and that the temperature will no longer increase thereafter. This was applied to all gasification tests to ensure consistency. Three runs were conducted for each test.

Condensed tar from the gaseous products in the liquid traps were collected and separated from the water by filtration (Advantec filter paper, 125 mm diameter, 6 μm particle retention) and left to dry for at least 12 hours. The tar was then weighed on an analytical balance (Ohaus SPS202F, US).

The rate of conversion (R) of biomass to gaseous products, measured in g/min was calculated according to the following:

$$R = \frac{M_i - M_f}{t_g} \tag{3.1}$$

where M_i is the initial mass of the biomass (g), M_f the final mass of the feedstock remains and t_g is the time taken for gasification (min). The time taken for

gasification t_g is the time between the introduction of gasification agents to the time the experiment was stopped, five minutes after the first drop in temperature was observed.

The amount of tar (%) was calculated by:

$$\frac{m_T}{M_i} \times 100\% \tag{3.2}$$

where m_T is the mass of tar (g) and M_i is the initial mass of the biomass (g).

3.6.4 Variation of Feedstock Form

Palm kernel shells with size 2.36-4.75 mm, powder with particle size 150-300 μm and pellets compacted from powder with particle size 150-300 μm (6 mm diameter with aspect ratio 1 and compacted at 195 MPa) were used as feedstock to study their effects on the rate of conversion of biomass to gaseous products during gasification. 20 g of biomass feedstock was used for each test and all tests were run based on the experimental steps described in Section 3.6.3. The rate of conversion of biomass to gaseous products was calculated according to equation (3.1).

3.6.5 Gasification of Binary Palm Kernel Shell and Zeolite Pellets

Pellets with varied concentration of zeolite catalyst incorporated (5% zeolite-95% PKS, 10% zeolite-90% PKS and 15% zeolite-85% PKS) were used as feedstock to study the effects of the amount of catalyst on the tar amount produced and the effectiveness of the catalyst in reducing tar. The mass of the biomass was fixed at 100 g while the amount of zeolite was varied.

ZSM-5 zeolite was calcined in the furnace at 600°C for 4 hours. Nayak and Choudhary (1983) discovered that the acidity, catalytic activity and product

selectivity of the zeolites were strongly affected when the temperature was increased above 600°C. Hence the temperature for calcination of ZSM-5 was set at 600°C for a duration of 4 hours in the furnace.

The calcined HZSM-5 zeolite was mixed with palm kernel shell powder (150-300 μm) using a blender to achieve homogeneity. The mixes comprised zeolite in different percentage by weight (5%, 10% and 15%). For every concentration, the mass of the biomass palm kernel shell powder was fixed at 100 g. As such, the composition of each concentration was: 100 g palm kernel shell powder + 5.3 g zeolite (95% PKS + 5% zeolite), 100 g palm kernel shell powder + 11.1 g zeolite (90% PKS + 10% zeolite) and 100 g palm kernel shell powder + 17.6 g zeolite (85% PKS + 15% zeolite).

The pellets were compacted to a compacted porosity of 15%. To determine the compaction pressure to produce binary pellets at a desired porosity or relative density, the Heckel model (Heckel, 1961) was used:

$$-\ln \varepsilon = aP + c \tag{3.3}$$

where a is a constant that is dependent on the composition of the pellet and c is the logarithm of reciprocal porosity when $P = 0$. This method has been widely used to relate the logarithm of reciprocal porosity to the applied compaction pressure (P) (Buckner et al., 2010; Roopwani and Buckner, 2011; Veen et al., 2000).

Figure 3.8 shows the Heckel plot using the compaction pressure and porosity data from the binary compaction studies and this was used to determine the compaction pressure to obtain binary palm kernel shell and zeolite pellets at a compacted porosity of 15%. Compaction pressures of 170 MPa, 185 MPa and 199 MPa were used to compact binary pellets containing 5%, 10% and 15% zeolite respectively.

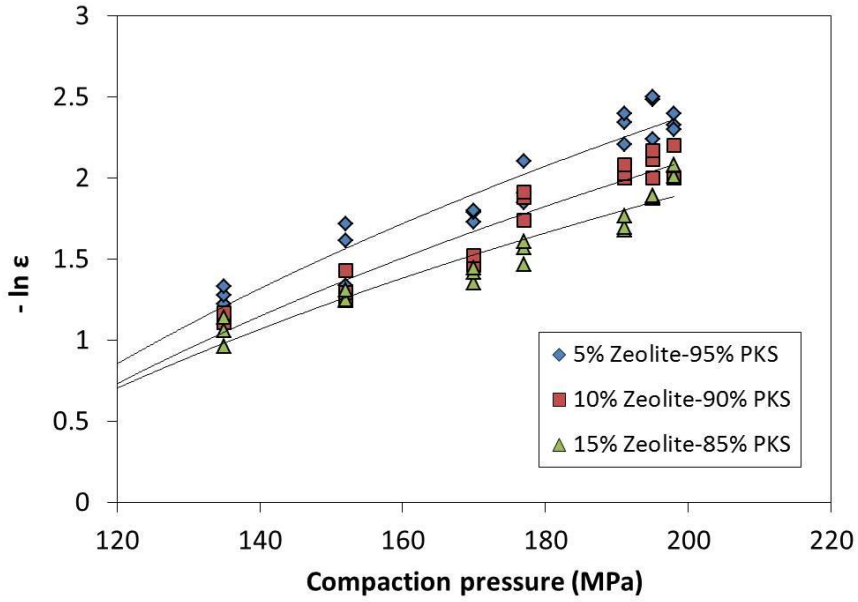

Figure 3.8 Heckel plot to relate the logarithm of reciprocal porosity during compaction to compaction pressure

A 25-ton XLP-series hydraulic press (Enerpac, USA) was used to produce the binary pellets. Each pellet had an aspect ratio of 1 and fabricated die with 15 mm diameter was used to produce the pellets. Preliminary data (not shown) showed that there was no notable difference in the strength of the pellets made from different diameter sizes.

Each pellet weighed nominally 2.97 g. The produced pellets were stored in fixed humidity chambers with a humidity level of 11% for at least 24 hours prior to gasification.

Gasification was carried out according to the same experimental procedures as described in Section 3.6.3. The ratio of the mass of tar collected to the mass of tar when pellets with 0% zeolite were gasified was calculated by the following equation:

$$\frac{m_{T_x}}{m_{T_0}} \tag{3.4}$$

where m_{T_0} is the mass of tar (g) when pellets with 0% zeolite were gasified. m_{T_x} is the mass of tar (g) when pellets with x% zeolite, where x = 5, 10 or 15, were gasified.

4 Strength and Gasification of Palm Kernel Shell Pellets

4.1 Introduction

In this chapter, the characterisation of biomass oil palm kernel shell powder in terms of true density and particle size analysis, as well as discussion on some of the factors that affect the strength of palm kernel shell pellets are reported. Both processing parameters during compaction and post-production conditions which could impact on the pellet strength were investigated. These findings could possibly be used to recommend optimum processing and storage conditions for palm kernel shell pellets in terms of compaction speed, hold time, compaction pressure and humidity conditions so as to enhance the pellet strength for handling and durability. Results from the gasification of various feedstock forms and sizes of palm kernel shell are also presented.

4.2 Characterisation of Powder and Pellet

4.2.1 Microscopy and Particle Size Analysis

Figure 4.1 shows the micrograph images of the three powders with particle size 75-150 μm, 150-300 μm and 300-425 μm. The particles of palm kernel shells were observed to be of irregular shapes and fibres (shown by the arrows) were noticeably present in the powder with size ranging from 300-425 μm as shown in Figure 4.1c.

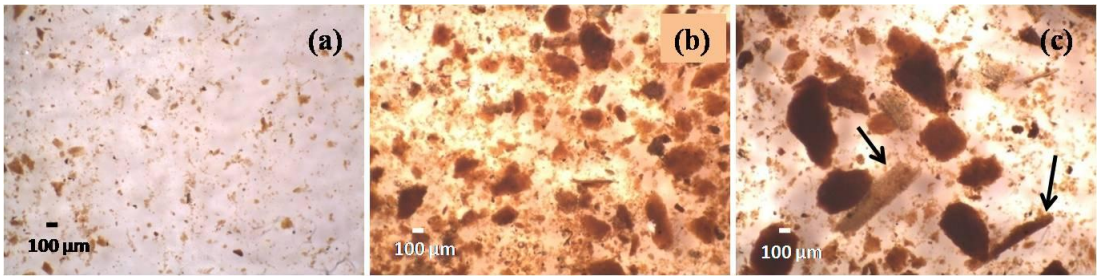

Figure 4.1 Micrographs of (a) 75-150 µm (b) 150-300 µm (c) 300-425 µm.

4.2.2 True Density of Powders

Table 4.1 summarises the true densities of the powders. The average densities of palm kernel and palm shell reported in literature (Luangkiattikhun et al., 2008) were 1.39 g/cm^3 and 1.42 g/cm^3 respectively hence the measured densities values were consistent with the literature. These densities values were used in the subsequent calculations in this work.

Sample	Measured True density (g/cm^3)
75-150 µm (A)	1.42±0.01
150-300 µm (B)	1.37±0.01
300-425 µm (C)	1.30±0.01

Table 4.1 A summary of true densities of powders measured using the pycnometer

4.2.3 Physical Appearance of Pellets

Figure 4.2 shows an optical image of the physical appearance of the pellets produced with particle sizes 75-150 µm, 150-300 µm and 300-425 µm while Figure 4.3 shows the micrograph images of the diametrical view of the pellets. It can be seen that the surface of the pellets made from the smallest particle size was smoother than the pellets made from the largest particle size. From Figure 4.2, there is noticeable difference in the physical appearance of pellets made from the three different particle sizes. The pellet made with the smallest particle size had a finer surface appearance and no chipping was observed. Chipping is a crack or flaw caused by the removal of

a small piece which occurs mostly at the edges (Ford et al., 2009). The pellet made with the largest particle size had a coarse surface and the edges of the pellet showed the most chipping. The pellet made with the medium particle size has relatively less chipping compared to the pellet made from the largest particle size. It should also be noted that since the surface of the pellet was not smooth, there could be possible errors in relaxed length measurement after the pellets were ejected from the die.

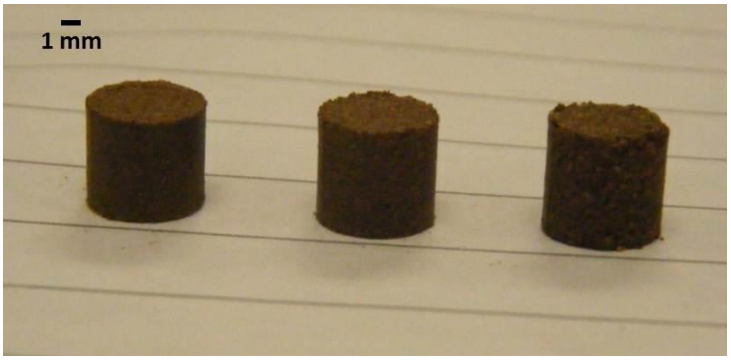

Figure 4.2 Optical image of the physical appearance of three pellets made from different particle sizes compacted at 188 MPa

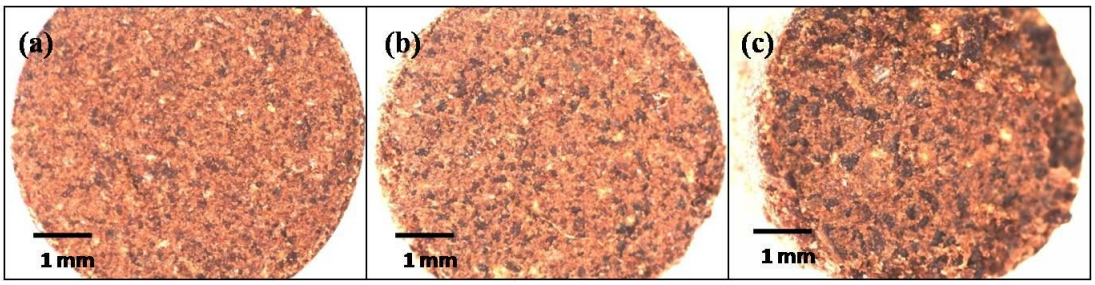

Figure 4.3 Micrographs of the diametrical view of pellets produced with particle size (a) 75-150 μm (b) 150-300 μm (c) 300-425 μm

4.3 Effect of Compaction Pressure on Pellet Strength

Figure 4.4 shows the relationship between the axial compressive strengths and the compaction pressure. The highest compressive strengths obtained were about 8.8 MPa and were similar for pellets made with particle size 75-150 μm and 150-300 μm. At the same compaction pressures, the compressive strength for pellets made with particle size 300-425 μm was evidently the lowest. A plateau in the strength

was observed at compaction pressures of approximately 190MPa although this was not evident for the pellets made with the largest particles. This plateau appears to correspond to no or near-zero porosities in the pellets during the compaction process as indicated in Figure 4.5. Some negative porosity values were obtained and this could probably be due to the deformability of the die at high compaction pressures which was not taken into account in the calculations. From a total of 24 measurements made for each particle size, the average elastic rebound of pellets made from 75-150 μm, 150-300 μm and 300-425 μm were (21±2)%, (24±3)% and (29±3)% respectively (Figure 4.7), i.e. pellets made from the largest particles exhibited the largest elastic rebound.

The radial tensile strengths of the pellets made from different particle sizes and compacted at various compaction pressures are shown in Figure 4.6. The range of radial tensile strength was between 0.07 MPa and 0.26 MPa, with the lowest values obtained for pellets made from the particle size of 300-425 μm. These radial tensile strength values were much lower compared to the compressive strengths. In addition, the radial tensile strength appeared to be increasing monotonically with increasing compaction pressures and there was an absence of a plateau at high compaction pressures.

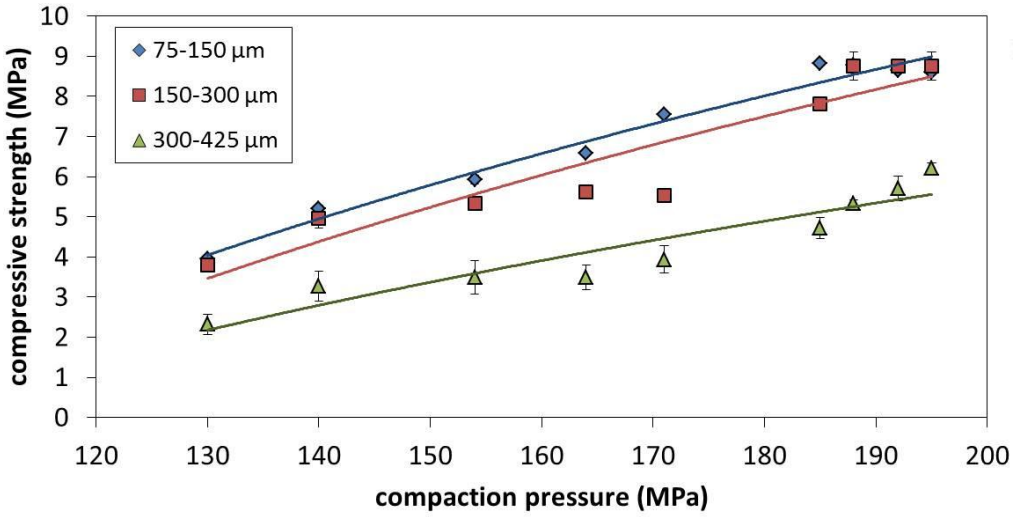

Figure 4.4 Influence of compaction pressure on compressive strength. Solid lines represent moving average of the ten data points for each particle size.

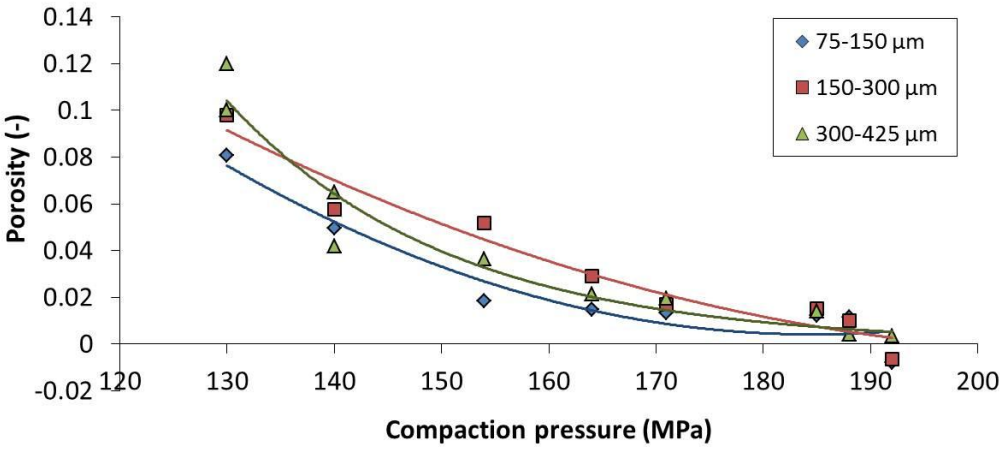

Figure 4.5 Variation of porosities during compaction with compaction pressure. Solid lines represent moving average of the ten data points for each particle size.

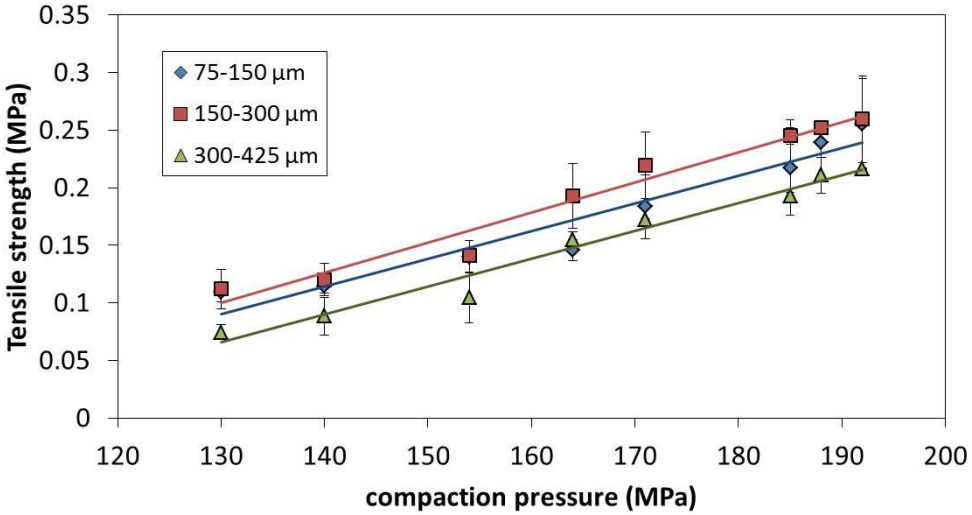

Figure 4.6 Tensile strength of palm kernel shell pellets compressed at various compaction pressures. Lines are best fits to the data.

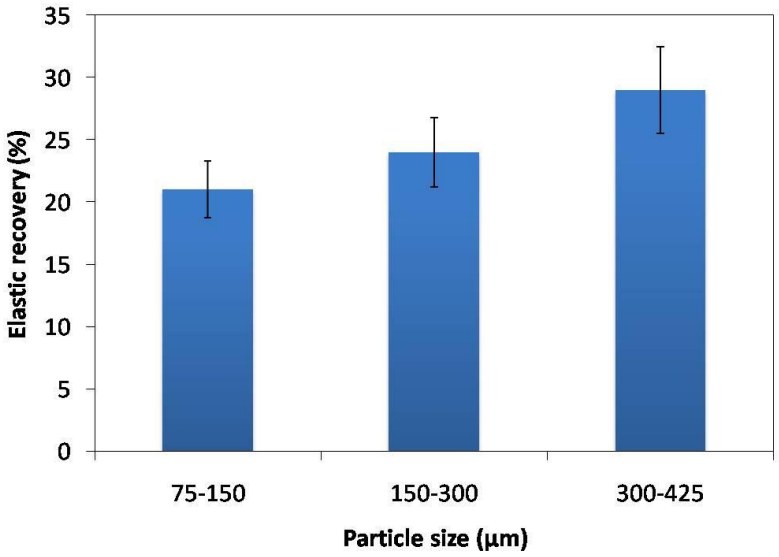

Figure 4.7 Average elastic recoveries of pellets made from different particle sizes

This study shows that pellets made from 100% raw ground kernel shells can be obtained through the compaction process. The compressive strength in the axial direction of the pellets was found to increase with compaction pressure and reached a maximum when no or near zero porosity during the compaction process was achieved. Thus, in the absence of any additional binders, the strength of the pellets did not exceed this maximum limit. Figure 4.8 shows the relationship between the compressive strengths of the pellets and the corresponding porosities in the pellets. The data was fitted with the Ryshkewitch-Duckworth empirical model (see equation (2.10)) which has been applied to a variety of systems to determine the strength at zero porosity and the bonding capacity constant (Etzler et al., 2011; Maarschalk et al., 1997b; Michrafy et al., 2007; Patel and Bansal, 2011; Wu et al., 2005).

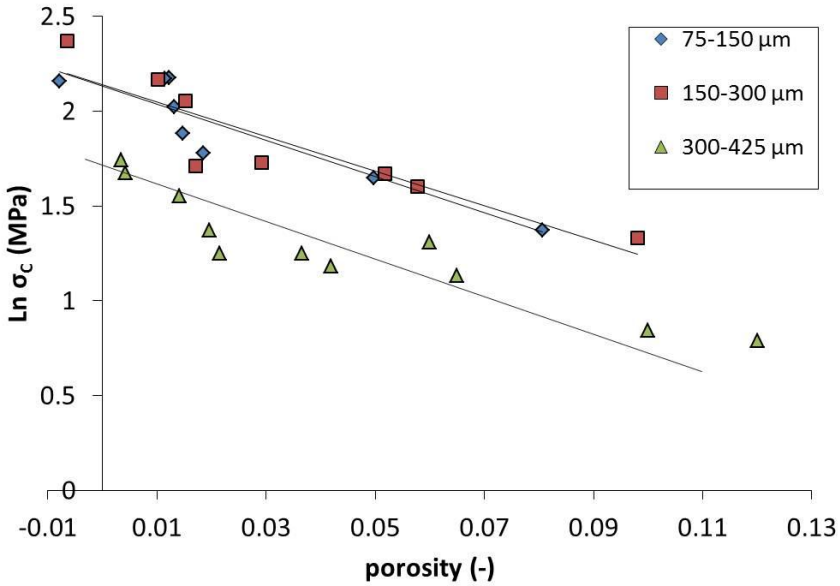

Figure 4.8 Relationship between porosity and compressive strength (natural logarithm)

The fitted parameters for the Ryshkewitch-Duckworth model for the palm kernel shell pellets are presented in Table 4.2. There do not appear to be any similar characterisation of palm waste in the literature, but the bonding capacities of the palm kernel shell pellets appear somewhat lower than those of sorbitol (Maarschalk et al., 1996b), lactose (Maarschalk et al., 1997b; Michrafy et al., 2007) and some binary systems such as microcrystalline cellulose/lactose and silicified microcrystalline cellulose-HD/lactose (Michrafy et al., 2007). The maximum compressive strength obtained for the three particle sizes were generally higher than that of palm biomass briquettes with binders (7.9 MPa as found by Nasrin et al., 2008). Pellets made with particle size 300-425 µm gave the lowest values of σ_0 and k while similar values were obtained for the pellets made with particle size 75-150 µm and 150-300 µm. The lower strength and bonding capacity in the pellets made from particle size 300-425 µm could be due to the presence of fibrous content in the powder (Figure 4.1c). The fibres were present in the sieved powder and were not possible to separate. Such fibres, which were also observed in the pellets after breakage, may have occupied spaces within the pellet and devoid the bonding between the particles, leading to weaker bonds. The bonding capacity may also be associated with the elastic rebound as the elastic rebound results in the breakage of bonds that are already formed during compaction (Maarschalk et al., 1996b). Thus,

the low bonding capacity of pellets with the largest particle size 300-425 μm is consistent with the observation that these pellets showed the largest elastic rebound.

Particle size (μm)	k (-)	σ_0 (MPa)
75-150	9.55	9.12
150-300	9.14	9.03
300-425	7.23	6.36

Table 4.2 Fitted parameters from Ryshkewitch-Duckworth relation to the data in Figure 4.8

The radial tensile strengths obtained for the palm kernel shell pellets were of much lower values compared to their compressive strengths at the corresponding compaction pressures. This was also observed by Newton et al (1993), who conducted compressive and tensile strength tests on lactose and microcrystalline cellulose compacts and concluded that the radial tensile strength of these compacts were lower than compressive strength. Large differences between the compressive (7.9 MPa) and tensile strength (0.34 MPa) were also observed in palm biomass briquettes with sawdust added as binders (Nasrin et al., 2008). For the palm kernel shell pellets with a diameter of 6 mm, the maximum strength corresponds to a compressive breaking force in the axial direction of approximately 250 N, which is sufficiently high to withstand handling loads. However, the radial tensile strength, which corresponds to the strength in the diametrical direction, was found to be much lower and the peak breaking force obtained from this study corresponds to a value of approximately 6 N. Thus, it is expected that the pellets would fail, not in the axial direction due to compressive stresses, but in the diametrical direction due to tensile stresses. Additional reinforcement, such as steam conditioning (Kaliyan and Morey 2009) may be required to strengthen the pellets. Pretreatment of the shells may also be beneficial as has been shown in some wood products (Yasin and Qureshi, 1990).

4.4 Effect of Compaction Speed on Pellet Strength

The compressive strength of the pellets were found to decrease with increasing compaction speed for the two smallest particle sizes as shown in Figure 4.9.

Although there is considerable scatter in the data, the changes seem to be significant when comparing the compaction speed of 1 mm/min and 100 mm/min. For the largest particle size, the changes due to different compaction speeds were within the scatter in the data. The increase in the compaction speed also resulted in an increased elastic rebound for the pellets as shown in Figure 4.10. At a compaction rate of 1 mm/min, there was considerable difference between the elastic rebound for the largest particle size and the other sizes. However, at 100 mm/min, the effect of the compaction speed was much lower. The significant scatter in the elastic rebound could be attributed to some degree of error in obtaining the length of the pellet during compaction through indirect measurement. Nevertheless, the mean values obtained were reasonable and showed a trend between elastic rebound and compaction speed.

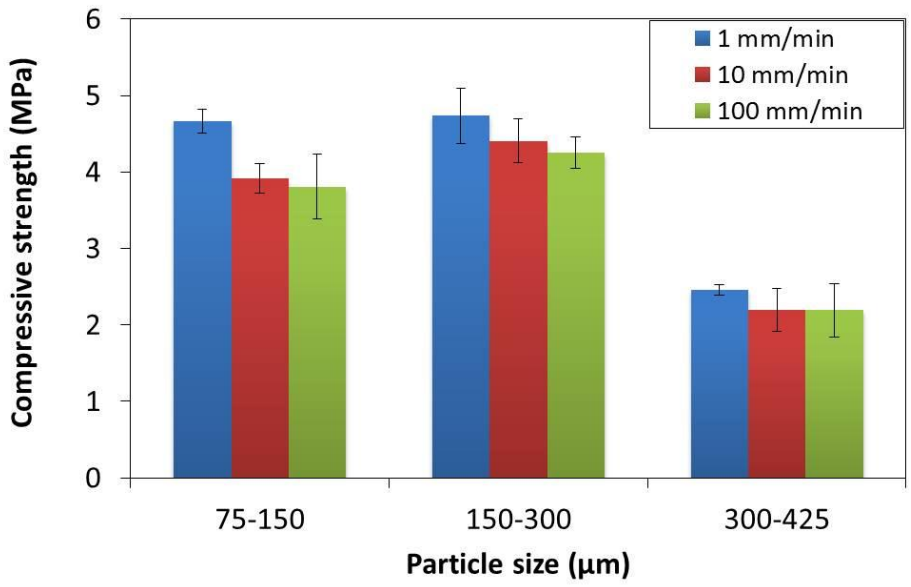

Figure 4.9 Variation of compressive strength with compaction speed for pellets with particle sizes 75-150 µm, 150-300 µm and 300-425 µm compacted at 164 MPa

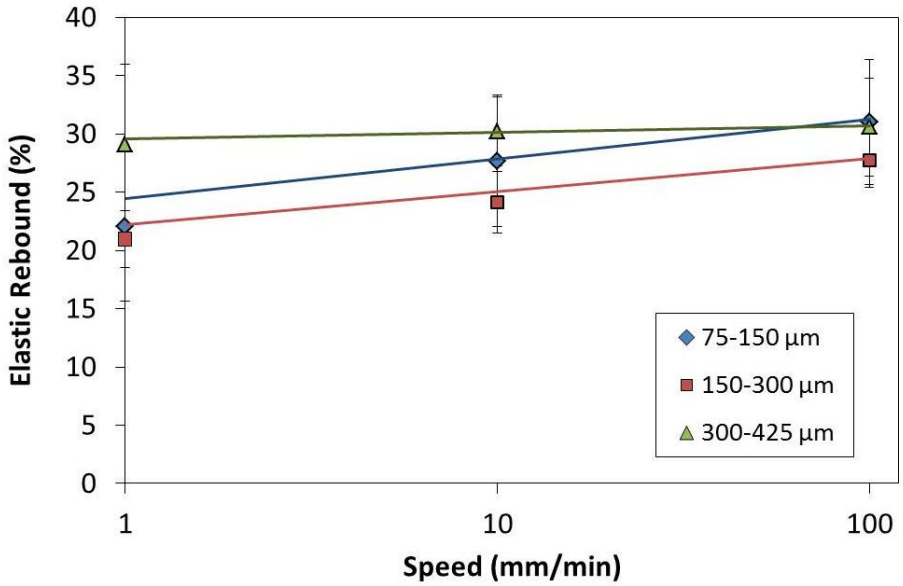

Figure 4.10 Effect of compaction speed (in logarithmic scale) on elastic rebound of pellets. Lines are best fits to the data.

Studies on the effect of compaction speed on the strength of tablets generally found that as the compaction speed increases, the strength of tablet decreases (Akande et al., 1997; Baba and Nagafuji, 1965). A similar trend was observed for the palm kernel shell pellets in this work. Armstrong (1989) suggested that materials which deform under stress are more sensitive to changes in the compaction speed as the consolidation mechanism depends on the time-dependent properties of the material. On the other hand, for materials which are brittle, the strength typically shows little dependence on the compaction speed (David and Augsburger, 1977; Rees and Rue, 1978). This study shows that palm kernel shell powders are possibly viscoelastic materials since they were sensitive to changes in compaction speed.

4.5 Effect of Hold Time on Pellet Strength

Figure 4.11a and Figure 4.11b show the variation of the porosity and volume with the hold time at maximum compaction. All pellets showed a decrease in both the porosity and volume during compaction with increasing hold time. Correspondingly, the strength of the pellets during compaction increased with increasing hold time (Figure 4.11c). These changes appeared to reach a plateau after a hold time of 60 s as

no or near-zero porosities in the pellets were reached. The study was conducted for pellets compacted at a compaction pressure of 164 MPa and compaction speed of 100 mm/min. As such, it would be expected that the hold time at which a plateau is reached may change if different processing parameters such as compaction pressure and compaction speed were used.

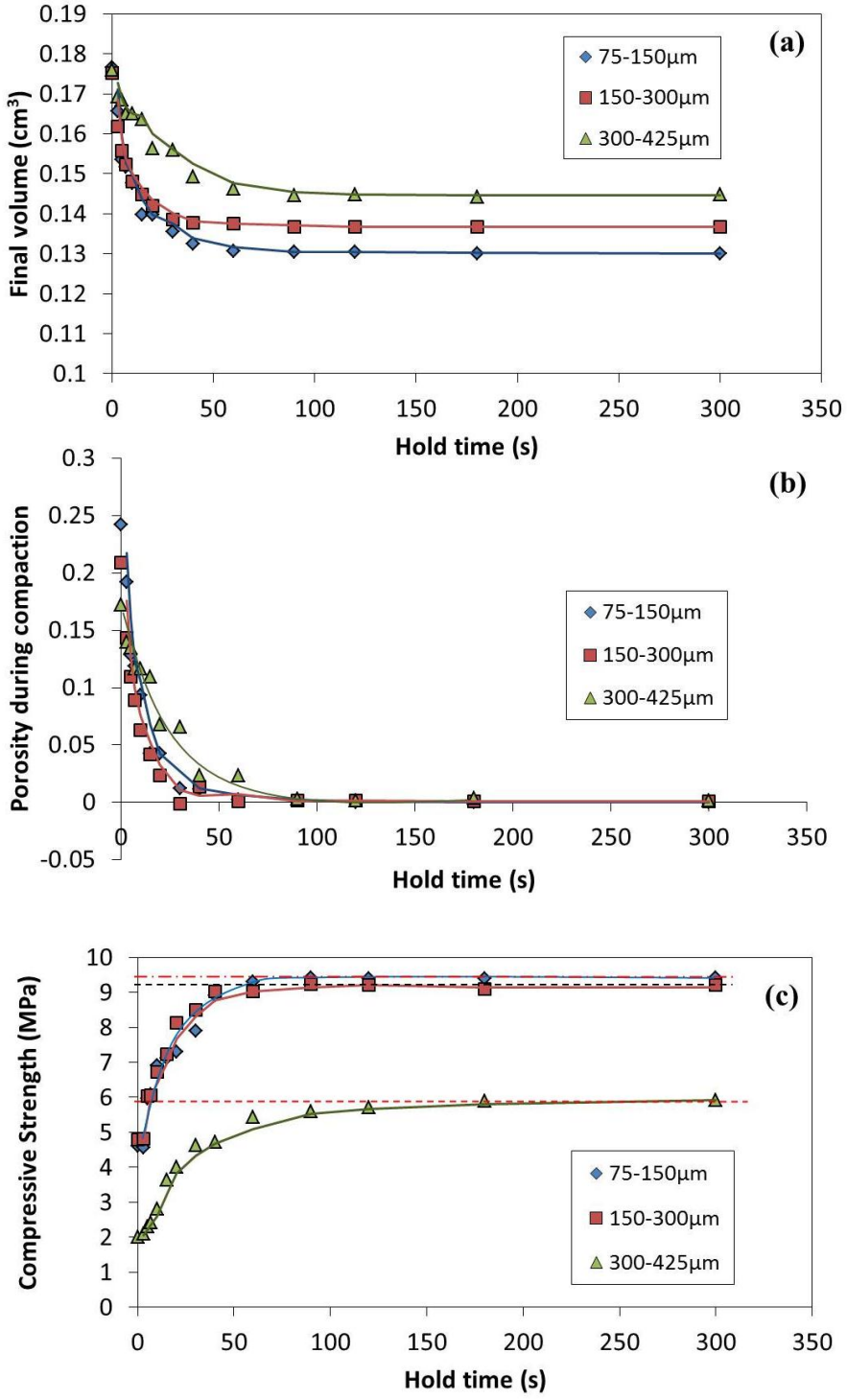

Figure 4.11 (a) Final volume achieved during compaction with increasing hold time. The plateaus corresponded to close-to-zero porosities (b) Changes in porosity during compaction with hold time (c) Variation of compressive strength with hold time for pellets compacted at 164 MPa at a compaction speed of 100 mm/min. Solid lines represent moving average of the data.

During the hold time, the porosity during compaction (ε) can be expressed as a function of hold time t by an exponential function in equation (4.1):

$$\varepsilon = \varepsilon_0 \exp(-\lambda t) \tag{4.1}$$

where ε_0 and λ are constants. The values of ε_0 and λ as obtained from the fitting of equation (4.1) to the porosity data in Figure 4.11b are shown in Table 4.3. ε_0 represents the porosity during compaction when hold time is zero and λ is a fitted parameter that is dependent on particle size. The variation of porosity with hold time may be included in a modified Ryshkewitch-Duckworth model such that:

$$\frac{\sigma}{\sigma_0} = \exp[-k\varepsilon_0 \exp(-\lambda t)] \tag{4.2}$$

Equation (4.2) shows good agreement when fitted to the strength data as shown in Figure 4.12, which suggests that during the holding time, the porosity of the pellets decreased with time until the pellets achieved no or near-zero porosity. When this condition was reached, the maximum strength was achieved and the holding time no longer affected the strength of the compact.

Particle size (µm)	ε_0	λ
75-150	0.22	0.09
150-300	0.19	0.10
300-425	0.17	0.04

Table 4.3 Fitted parameters from the Ryshkewitch-Duckworth model for hold time

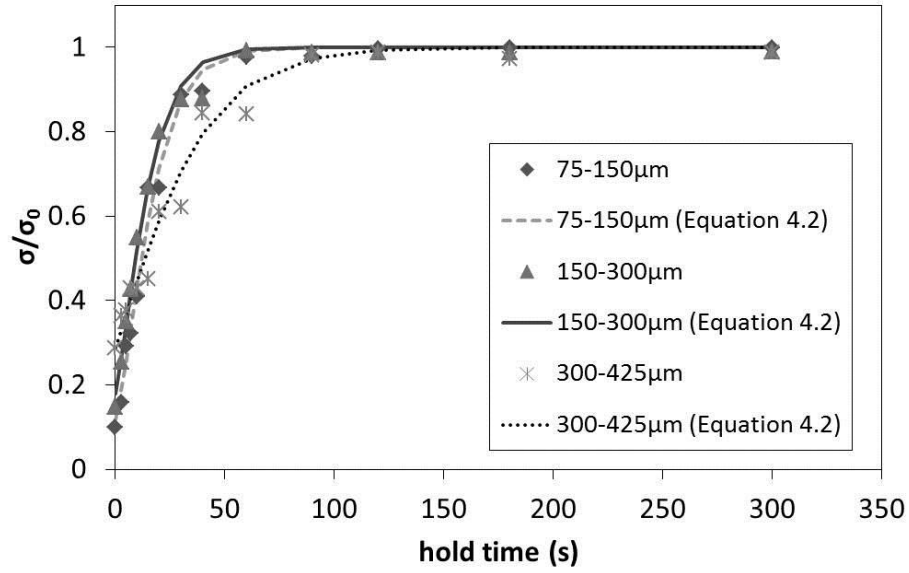

Figure 4.12 σ/σ_0 against hold time for different particle sizes with the fitted model. The points represent experimental data for each particle size. Solid and dotted lines represent the fitted model of equation (4.2) for each particle size.

This observation has some practical implications as it suggests that the maximum strength of the pellets could be achieved at low pressures, as long as the hold time is increased to allow gradual compaction of the particles until the condition of no or near zero porosity is achieved. Similar observation was obtained by Li and Liu (2000) for compacted oak sawdust. However, the increase in hold time may not be favourable as a means to increase the strength of the pellets in practice as this would reduce the production rate of the pellets.

4.6 Effect of Humidity and Storage Time on Pellet Strength

The compressive strength of the pellets decreased with increasing storage time, with significant loss in strength after one day (24 hours) of storage and relatively minor changes thereafter (Figure 4.13a). This trend was observed at all humidity conditions, with the greatest decrease in strength being observed for pellets stored at the humidity level of 57% (note that the pellets were made with feedstock stored at a humidity level of 11%). The pellets appeared to take up moisture within the first day of storage, with relatively little change in the water activity thereafter (Figure 4.13b).

The volume of the pellets also appeared to gradually increase with time (Figure 4.13c).

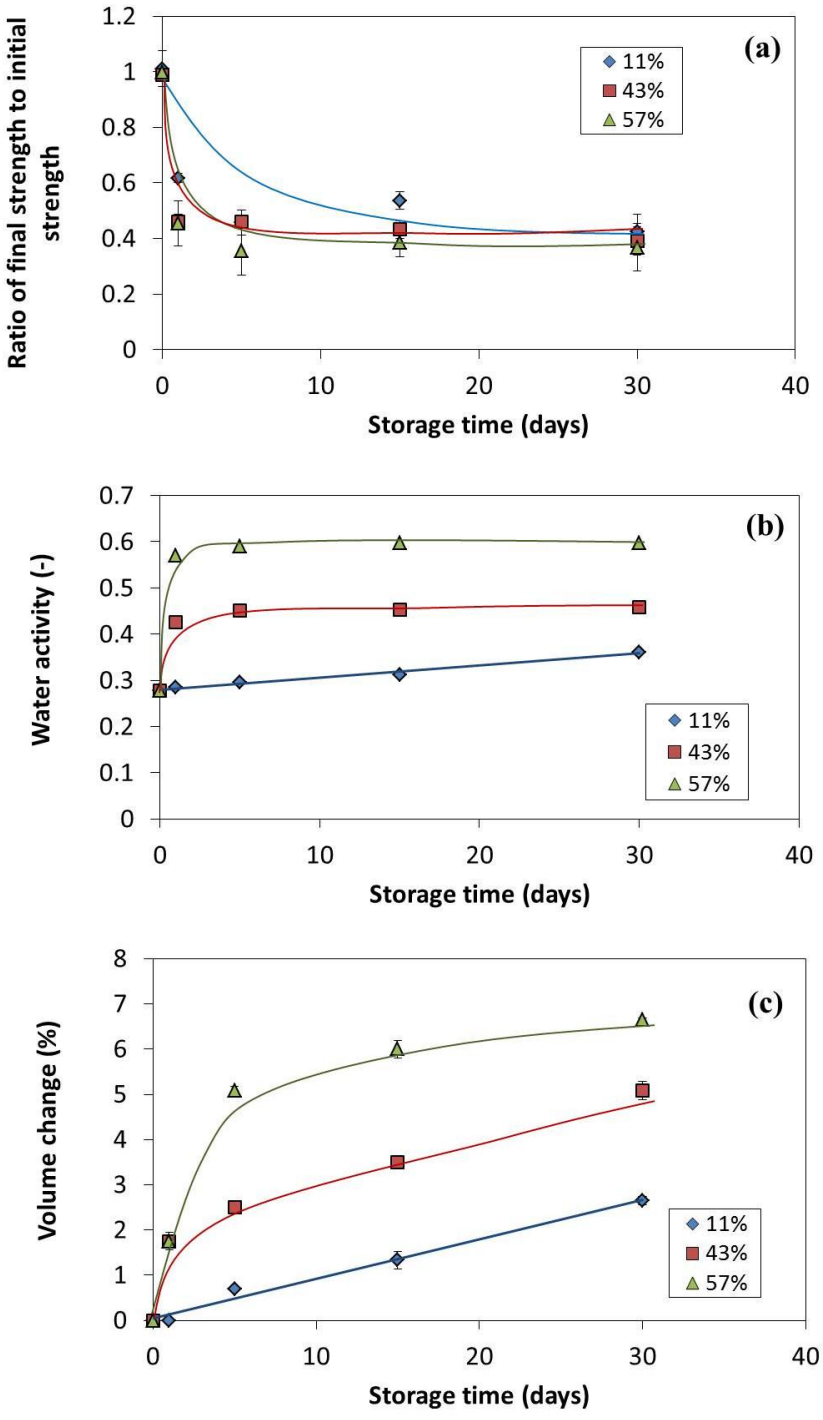

Figure 4.13 (a) Effect of storage conditions at three humidity levels on the strength of pellets (b) Changes in water activity in the pellets (c) Volume change of the pellets with storage time and humidity level. Volume change is the difference between the final and initial volume as a percentage of the initial volume. Solid lines represent moving average of five data points for each humidity level.

Storage at ambient temperature drastically decreased the strength of the pellets and this could be attributed to the gradual elastic rebound that occurs during the storage period. As the final porosity increases during the elastic rebound, and assuming a linear relationship between the compacted porosity and the final porosity, the relationship between the porosity during compaction (ε) and the storage time may be modelled using equation (4.3):

$$\varepsilon = \alpha \ln t_s + \beta \tag{4.3}$$

where α and β are constants, t_s is the storage time in days, and $t_s > 0$. α is a constant that is dependent on the storage condition such as humidity level and β represents the porosity of the pellet after 1 day of storage, t_s = 1. Similar to the hold time effect, equation (4.3) may be used to modify the Ryshkewitch-Duckworth equation such that:

$$\frac{\sigma}{\sigma_i} = \exp[-k(\alpha \ln t_s + \beta)] \tag{4.4}$$

where σ_i is the strength of the pellet at $t_s = 0$. k is the bonding capacity of the palm kernel shell particles from the results in Table 4.2 . Figure 4.14 shows the fit of equation (4.4) to the experimental data of Figure 4.13a and a good agreement is found, with the fitted parameters as shown in Table 4.4. These relationships indicated that the storage time affected the porosity adversely which negatively impacted on the strength of the pellets. The changes in porosity over the period of storage time were caused by the higher water activity or moisture level in the pellet (Figure 4.13a) and consistent with observations noted by other researchers (Shi et al., 2011; Sun, 2008). The gradual increase in porosity is also observed in some wood products (e.g. Hann et al., 1963) where 'springback' causes a decrease in density as well as a reduction in the mechanical locking of compressed particles.

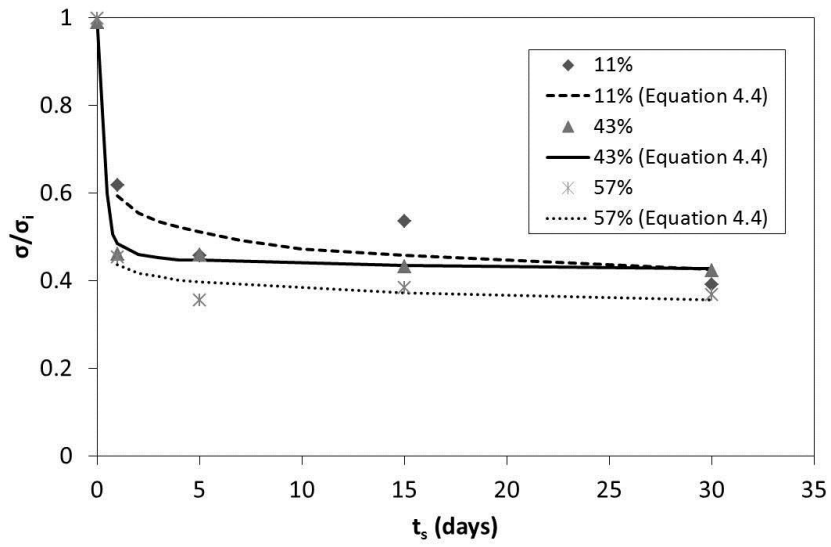

Figure 4.14 σ / σ_i against storage time, at various humidity levels with the fitted model. The points represent experimental data for each particle size. Solid and dotted lines represent the fitted model of equation (4.4) for each particle size.

Humidity level (%)	α	β
11	0.011	0.06
43	0.003	0.08
57	0.006	0.09

Table 4.4 Fitted parameters from the modified Ryshkewitch-Duckworth model for storage time

Based on the results from Figure 4.12 and Figure 4.14, it is proposed that equation (4.2) for the hold time (t) to produce the pellets when storage time t_s = 0 can be combined with equation (4.4) as follows:

$$\frac{\sigma}{\sigma_0} = \exp\left[-k\left(\alpha \ln t_s + \beta\right)\right] \cdot \exp\left[-k\varepsilon_0 \exp(-\lambda t)\right] \qquad (4.5)$$

Equation (4.5) can be further simplified as follows to estimate the strength based on hold time and storage time:

$$\frac{\sigma}{\sigma_0} = \exp\left\{-k\left[\left(\alpha \ln t_s + \beta\right) + \varepsilon_0 \exp\left(-\lambda t\right)\right]\right\} \quad (4.6)$$

In addition to the storage time, the humidity at which the pellets were stored additionally influenced the extent of reduction in strength of the pellet. The strength differences of pellets stored under different humidity conditions were probably due to the presence of water which influenced the bonding within the pellet. Mollan and Celik (1995) suggested two possible reasons for the lower compressive strength for pellets stored in high humidity conditions. Firstly, hydrodynamic resistance might occur from the water during compression and this energy might then be released on decompression, thus disrupting the bonds. Secondly, water may dissolve some bonds and weaken others so the pellets had low strength due to porosity expansion.

The storage tests suggest that the pellet quality may deteriorate during storage. Pellets with poor quality fracture easily and this will create difficulties in handling and transportation. In addition, long-term storage also has a negative impact on the combustion characteristics of biomass pellets. The increase in moisture content in the pellets due to long-term storage may result in pellets with lower reactivity and peak temperature during combustion when utilized as a biofuel (Casal et al., 2010). It is recommended that dry storage conditions, possibly vacuum-packed pellets or low relative humidity of less than 11% are necessary to minimize the deterioration of the pellet quality.

4.7 Gasification of Palm Kernel Shells, Powder and Pellets

Figure 4.15 shows the temperature and time profile for the gasification of the three feedstock forms. During pyrolysis, between time 0 to approximately 50 minutes, the temperature and time profile in Figure 4.15 show a gradual increase in temperature with time. At this stage, some fluctuations in the temperature were observed when shells and powder were gasified but a more steady increase in temperature was observed when pellets feedstock was used. When the temperature reached 250°C, air and nitrogen were introduced to react with the volatile matter released by the biomass feedstock and the temperature increased sharply at this stage of gasification. When gasifying palm kernel shell in the pelletised form, the time taken for

gasification (t_g) was approximately 10 minutes and relatively shorter compared to the raw, ungrounded and powder form which took approximately 16 minutes and 18 minutes for gasification respectively.

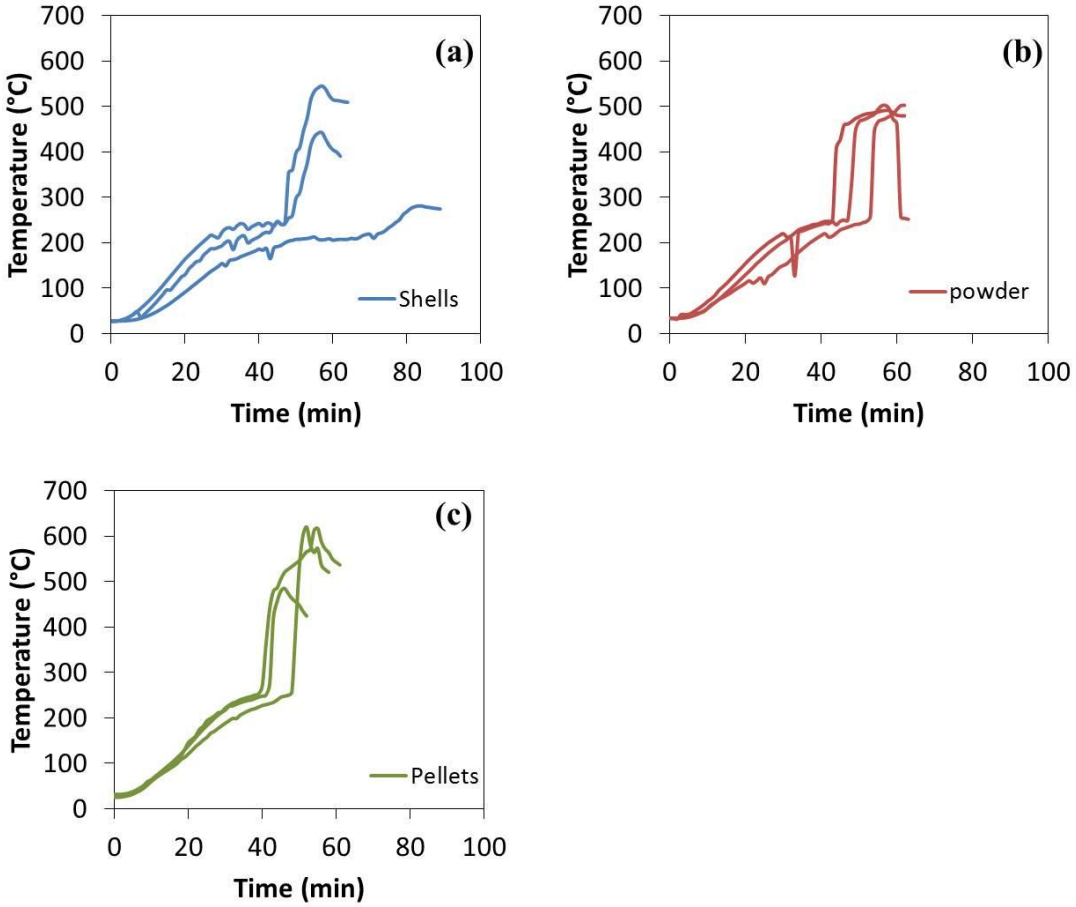

Figure 4.15 Temperature and time profile for the gasification of (a) raw, ungrounded palm kernel shells (b) palm kernel shells in grounded form (powder) (c) palm kernel shell in pelletised form (pellets)

Figure 4.16 compares the conversion rate of the three forms of the feedstock to gaseous products during gasification. The conversion rate of the pellets was found to be the highest, followed by those for the powder and raw, unprocessed feedstock.

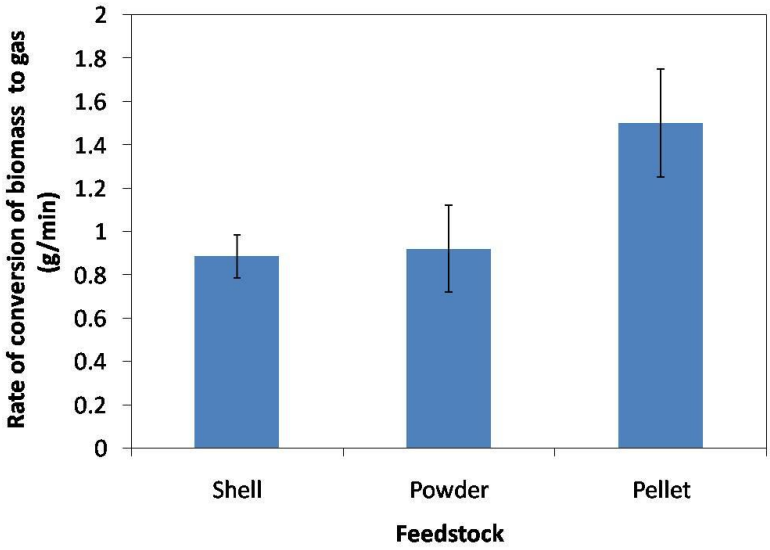

Figure 4.16 The conversion rate of the biomass to gaseous products for the three different forms of the feedstock

One possible explanation for the observations in Figure 4.16 could be taken from a heat transfer perspective. During gasification, heat is transferred from the source to the feedstock and propagated by heat or thermal conduction through the solid phase (solid particles of the feedstock). The total heat transfer may be described by two mechanisms (i) fluid-to-particle heat transfer and (ii) particle-to-particle heat transfer, whereby heat conduction occurs between points of contact of the solids. The differences in rate of conversion of biomass to gaseous products between the various feedstock may be due to the differences in heat conduction of the feedstock which affects the thermochemical performance (Onyekonwu, 1988; Pabst and Gregorova, 2007).

The palm kernel shells, powder and pellets can be classified as external porosity material as air makes up the continuous phase between the palm shells and powder particles. In addition, the porosity within each palm kernel shell and powder particle may be assumed to be zero. On the other hand, there is non-zero porosity within the pellets. However, the porosities within pellets are quite small hence the pellet may be treated as a consolidated granular material that is made up of discrete particles to form a larger solid and thus also considered as an external porosity material, where air is the continuous phase between the pellets. This classification for pellets is

similar to sandstone, a consolidated granular material that behaved like an external porosity material as found by Carson et al. (2005).

The bulk density of palm kernel shell, powder and pellets were found to be (0.49±0.02) g/cm^3, (0.50±0.03) g/cm^3 and (0.65±0.02) g/cm^3 respectively. The bulk density values of palm kernel shells and powder are relatively close and it may be deduced that the packing of palm kernel shells and powder particles might be similar to each other. As such, the heat transfer pathways for palm kernel shells and powder particles are comparable and both cases will have relatively similar rate of conversion of biomass to gaseous products, as depicted in Figure 4.16. On the other hand, pellets had a higher bulk density compared to shells and powder feedstock. More pellets occupy a given volume and hence more heat transfer pathways to facilitate heat transfer are available as compared to shells and powder particles. Since the heat conduction pathways for external porosity materials depend strongly on the contact between neighbouring particles (Carson et al., 2005; Felske, 2004), the close packing of pellets led to better thermal conductivity and heat transfer in the pellet feedstock, thus the rate of biomass conversion to gaseous products was higher. Such observations are consistent with other research which found that factors such as porosity and thermal conductivity of the fuels could affect thermochemical performance (Onyekonwu, 1988).

The physical appearances of the three forms of feedstock before and after gasification are shown in Figure 4.17. The black solid carbonaceous residue after gasification is char while the grey solid residue is ash. Char is the carbon remains from the biomass after devolatisation and when char is gasified in limited oxygen, gaseous products, tar and ash are produced (Hwang et al., 2008). The main difference between ash and char is that ash may not preserve any of the original morphology of the precursor and it may have a higher concentration of inorganic components due to the complete consumption of the organic matrix (Alvin, 1995). More char residue of palm kernel shells and powder were observed in the residues after gasification whereas mainly ash was observed in the residues after the pellets were gasified. These observations indicate that the gasification of pelletised feedstock was more complete. The contaminant tar was concluded to be present in

the gaseous products when palm kernel shell biomass was gasified as condensed tar was collected in the liquid traps as shown in Figure 4.18. Hence gas-cleaning processes would be necessary in order to remove the tar from the gaseous products.

Figure 4.17 Physical appearances of (a) raw, ungrounded palm kernel shells (b) grounded palm kernel shells in powder form (c) palm kernel shell pellets before and after gasification

Figure 4.18 Collection of condensed tar from the gaseous products in the four liquid traps

4.8 Conclusion

In summary, the characterisation of palm kernel shell powder and pellets as well as factors that affected the strength of binderless palm kernel shell pellets were presented and discussed. It has been established that oil palm kernel shell powders without binders can be pelletised to relatively low porosities. The optimum compaction pressure was found to be approximately 188 MPa which produced the strongest pellets from 75-150 μm and 150-300 μm particle sizes with a maximum compressive strength of around 8.5-9 MPa. However, the tensile strengths of the pellets were found to be much weaker than the compressive strengths when compacted at the same compaction pressure. Porosity was found to be a primary factor influencing the strength of a pellet and an empirical model was proposed to predict the strength of the pellets, given the hold time (t) and storage time (t_s) information: $\frac{\sigma}{\sigma_0} = \exp\{-k[(\alpha \ln t_s + \beta) + \varepsilon_0 \exp(-\lambda t)]\}$.

Low speeds and increased hold time could enhance the strength of the pellet, however these would reduce the production rate of the pellets. Exposure of the

pellets to higher humidity levels caused the pellets to become longer, more porous and weaker and the decrease in strength of the pellet was most significant after one day of storage. It is recommended that dry storage conditions are necessary to minimize the deterioration of palm kernel shell pellet quality over time and thermal treatment of pellets may be considered to further enhance the strength of the pellet. These results are expected to be useful in the selection of the appropriate conditions necessary for efficient gasification. A higher density of the biomass would also provide benefits in terms of transportation costs, size of fuel storage and handling equipment.

From the gasification studies, it was found that the pelletised form of the feedstock increases the efficiency of the gasification process as compared to raw ungrounded and powder forms of palm kernel shells. Tar was found to be present in the gaseous products from the gasification of palm kernel shell biomass hence gas cleaning processes are necessary and will be looked into in the following Chapter 5.

5 Strength and Gasification of Binary Palm Kernel Shell Pellets

5.1 Introduction

In Chapter 4, it was established that oil palm kernel shell powders without binders can be pelletised to relatively low porosities and oil palm kernel shell pellets can increase the efficiency of gasification. However, tar was found as a contaminant in the gaseous product when palm kernel shell biomass was gasified. The effect of HZSM-5 zeolite on tar reduction for palm shell gasification had been investigated by Chin et al. (2010). The catalyst was added into the gasifier with the palm shells. In extension to the previous work, the catalyst would now be incorporated into palm kernel shell powder and compacted into binary pellets. Thereafter, these pellets would be gasified to study their effectiveness in tar reduction. Perego et al. (2011) commented that the next generation of biofuels should be produced by more sustainable avenues to ensure competitive energy supplies for transportation, bearing in mind that the biofuel should also have emission compliance, low environmental impacts and carbon balance. Incorporating the catalyst into palm kernel shell pellets may then be a viable option to explore into, similar to impregnation of pellets (Kutty et al., 2008; Spieker and Regalbuto, 2001).

It is also important to study the mechanical strength of the binary palm kernel shell and zeolite pellets to ensure good handling and ease of transportation. Michrafy et al. (2007) and Wu et al. (2005) had proposed models to predict the mechanical properties of compacts containing two components and these models will be applied in the study of the strength of binary palm kernel shell and zeolite pellets. The compaction of single-component formulation was investigated and characterised in Chapter 4 and these results will be used for the prediction of the strength of binary pellets using suitable models. The final results were expected to help in the selection

of components to enable compacts of good strength to be made. Lastly, the binary palm kernel shell and zeolite pellets were gasified to study its effectiveness of tar reduction in the gaseous product.

5.2 Characteristics and Properties of Binary Palm Kernel Shell and Zeolite Powder Mixtures

The true densities of binary mixtures palm kernel shell and zeolite are reported in Table 5.1. The predicted and measured true densities of the binary mixture are generally in good agreement.

Percentage mass of zeolite in mixture (%)	Volume fraction of palm kernel shell, V_{PKS}	Volume fraction of Zeolite, V_Z	Measured true density of mixture, $\rho_{T,m}$ (g/cm^3)	Predicted true density of mixture, $\rho_{T,m}$ (g/cm^3)
0	1.00	0.000	1.37 ± 0.01	1.37
5	0.97	0.005	1.39 ± 0.01	1.39
10	0.93	0.009	1.42 ± 0.01	1.42
15	0.90	0.014	1.46 ± 0.01	1.44
25	0.82	0.023	1.52 ± 0.01	1.50
50	0.60	0.046	1.60 ± 0.02	1.65
100	0.00	1.000	2.08 ± 0.02	2.08

Table 5.1 Measured and predicted true densities of binary palm kernel shell and zeolite mixture

Figure 5.1 compares the micrograph images of binary powder with different mass fraction of zeolite. The palm kernel shell particles were irregularly shaped and appear to be larger than the white zeolite. In Figure 5.1b and Figure 5.1c, the white zeolite particles were observed to agglomerate and this resulted in lumps of zeolite within the binary powder mixture. More agglomeration of zeolite particles, as indicated by circles, were noticed in the binary powder with 50% zeolite (Figure 5.1c) than that with 25% zeolite (Figure 5.1b). No agglomeration was observed in

Figure 5.1a where zeolite particles were absent in the palm kernel shell powder, as expected. The HZSM-5 zeolite particles are relatively smaller in particle sizes that range between 0.1 to 1.1 μm (Martinez and Lopez, 2005; Ren et al., 2010) in contrast with the larger size (150-300 μm) and irregular shapes of palm kernel shell particles. Hence the zeolite particles may have a higher tendency to agglomerate and form bulks within the binary powder mixture (Hartley et al., 1985).

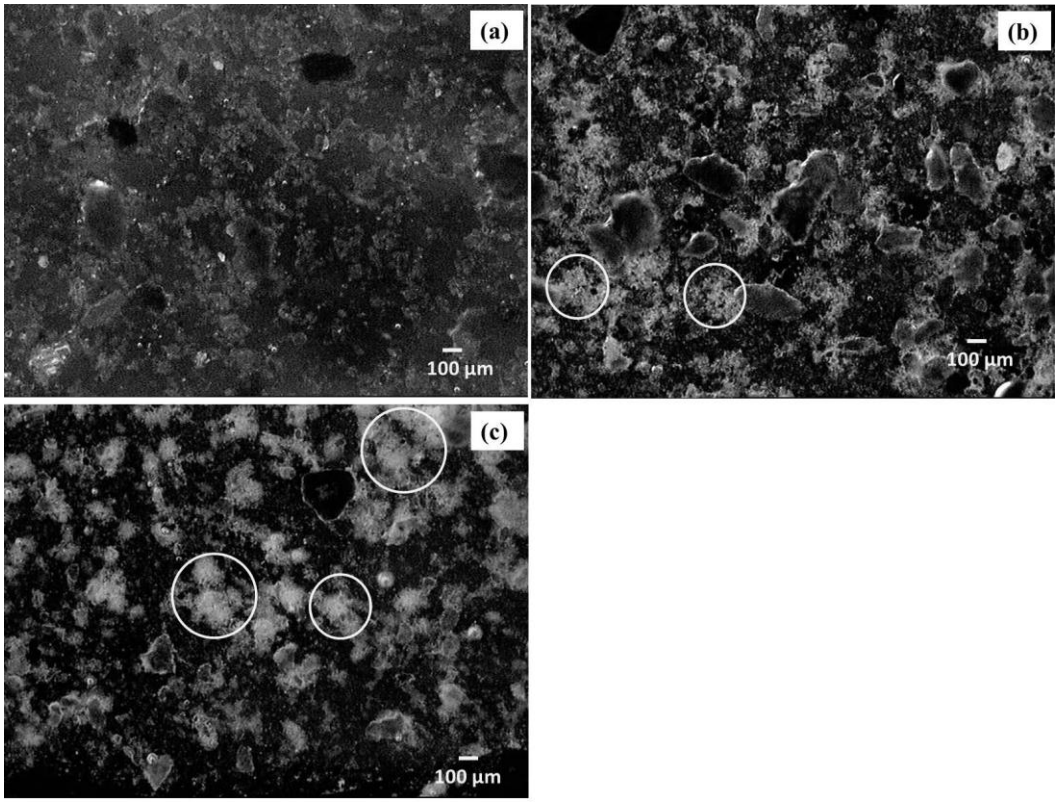

Figure 5.1 Micrographs through a 5× objective: (a) binary powder of 0% zeolite-100% PKS (b) binary powder of 25% zeolite-75% PKS (c) binary powder of 50% zeolite-50% PKS. The circles indicate agglomeration of zeolite particles.

5.3 Compaction of Binary Palm Kernel Shell and Zeolite Pellets

The pellets with varying formulations were compacted at different compaction pressures ranging from 134 to 198 MPa and subjected to uniaxial compression tests. Figure 5.2 reflects the relationship between the compressive strength and compaction pressure of binary palm kernel shell and zeolite pellets and Figure 5.3 shows the relative density and compressive strength for the various formulations of binary palm kernel shell and zeolite pellets.

The results in Figure 5.2 show that for the same compaction pressure, the highest average compressive strength was obtained for the formulation with 5% zeolite whereas the lowest average compressive strength was obtained for the formulation with 50% zeolite. However, the highest compressive strength of ~7.5 MPa obtained for the binary pellets with 5% zeolite was still lower than that of pure palm kernel shell pellets. A plateau in the strengths was observed at high compaction pressures of approximately 188 MPa, 191 MPa and 195 MPa for binary pellets that contain 5%, 10%, 25% and 50% zeolite respectively. These plateaus in strengths for binary pellets that contain 5%, 10% and 25% zeolite correspond to a relative density ~1 as shown in Figure 5.3. Although a plateau in strength was observed for the binary pellets with 50% zeolite, it does not correspond to a relative density of 1. The range of compaction pressures applied was probably not sufficient to increase the strength of the binary pellet containing 50% zeolite beyond ~1.4 MPa. This observation was also supported by the results in Figure 5.3 which show that the relative density for the binary pellets with 50% zeolite could not increase beyond ~0.80. Higher compactions will be required to increase the relative density for the binary pellets containing 50% zeolite beyond 0.80. However, this was beyond the capacity of the equipment and not possible to achieve in this study.

The variation of compressive strength with the compacted relative density during the compaction of the binary palm kernel shell and zeolite pellet is shown in Figure 5.3. The changes in compressive strength with relative densities for the binary pellets containing 5%, 10% and 15% zeolite were greater compared with that of the binary pellets containing 25% and 50% zeolite. The 50% zeolite-50% PKS formulation which had the lowest relative density corresponded to the weakest pellet strength.

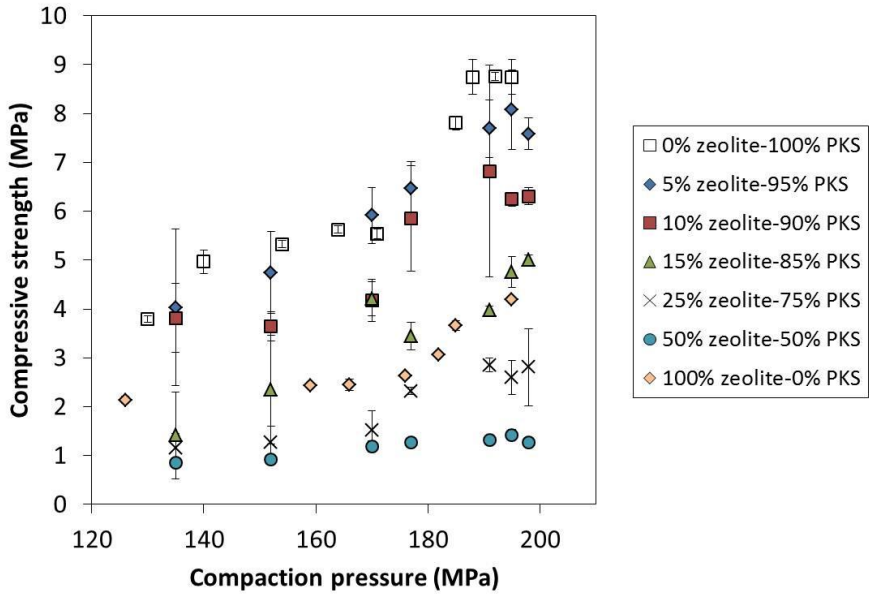

Figure 5.2 Compressive strength against compaction pressure for binary zeolite and palm kernel shell powder mixture

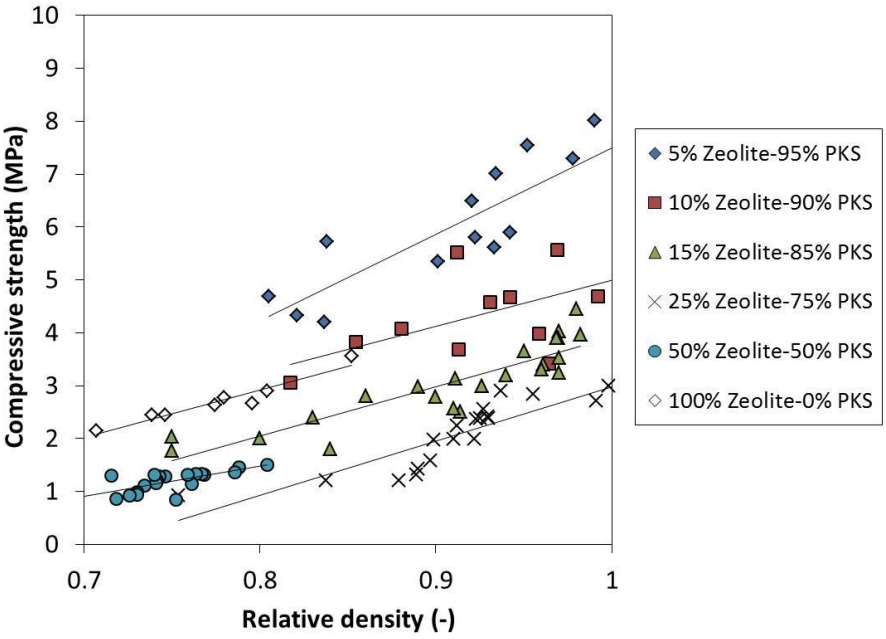

Figure 5.3 Compressive strength against relative density during compaction of the binary palm kernel shell and zeolite pellets

Porosity and strength (natural logarithm) data were used to determine the strength of binary pellets at zero porosity. The values of the maximum strength of binary pellets at zero porosity ($\sigma_{0,m}$) and bonding capacity (k_m) are summarised in Table 5.2. Table 5.3 reports the properties of individual powder components. The bonding capacity

and maximum strength of pure palm kernel shell at zero porosity was obtained from the results in Chapter 4. The maximum compressive strengths obtained for the binary pellets at zero porosity were lower than that obtained from pellets made from the single component powders containing only palm kernel shell.

Binary mixtures	k_m (-)	$\sigma_{0,m}$ (MPa)
5% Zeolite-95% PKS	1.91	6.89
10% Zeolite-90% PKS	1.55	4.69
15% Zeolite-85% PKS	1.52	3.97
25% Zeolite-75% PKS	1.35	2.15
50% Zeolite-50% PKS	0.51	1.32

Table 5.2 Strength and bonding capacity of binary pellets from porosity-strength measurements of binary mixtures during compaction

Individual components	k (-)	σ_0 (MPa)
Palm kernel shell	9.14	9.03
Zeolite	2.57	7.94

Table 5.3 Properties of individual components derived from porosity-strength measurements during compaction

From a total of 21 replicates for each binary mixture, the average elastic rebound was calculated. Figure 5.4 shows the average elastic rebound for each binary mixture. It was noted that there was significant elastic rebound in the binary pellets. The average elastic rebound of the pellets with 5%, 10%, 15%, 25% and 50% zeolite incorporated were (25±1)%, (34±2)%, (35±3)%, (37±2)%, (38±3)% respectively. Pellets with 50% zeolite formulation exhibited the largest elastic rebound. The elastic rebound of binary pellets were generally larger compared to that of pure palm kernel shell pellets (i.e. (24±3)%).

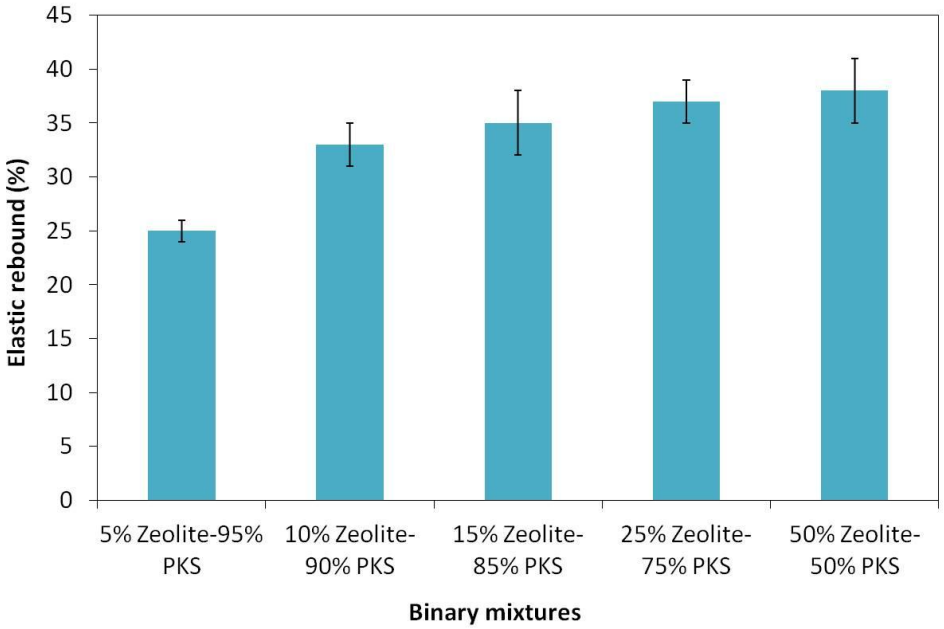

Figure 5.4 Average elastic rebound of binary mixtures

5.4 Predicting the Strength of Binary Palm Kernel Shell and Zeolite Pellets

Equations (2.12) and (2.16) were incorporated into equation (2.11) and the following equation was obtained to predict the strength of binary pellets:

$$\ln \sigma_m = -\varepsilon(k_1 V_1 + k_2 V_2) + \ln\left(\sigma_{0,1} V_1 + \sigma_{0,2} V_2\right) \tag{5.1}$$

Figure 5.5 compares the strength of binary pellets obtained experimentally with the predicted outcomes using the model proposed by Michrafy et al. (2007) and Wu et al. (2006) from equation (5.1). The predicted strength was relatively close to the experimentally obtained strength for the binary pellet containing 5% zeolite. However, the predicted binary pellet strengths were generally over-estimations compared to the experimental pellet strengths for the other binary pellets. This could be due to the fact that the pellets experienced elastic rebound after ejection from the die which resulted in higher porosities and lower strengths. The interfacial interaction between zeolite and palm kernel shell particles may be low and this could have resulted in weak bonds within the pellet matrix (Veen et al., 2004). Such

phenomenon was not taken into account by the Michrafy et al. (2007) and Wu et al. (2006) model.

The model from equation (5.1) considered only porosities of binary pellets during compaction and this may have led to over-estimations of the binary pellet strengths. Pharmaceutical binary tablets may have elastic rebound that is relatively less significant as compared to biomass binary pellets. As such, the final porosity of pharmaceutical tablets may not vary too far from the porosity during compaction. Hence the model by Michrafy et al. (2007) and Wu et al. (2006) may be suitable for predicting the strength of some pharmaceutical tablets but not biomass pellets.

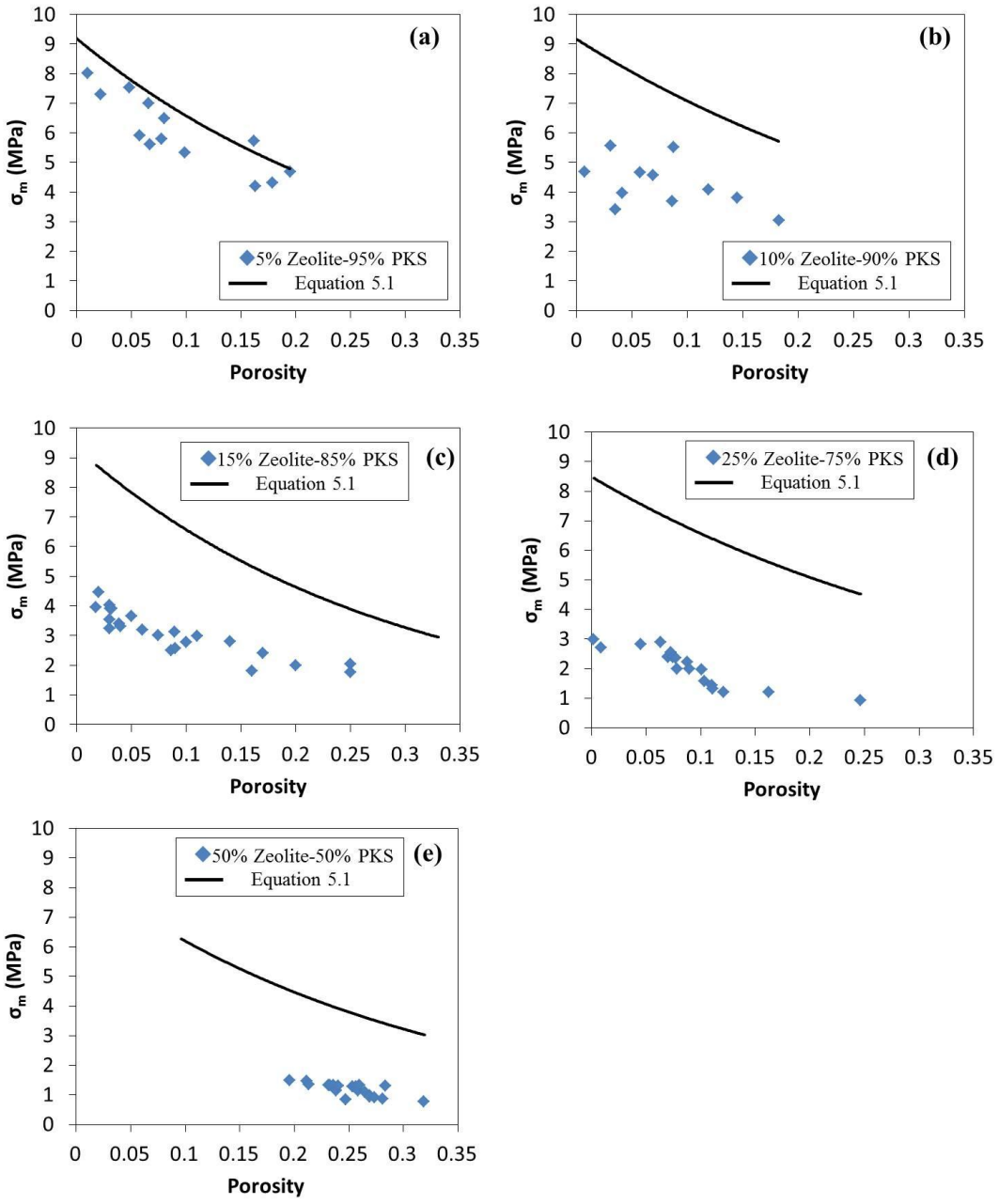

Figure 5.5 Compressive strength of binary mixtures as a function of porosity. The lines represent the predictive outcomes of the linear mixing rule and Ryshkewitch-Duckworth model from equation (5.1) on the strength of the binary mixtures.

Elastic rebound results in a change in relative density and hence affects the porosity of the pellet (Maarschalk et al., 1996b). Figure 5.6 shows the relationship between the final porosity (ε_f) and porosity during compaction (ε) of the pellets produced from different binary mixtures. A linear relationship between final porosity and porosity during compaction can be determined from the best fitting as follows:

$$\varepsilon_f = \gamma\varepsilon + \varphi \tag{5.2}$$

where γ and φ are fitted values from the final porosity and porosity during compaction relationship. Table 5.4 shows the fitted values for each binary mixture.

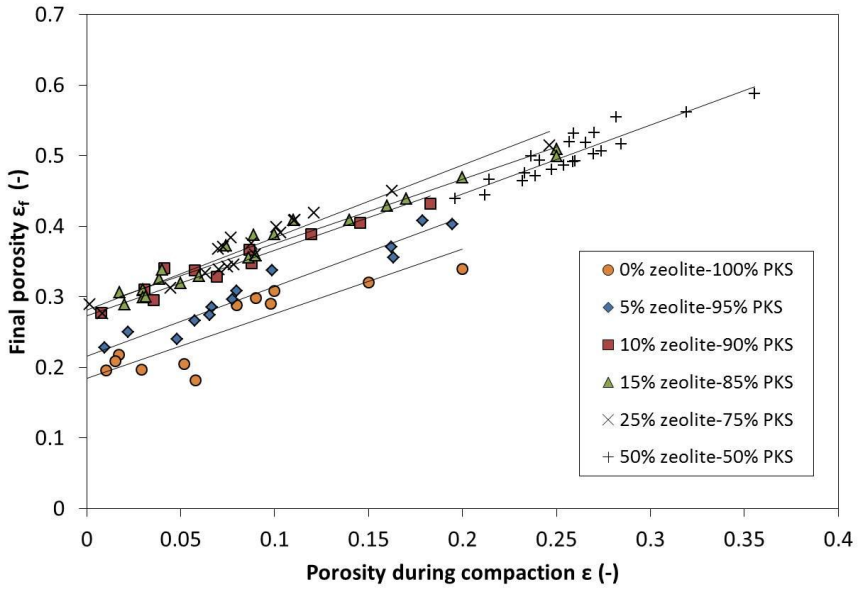

Figure 5.6 Relationship between final porosity and porosity during compaction from experiment

Binary mixtures	γ	φ
0% Zeolite-100% PKS	0.91	0.18
5% Zeolite-95% PKS	0.98	0.22
10% Zeolite-90% PKS	0.93	0.27
15% Zeolite-85% PKS	0.91	0.28
25% Zeolite-75% PKS	1.03	0.28
50% Zeolite-50% PKS	0.98	0.25

Table 5.4 Fitted values from the final porosity and porosity during compaction relationship

The change in porosity is defined as the difference between the final porosity (ε_f) and the porosity during compaction (ε). The average change in porosity with respect to porosity during compaction, $\overline{\Delta\varepsilon}$, for each binary mixture can be calculated as follows:

$$\overline{\Delta\varepsilon} = \frac{\sum \frac{\varepsilon_f - \varepsilon}{\varepsilon}}{n} \tag{5.3}$$

where n is the total number of points taken for calculation. The final porosity (ε_f) was determined by equation (5.2) for each binary mixture with the fitted values from Table 5.4.

Figure 5.7 shows the average change in porosity with respect to porosity during compaction ($\overline{\Delta\varepsilon}$) and the volume fraction of zeolite (V_Z) in the binary mixture when the zeolite composition is varied between 0% to 50%. The relationship between average change in porosity with respect to porosity during compaction and volume fraction of zeolite in a binary mixture could be fitted with an experimental equation which resulted in:

$$\overline{\Delta\varepsilon} = 5.42\exp(-34.7V_z) \tag{5.4}$$

As elastic rebound increases with increasing volume fraction of zeolite in the binary mixture, the difference between the final porosity and porosity during compaction also increases. The change in porosity (with respect to porosity during compaction or the initial compaction) was observed to decrease with increasing volume fraction of zeolite. This is because the porosity during compaction for binary mixtures with low volume fraction of zeolite was relatively lower compared to that with higher volume fraction hence the average change in porosity with respect to the porosity during compaction turns out to decrease with increasing volume fraction of zeolite in the binary mixture.

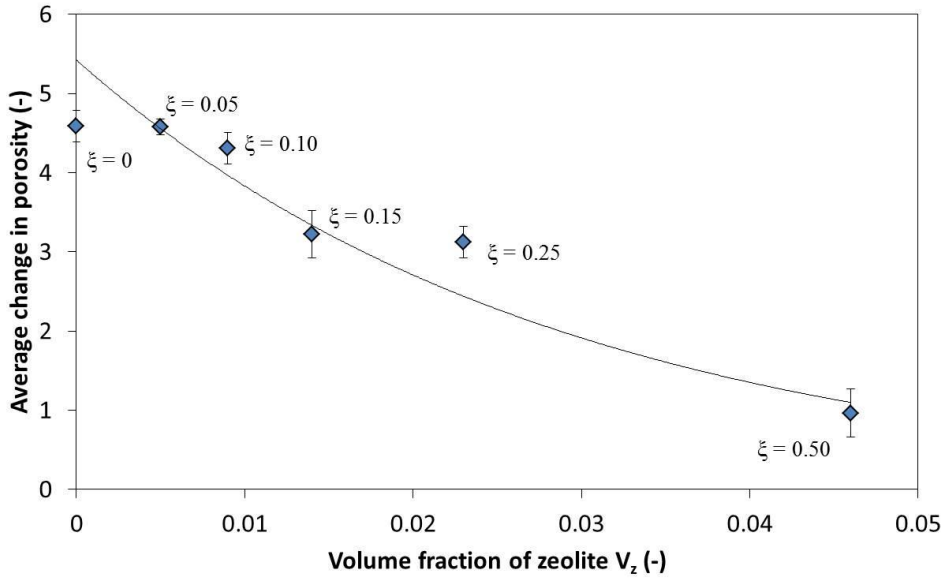

Figure 5.7 Relationship between average change in porosity from experiment and volume fraction of zeolite in a binary mixture. The line represents the fit to equation (5.4). The mass fraction (ξ) of zeolite that corresponds to each volume fraction of zeolite is represented on the graph.

The relationship between average reduction in strength and average change in porosity with respect to porosity during compaction for each binary mixture is shown in Figure 5.8. The average reduction in strength ($\overline{\Delta\sigma_m}$) between the predicted and experimental strengths for each binary mixture was determined by the following equation:

$$\overline{\Delta\sigma_m} = -\frac{\sum \frac{\sigma_{m,\exp} - \sigma_m}{\sigma_m}}{n} \tag{5.5}$$

where $\sigma_{m,\exp}$ is the experimental strength, σ_m is the predicted strength from equation (5.1) and n is the total number of points taken for calculation.

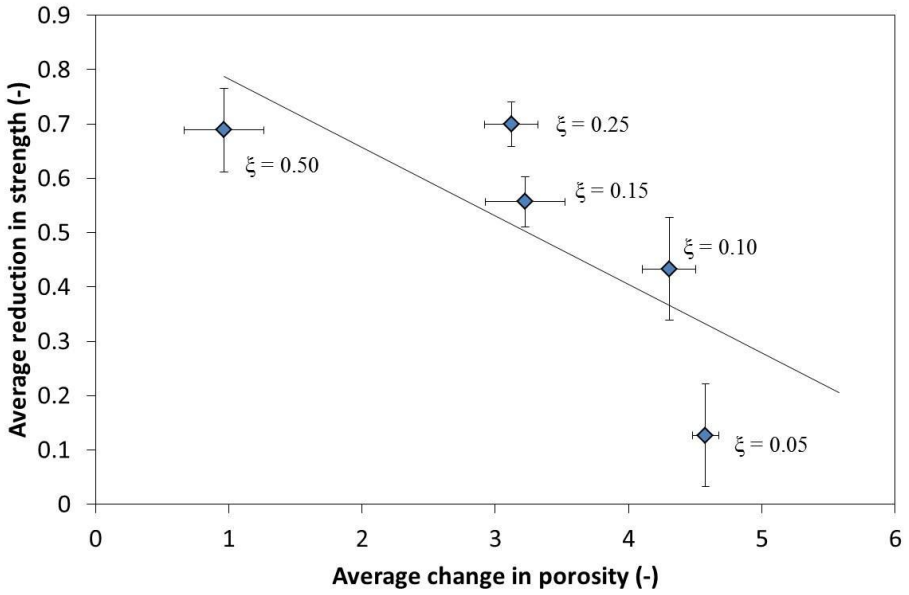

Figure 5.8 Relationship of average reduction in strength between predicted and experimental results with average change in porosity. The line represents the fit to equation (5.6). The mass fraction (ξ) of zeolite that corresponds to each volume fraction of zeolite is represented on the graph.

It was observed that the average strength reduction between the predicted and experimental results is larger when the average change in porosity of the binary mixture is low which corresponds to higher volume fraction of zeolite. Hence to enable a better prediction of the strength of binary pellets, the change in porosity of the binary mixture must be taken into consideration. The relationship between the average reduction in strength ($\overline{\Delta\sigma_m}$) and the average change in porosity with respect to porosity during compaction ($\overline{\Delta\varepsilon}$) was found as follows, assuming a linear relationship:

$$\overline{\Delta\sigma_m} = -0.13\overline{\Delta\varepsilon} + 0.91 \tag{5.6}$$

Incorporating equation (5.6) into the predicted strength of the binary mixtures of equation (5.1), the following could be obtained, which relates the strength of the binary mixture to the elastic rebound or porosity of the pellets:

$$\ln\sigma_m = \left(1-\overline{\Delta\sigma_m}\right)\cdot\left[-\varepsilon(k_{PKS}V_{PKS} + k_Z V_Z) + \ln\left(\sigma_{0,PKS}V_{PKS} + \sigma_{0,Z}V_Z\right)\right] \tag{5.7}$$

The predicted strength of the binary mixtures of equation (5.1) was assumed a factor 1. Hence the reduction in strength has to be subtracted from 1 to obtain the factor to be multiplied to equation (5.1) for the prediction of the strength of the binary mixtures in equation (5.7). Incorporating equations (5.4) and (5.6) into equation (5.7), the modified model to predict the strength of binary mixture from the properties of the individual constituent components is as follows:

$$\ln \sigma_m = [0.70\exp(-34.7V_z) + 0.09][-\varepsilon(k_{PKS}V_{PKS} + k_Z V_Z) + \ln(\sigma_{0,PKS}V_{PKS} + \sigma_{0,Z}V_Z)] \qquad (5.8)$$

The variations of strength with porosity for each binary mixture with the modified model are shown in Figure 5.9. The symbols represent the experimental data; the solid lines are the predictions using equation (5.1) and the dashed lines are the predictions using equation (5.8). The experimental data appear to be closer to the fitted model given by equation (5.8) compared to the fitted model by equation (5.1) for the range of porosities studied. Extrapolating the fitted model given by equation (5.8) in the strength and porosity graph allows the determination of the strength of the binary mixture at zero porosity. Table 5.5 shows the predicted maximum strength of the binary mixtures at zero porosity. The predicted maximum strengths from equation (5.8) are rather close to those obtained from porosity-strength measurement as shown in Table 5.2.

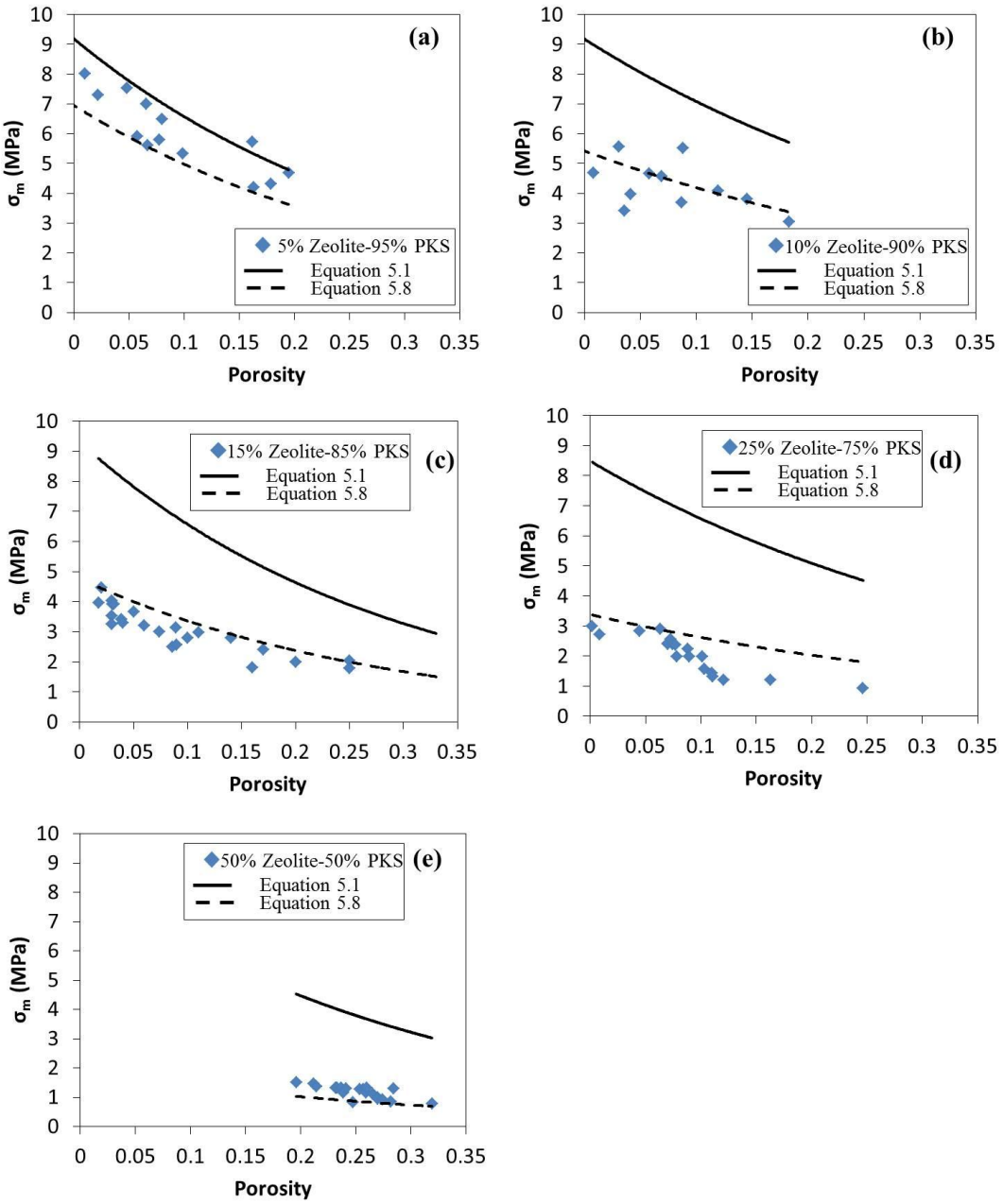

Figure 5.9 The variation of strength with porosity for various binary mixtures. The solid lines represent the predictive outcomes of the linear mixing rule and Ryshkewitch-Duckworth model from equation (5.1) on the strength of the binary mixtures. The dashed lines represent the modified model from equation (5.8).

Binary mixtures	$\sigma_{0,m}$ [from equation (5.8)] (MPa)
5% Zeolite-95% PKS	6.12
10% Zeolite-90% PKS	5.43
15% Zeolite-85% PKS	4.76
25% Zeolite-75% PKS	3.34
50% Zeolite-50% PKS	1.97

Table 5.5 Maximum strength of binary mixtures at zero porosity from the fitted model by equation (5.8)

As the volume fraction of zeolite increases in the binary mixture, the strength of the binary pellet decreases. Porosity influences the strength of a compact and high porosities negatively impacts on the strength (Adolfsson and Nystrom, 1996). It was shown in Chapter 4 that high porosities led to lower palm kernel shell pellet strengths and the same observation may also be made for binary palm kernel shell and zeolite pellets and consistent with other binary pharmaceutical compacts (Michrafy et al., 2007; Tye et al., 2005; Wu et al., 2006).

The higher porosity in the binary palm kernel shell and zeolite pellet was a result of the larger elastic rebound. Elastic rebound results in the breakage of bonds that are already formed during compaction (Anuar and Briscoe, 2009). The micrographs in Figure 5.1 show that the white zeolite particles agglomerate and this resulted in lumps of zeolite within the binary powder mixture. More agglomeration of zeolite particles were noticed in the binary powder with 50% zeolite (Figure 5.1c) than that with 25% zeolite (Figure 5.1b). Such agglomeration behaviour may affect porosity, relative density and cohesion which can lead to changes in the properties of a material (Lee et al., 2009). Agglomeration depends on the size of the individual particles and fine particles are more cohesive than coarse particles (Hartley et al., 1985). HZSM-5 zeolite particles have relatively smaller particle sizes ranging between 0.1 to 1.1 μm and more regular shapes (Martinez and Lopez, 2005; Ren et al., 2010) in contrast with the larger size (150-300 μm) and irregular shapes of palm kernel shell particles hence zeolite particles may have a higher tendency to agglomerate and form bulks within the binary powder mixture.

The interfacial interaction between zeolite and palm kernel shell particles may be low and this resulted in weak bonding within the binary pellet structure as the volume fraction of zeolite increases. This is consistent with some binary compacts studied by other researchers (Hadzovic et al., 2011; Veen et al., 2004). The elastic rebound which occurred after the compaction pressure was removed further led to the breakage of bonds which were already formed during compaction. Hence the porosity increased and the strength of the binary pellet weakened. Unlike pharmaceutical binders such as microcrystalline cellulose (MCC) and silicified microcrystalline cellulose (SMCC) which undergo fragmentation into fine binder particles to fill the voids between the compound particles that lower tablet porosity (Adolfsson et al., 1997; Nystrom et al., 1993), the higher porosity from the results suggested that zeolite particles do not behave like binders.

Binary pellets made from the formulations with 5%, 10% and 15% zeolite can withstand handling loads up to 212 N, 183 N and 127 N respectively (i.e. corresponding to 7.5 MPa, 6.5 MPa and 4.5 MPa respectively) while binary pellets containing 25% and 50% zeolite can only withstand handling loads up to 70 N and 28 N respectively (i.e. corresponding to 2.5 MPa and 1.0 MPa respectively). It is thus recommended that if zeolite catalyst was to be incorporated into palm kernel shell pellets to produce feedstock for gasification, the composition of the zeolite should be limited to between 5 to 15%.

5.5 Gasification of Binary Palm Kernel Shell and Zeolite Pellets

Studies on the effect of zeolite amount on tar reduction for gas cleanup had been done previously on the gasification of raw, ungrounded palm kernel shells (Chin, 2011). The zeolite was added in situ with the raw palm kernel shells in the gasifier and it was found that the tar was reduced from a weight fraction of 1 to 0.05 as zeolite percentage was increased from 0% to 10% (Chin, 2011). In this part of the project, the feasibility of gasifying pelletised palm kernel shell with zeolite and its effectiveness in tar reduction for gas cleanup was studied.

5.5.1 Effect of Zeolite Composition on Gas Cleaning

Figure 5.10 compares the amount of tar by mass ratio in the gaseous products obtained from the gasification of pelletised binary palm kernel shell and zeolite mixture and that from palm kernel shells and zeolite added in-situ. The results for the gasification of raw, ungrounded palm kernel shells and zeolite were adapted from Chin (2011). As the zeolite percentage was increased from 0% to 15% in the binary pellets, tar was reduced from a mass ratio of 1 to 0.27.

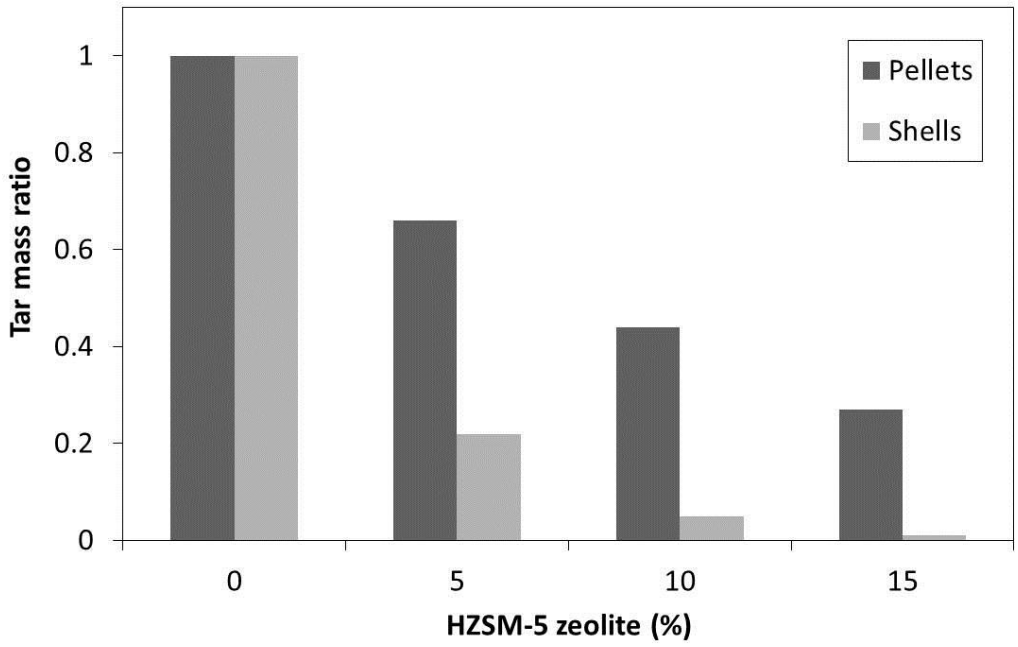

Figure 5.10 Amount of tar by mass ratio in the gaseous products as a function of percentage of catalyst for gasification of binary palm kernel shell and zeolite pellets and raw palm kernel shells with zeolite added in-situ

HZSM-5 zeolite was found to be effective in removing some chemical components in tar. The chemical components and their concentration in the tar analysed by gas chromatography are presented in Figure 5.11 (adapted from Chin, 2011). Chemical components such as carbolic acid, o-methoxy phenol, 2-methoxy p-cresol and diethyl phthalate were found in tar when no HZSM-5 zeolite was added to the palm shell feedstock. When 5% or 10% zeolite was added to the feedstock, carbolic acid in the tar was reduced significantly and the concentration of most of the other chemical components dropped to near-zero (Chin, 2011).

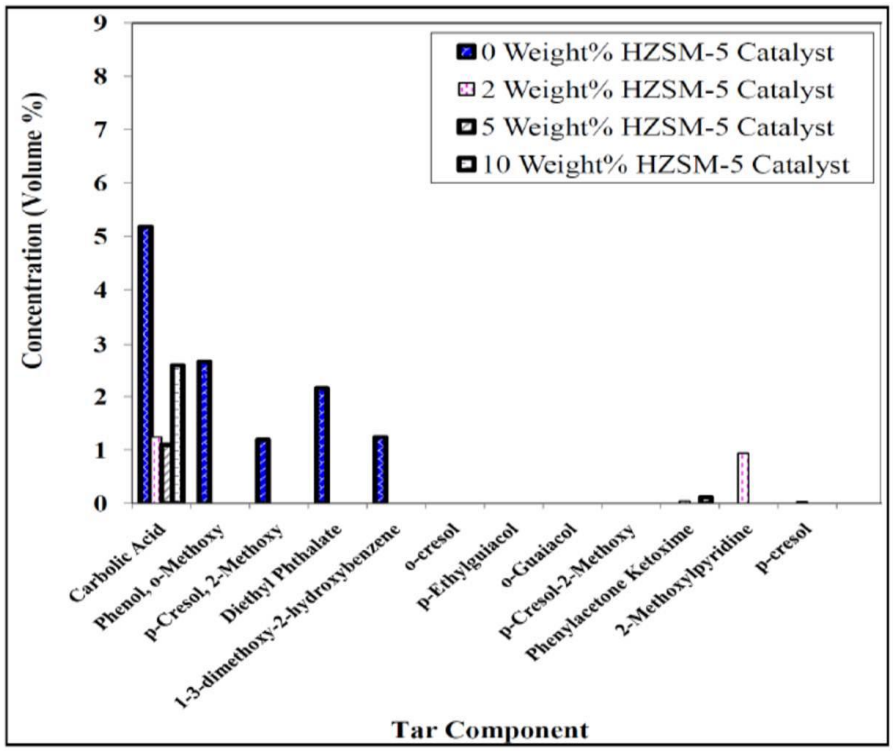

Figure 5.11 Chemical components and their concentration in tar (adapted from Chin, 2011)

In comparison with the previous work by Chin (2011), it seems that an increase of zeolite to 10% in the pelletised palm kernel shells only caused a 56% reduction in tar whereas the same amount of zeolite resulted in 95% of tar reduction for the gasification of raw, ungrounded palm kernel shells. This could be due to zeolite being trapped within the binary palm kernel shell and zeolite pellet hence not all of the zeolite catalyst were available to crack tar. To further decrease the amount of tar in the gaseous products, the composition of zeolite in the pelletised feedstock has to be increased. However, this will compromise the strength of the binary pellet as shown in the earlier sections of Chapter 5. Increasing the composition of zeolite in the binary pellet to 25% or 50% will decrease the strength of the binary pellet and result in difficulties in handling.

From the gasification results, it is shown that pelletised HZSM-5 zeolite with palm kernel shell was not as effective in reducing tar as compared with zeolite added in-situ with the palm kernel shell feedstock for gasification. Although adding zeolite in-situ with the palm kernel shell feedstock was effective in tar reduction, the zeolite

was not recoverable after gasification and this may induce high costs in gas cleaning due to the one-time usage of zeolite. It is suggested that a secondary catalytic tar cracking unit containing HZSM-5 zeolite be installed with the fixed bed updraft gasifier such that the gaseous products can be channeled to this cracking unit for tar removal. In this way, the catalyst can be used for a longer time and it will also be more cost effective. Pelletised 100% palm kernel shell feedstock can be used in place of raw palm kernel shells as the gasification of pelletised feedstock was shown to be more efficient.

5.6 Conclusion

This study shows that the constituents of the pellets are pertinent parameters that could affect the strength of the pellets formed from binary mixtures. For the range of zeolite composition (5% to 50%) studied, the porosity of the binary palm kernel shell and zeolite pellet increased with zeolite composition and the strength decreased correspondingly. Porosity is the primary factor that influences the strength of a binary pellet. Binary palm kernel shell and zeolite pellets with higher porosities were found to have lower strengths and binary pellet containing 50% zeolite had the weakest strength. As the composition of zeolite in the binary pellet increased, the elastic rebound of the pellet also increased. More agglomeration of zeolite particles were noticed in the binary mixture and this could have reduced the contact points between palm kernel shell particles and led to weak bonding. The elastic rebound which occurred after the compaction pressure was removed further led to the breakage of bonds which were already formed during compaction. Hence the porosity increased and the strength of the binary pellet weakened.

An empirical model was developed on the basis of the Ryshkewitch-Duckworth model to predict the strength of the binary mixture pellet, based on the properties of the zeolite and palm kernel shell. The validity of the model has been demonstrated to give a good fit with the experimental data. It has been shown that the properties of the individual components in the binary mixture, namely zeolite and palm kernel shell can be used to predict the strength of the binary pellets. It should be noted that the predictions from the model depend on the constituents of the pellet and these

results may only be valid for the studied powders and the range of zeolite composition. The results were used to help in the selection of the appropriate constituents and its amount for mixing to produce binary palm kernel shell and zeolite pellets of good strength for gasification.

Binary pellets with zeolite composition 5%, 10% and 15% were selected for gasification due to their higher strengths for handling compared with binary pellets of 25% and 50% zeolite composition. The gasification of palm kernel shell with zeolite being incorporated as a catalyst in the pelletised form was proven to be feasible but not as effective in reducing tar from the gaseous products as zeolite added in-situ with raw palm kernel shells. For the same amount of catalyst used, the amount of tar reduced when the pelletised form was gasified was less than that when the raw, ungrounded form was gasified in situ with zeolite. This could probably be due to zeolite being trapped within the binary pellet and hence not all the zeolite is available to crack the tar.

Increasing the composition of zeolite in the binary pellet may improve the tar cracking but this will compromise the strength of the binary pellet, leading to lower pellet strength and making handling of the feedstock difficult. Although the adding of zeolite in-situ with the feedstock was more effective in reducing tar, the zeolite was not recoverable once it was gasified and this may lead to higher costs. It is suggested that a secondary catalytic cracking unit containing HZSM-5 zeolite be installed with the gasifier such that the gaseous products can be channeled to the unit for tar removal. The recommended feedstock form for gasification is 100% pelletised palm kernel shell as it leads to more efficient gasification as shown in Chapter 4.

6 Conclusion

6.1 Conclusion

The influence of processing parameters during compaction and post-production conditions that could impact the mechanical strength of palm kernel shell pellets was investigated. It has been established that oil palm kernel shell powders without binders can be pelletised to relatively low porosities. The optimum compaction pressure was found to be 188 MPa which produced the strongest pellets from 75-150 μm and 150-300 μm particle sizes with a maximum compressive strength of 8.8 MPa. However, the radial tensile strengths of the pellets were found to be much weaker than the compressive strengths when compacted at the same compaction pressure. The properties, namely bonding capacities and maximum strengths of the pellets produced from 75-150 μm, 150-300 μm and 300-425 μm were determined from the Ryshkewitch-Duckworth model. Low speeds and increased hold time could enhance the strength of the pellet, however these would reduce the production rate of the pellets. Exposure of the pellets to higher humidity levels caused the pellets to become longer, more porous and weaker and the decrease in strength of the pellet was most significant after one day of storage. Porosity was found to be a primary factor influencing the strength of a pellet and an empirical model based on the Ryshkewitch-Duckworth model was developed to predict the strength of the pellets, given the hold time and storage time information. It is recommended that dry storage conditions are necessary to minimise the deterioration of palm kernel shell pellet quality over time and thermal treatment of pellets may be considered to further enhance the strength of the pellet.

Pellets produced from the optimum compaction pressure and stored under low humidity condition for good mechanical strength were gasified and it was found that its rate of conversion of biomass to gaseous products were highest, compared to the gasification of palm kernel shell in raw, ungrounded and powder forms. Hence palm kernel shell biomass in pelletised form is recommended as the feedstock to enhance

the efficiency of gasification. Tar was found as a contaminant in the gaseous product during gasification. As such, gas-cleaning processes are necessary.

To reduce the tar contaminant in the gaseous products during gasification, the catalyst HZSM-5 zeolite was used and incorporated into the palm kernel shell pellet. Studies on compaction and strength tests of binary palm kernel shell and zeolite pellets were conducted to understand their mechanical properties prior to gasification. The mechanical strength of binary palm kernel shell and HZSM-5 zeolite pellets was affected by the constituents of the pellet. The porosity of the binary palm kernel shell and zeolite pellet increased with the composition of zeolite and the strength decreased correspondingly. An empirical model was developed on the basis of the Ryshkewitch-Duckworth model to predict the strength of the binary mixture pellet, based on the properties of the zeolite and palm kernel shell. The validity of the model has been demonstrated to give a good fit with the experimental data. It has been shown that the properties of the individual components in the binary mixture, namely zeolite and palm kernel shells can be used to predict the strength of the binary pellets. These results were used to select the appropriate constituents and its amount for mixing to produce binary palm kernel shell and zeolite pellets of good strength for gasification.

The gasification of binary palm kernel shell and HZSM-5 zeolite pellets was proven to be feasible but not as effective in reducing tar from the gaseous products as zeolite added in-situ with raw palm kernel shells. For the same amount of catalyst used, the amount of tar reduced when the pelletised form was gasified was less than that when the raw, ungrounded form was gasified in situ with zeolite which could probably be due to zeolite being trapped within the binary pellet and hence not all the zeolite is available to crack the tar. It is suggested that a secondary catalytic cracking unit containing HZSM-5 zeolite be installed with the gasifier for the gasification of pelletised 100% palm kernel shells, such that the gaseous products can be channeled to the unit for tar removal and efficient gasification can also be achieved.

The results from this research are expected to be useful in the selection of the appropriate conditions necessary for the production of strong palm kernel shell

pellets that can withstand handling and transportation. Such findings could serve as new knowledge for further developments of palm kernel shell feedstock in pelletised form that enhance the efficiency of gasification.

6.2 Future Work

The strength of the pellets with the largest particle size range of 300-425 µm was found to be the weakest and the strength of binary pellets containing different amount of zeolite was also found to be lower than that of pellets made from 100% palm kernel shell. As such, it will be worthwhile to investigate methods to strengthen these pellets.

Results from section 4.4 and section 4.5 show that compaction speed and hold time are factors that affect the strength of pellets made from 100% palm kernel shell. However, studies on the effects of compaction speed and hold time on binary palm kernel shell pellets were not carried out in this work. It was also observed that there were limitations of the equipment as it was not possible to increase the compaction pressures further for binary pellets containing 50% zeolite to improve the strength of the binary pellets. Future experiments can be conducted by increasing the hold time instead of the compaction pressure to overcome this limitation and to investigate the effects of compaction speed and hold time on binary pellets. The results may be used to determine the optimum compaction speed and hold time that can strengthen the binary pellets.

It is also worthwhile to investigate if thermal treatment such as heat or steam treatment would give rise to palm kernel shell pellets with better strength properties. The palm kernel shell powder may be subjected to steam or heat treatment before compaction or the pellets may be subjected to steam or heat post-treatment to study the impact of thermal treatments on the strength of the pellets. An investigation into the mechanisms and rate of water uptake by the pellets can also be looked into.

100% palm kernel shell pellets and binary pellets were compacted in the absence of binders in this work. Biomass pellets are typically made by combining a binder with

the biomass (see e.g. patents by Aunsholt 1986; Gunnerman 1977; Murcia 2007, Johnston and Houseman 1985) for better strength. In future studies, a suitable binder, possibly palm fat which is low in cost, may also be combined with palm kernel shells to enhance the strength of the pellets without increasing the contamination of the syngas during gasification. Binary pellets may also require strengthening by the addition of a suitable binder.

As gaseous products from gasification that are rich in hydrogen are vital to energy generation, future studies on the gasification of palm kernel shell pellets may investigate on using steam as a gasification agent to obtain syngas; and whether this could lead to higher yield of hydrogen. Other cheaper catalysts such as dolomite can also be considered for incorporation with palm kernel shell pellets to remove contaminants in the gaseous products before syngas applications.

7 References

Abu ERZ, Bramer EA, Brem G. 2004. Review of catalysts for tar elimination in biomass gasification processes. *Industrial & Engineering Chemistry Research*, 43, 6911-6919

Adapa P., Tabil L., Schoenau G. 2009. Compression Characteristics of Selected Ground Agricultural Biomass. *Agricultural Engineering International: the CIGR Ejournal*. Manuscript 1347. Vol. XI

Adolfsson A., Nystrom C. 1996. Tablet strength, porosity, elasticity and solid state structure of tablets compressed at high loads. *International Journal of Pharmaceutics*, 132, 95-106

Adolfsson A., Olsson H., Nyström C. 1997. Effect of particle size and compaction load on interparticulate bonding structure for some pharmaceutical materials studied by compaction and strength characterization in butanol. *European Journal of Pharmaceutics and Biopharmaceutics*, 44, 243-251

Adolfsson A ., Caramella C., Nystrom C. 1998. The effect of milling and addition of dry binder on the interparticulate bonding mechanisms in sodium chloride tablets. *International Journal of Pharmaceutics,* 160, 187-195

Ahlneck C., Alderborn G. 1989. Moisture adsorption and tabletting: II. The effect on tensile strength and air permeability of the relative humidity during the storage of tabtets of 3 crystalline materials. *International Journal of Pharmaceutics*, 56, 143-150

Ahmad S., Mohd Zainal Abidin Ab Kadir, Suhaidi Shafie. 2011. Current perspective of the renewable energy development in Malaysia. *Renewable and Sustainable Energy Reviews*, 15, 897-904

Akande O.F., Rubinstein M.H., Rowe P.H., et al. 1997. Effect of compression speeds on the compaction properties of a 1:1 paracetamol–microcrystalline cellulose mixture prepared by single compression and by combinations of pre-compression and main-compression. *International Journal of Pharmaceutics*, 157, 127-136

Al-Khattaf S. 2002. The influence of Y-zeolite unit cell size on the performance of FCC catalysts during gas oil catalytic cracking. *Applied Catalysis A: General*, 231, 293-306

Alderborn G. 1996. Chapter 10: Particle Dimensions. *Pharmaceutical Powder Compaction Technology, Informa Healthcare*, 1st Edition, ISBN-13:978-0824793760, 245-282

Alvin M.A. 1995. Characterization of ash and char formations in advanced high temperature particulate filtration systems. *Fuel Processing Technology,* 44, 237-283

Anis S., Zainal Z.A. 2011. Tar reduction in biomass producer gas via mechanical, catalytic and thermal methods: A review. *Renewable and Sustainable Energy Reviews*, 15, 2355-2377

Anuar M.S., Briscoe B.J. 2009. The elastic relaxation of starch tablets during ejection. *Powder Technology*, 195, 96-104

Armstrong N.A. 1989. Time-dependent factors involved in powder compression and tablet manufacture. *International Journal of Pharmaceutics*, 49, 1-13

Aunsholt K.E.H. 1986. *Fuel briquettes and method of making*. US Patent 4589887

Ayhan D. 2005. Potential applications of renewable energy sources, biomass combustion problems in boiler power systems and combustion related environmental issues. *Progress in Energy and Combustion Science*, 31, 171-192

Azali A., Nasrin A.B., Choo Y.M., et al. 2005. Development of gasification system fuelled with oil palm fibres and shells. *American Journal of Applied Sciences*, ISSN 1546-9239, 72-75

Baba M., Nagafuji N. 1965. Studies on tablet compression II: The stress relaxation and strain recovery of tablets. *Annu Rep Shionogi Res Lab*, 15, 147-151

Bacher C., Olsen P.M., Berthelsen P., et al. 2007. Improving the compaction properties of roller compacted calcium carbonate. *International Journal of Pharmaceutics*, 342, 115–123

Bacher C., Olsen P.M., Bertelsen P., et al. 2008. Compressibility and compactibility of granules produced by wet and dry granulation. *International Journal of Pharmaceutics*, 358, 69-74

Balat M., Balat M., Kırtay E., et al. 2009. Main routes for the thermo-conversion of biomass into fuels and chemicals. Part 2: Gasification systems. *Energy Conversion and Management*, 50, 3158-3168

Basiron Y., Simeh M.D. 2005. Vision 2020-the palm oil phenomenon. *Oil Palm Industry Economic Journal*, 5, 1-10

Belgiorno V., De Feo G., Della Rocca C., et al. 2003. Energy from gasification of solid wastes. *Waste Management*, 23, 1-15

Bhattacharya S.C., Saunier G.Y., Shah N., et al. 1985. Densification of biomass residues in Asia. Bioenergy 84. *Biomass conversion*, 3, 559–63

Bolhuis G.K., Holzer A.W. 1996. *Chapter 16: Lubricant Sensitivity, Pharmaceutical Powder Compaction Technology*, Informa Healthcare, 1st Edition, ISBN-13:978-0824793760, 517-560

Bridgwater A.V. 1994. Catalysis in thermal biomass conversion. *Applied Catalysis A: General*, 116, 5-47

Bridgwater A.V. 1995. The technical and economic feasibility of biomass gasification for power generation. *Fuel*, 14, 631-653

Briscoe B.J., Evans P.D. 1991. Wall friction in the compaction of agglomerated ceramic powders. *Powder Technology*, 65, 7–20

Briscoe B.J., Rough S.L. 1998. The effects of wall friction in powder compaction. *Colloids and Surfaces: Physicochemical and Engineering Aspects*, 137, 103–16

Buchireddy P.R., Bricka R.M., Rodriguez J., et al. 2010. Biomass gasification: catalytic removal of tars over zeolites and nickel supported zeolites. *Energy and Fuels*, 24, 2707-2715

Buckner I.S., Wurster, D.E., Aburub, A. 2010. Interpreting deformation behavior in pharmaceutical materials using multiple consolidation models and compaction energetics. *Pharmaceutical Development and Technology*, 15 492-499

Carlson T.R., Tompsett G.A., Conner W.C., et al. 2009. Aromatic Production from Catalytic Fast Pyrolysis of Biomass-Derived Feedstocks. *Topics in Catalysis*, 52, 241-252

Carson J.K., Lovatt S.J., Tanner D.J., et al. 2005. Thermal conductivity bounds for isotropic, porous materials. *International Journal of Heat and Mass Transfer*, 48, 2150-2158

Casal M.D., Gil M.V., Pevida C., et al. 2010. Influence of storage time on the quality and combustion behaviour of pine woodchips. *Energy*, 35, 3066-3071

Cheng J. 2010. *Biomass to renewable energy processes*. Taylor and Francis Group, ISBN: 978-1-4200-9517-3

Chin L.F.B., Gorin A., Twaiq F., et al. 2010. *Effect of HZSM-5 Zeolite on Tar Reduction for Biomass Palm Shell Gasification in Fixed Bed Reactor*. 2010 International Conference on Environmental Science and Technology (ICEST 2010), April 23-25, Bangkok Thailand. doi: 10.3850/978-981-08-5716-5_T107

Chin L.F.B. 2011. *Studies of syngas cleaning technologies suitable for power generation from biomass oil palm shells*. M.Phil. thesis, Curtin University. (Publication No. PID: 168995)

Chok V.S., Gorin A., Chua H.B. 2010. Minimum and complete fluidization velocity for sand-palm shell mixtures, Part II: characteristic velocity profiles, critical loading and binary correlations. *American Journal of Applied Sciences*, 7, 773-779

Cooper A.R., Eaton L.E. 1962. Compaction behavior of several ceramic powders. *Journal of the American Ceramic Society*, 45, 97–101

Corley R.H.V., Tinker P.B. 2003. *The Oil Palm*, Fourth Edition, Blackwell Science Ltd

Corma A. 2003. State of the art and future challenges of zeolites as catalysts. *Journal of Catalysis*, 216, 298-312

Dahlan I., Islam M., Rajion M.A. 2000. Nutrient intake and digestibility of fresh, ensiled and pelleted oil palm (Elaeis guineensis) frond by goats. *Asian-Australasian Journal of Animal Sciences*, 13, 1407-1413

Daily Express. 2009. *QL Resources outlook bright amid new palm pellet project*. http://www.dailyexpress.com.my/news.cfm?NewsID=68691 (accessed 21 March 2011)

Dam J.V., Junginger M., Faaij A., et al. 2008. Overview of recent developments in sustainable biomass certification. *Biomass and Bioenergy*, 32, 749-780

David S.T., Augsburger L.L. 1977. Plastic flow during compression of directly compressible fillers and its effect on tablet strength. *Journal of Pharmaceutical Science*, 66, 155-159

Delgado J., Aznar M.P., Corella J. 1997. Biomass gasification with steam in fluidized bed: effectiveness of CaO, MgO, and CaO–MgO for hot raw gas cleaning. *Industrial and Engineering Chemistry Research*, 36, 1535-1543

Demirbas A. 2007. Combustion of biomass. *Energy Sources* Part A, 29, 549-561

Depner H., Jess A. 1999. Kinetics of nickel-catalyzed purification of tarry fuel gases from gasification and pyrolysis of solid fuel. *Fuel*, 78, 1369-1377

Devi L., Ptasinski K.J., Janssen F.J.J.G. 2002. A review of the primary measures for tar elimination in biomass gasification processes. Biomass and Bioenergy, 24, 125-140

Dimilia R.A., Reed J. S. 1983. Stress transmission during the compaction of a spray-dried alumina powder in a steel die. *Journal of the American Ceramic Society*, 66, 667- 72

Doelker E. 1993. Comparative compaction properties of various microcrystalline cellulose types and generic products. *Drug Development and Industrial Pharmacy,* 19, 2399 2471

Duberg M., Nyström C. 1986. Studies on direct compression of tablets. XVII. Porosity-pressure curves for the characterisation of volume reduction mechanisms in powder compression. *Powder Technology*, 46, 67-75

Duckworth W.H. 1953. Discussion of Ryshkewitch paper by Winston Duckworth. *Journal of the American Ceramic Society*, 36, 68

Eriksson M., Alderborn G. 1994. Mechanisms for post-compaction changes in tensile strength of sodium chloride compacts prepared from particles of different dimensions. *International Journal of Pharmaceutics*, 109, 59-72

Etzler F.M., Bramante T., Deanne R., et al. 2011. Tablet Tensile Strength: An Adhesion Science Perspective. *Journal of Adhesion Science and Technology,* 25, 501–519

FAO. 1986. Wood gas as engine fuel. *Forestry Paper* 72

Faaij A., Van Ree R., Waldheim L. et al. 1997. Gasification of biomass wastes and residues for electricity production. *Biomass and Bioenergy*, 12, 387-407

Fell J.T., Newton J.M. 1970. Determination of tablet strength by diametral compression test. *Journal of Pharmaceutical Sciences,* 59, 688-691

Fell J.T., Newton J. M. 1971. Effect of particle size and speed of compaction on density changes in tablets of crystalline and spray-dried lactose. *Journal of Pharmaceutical Sciences*, 60, 1866-1869

Felske J.D. 2004. Effective thermal conductivity of composite spheres in a continuous medium with contact resistance. *International Journal of Heat and Mass Transfer*, 47, 3453-3461

Feng Y., Xiao B., Goerner K., et al. 2011. Influence of Particle Size and Temperature on Gasification Performance in Externally Heated Gasifier. *Smart Grid and Renewable Energy*, 2, 158-164

Finney K.N., Sharifi V.N. and Swithenbank J. 2009. Fuel Pelletization with a Binder: Part II s The Impacts of Binders on the Combustion of Spent Mushroom Compost-Coal Tailing Pellets. *Energy & Fuels*, 23, 3203–3210

Ford C., Bush M.B., Lawn B.R. 2009. Effect of wear on stresses and potential failure modes in teeth. *Journal of Materials Science: Materials in Medicine*, 20, 2243-2247

Francl J., Kingery W.D. 1954. Thermal conductivity: IX, Experimental investigation of effect of porosity on thermal conductivity. *Journal of the American Ceramic Society*, 37, 99-107

Freitag F., Reincke K., Runge J., et al. 2004. How do roll compaction/dry granulation affect the tableting behaviour of inorganic materials? Microhardness of ribbons and mercury porosimetry measurements of tablets. *European Journal of Pharmaceutical Sciences*, 22, 325–333

Frosch R.A. 1981. *Solar heated fluidized bed gasification system*. US Patent 4290779

Fuhrer C., 1977. Substance behaviour in direct compression. *Labo-Pharma Problemes Techniques*, 25, 759-762

Garr J.S.M., Rubinstein M.H. 1991. The effect of rate of force application on the properties of microcrystalline cellulose and dibasic calcium phosphate mixtures. *International Journal of Pharmaceutics*, 73, 75-80

Ghebre-Sellassie I. 1989. Mechanism of Pellet Formation and Growth. *Pharmaceutical Pelletization Technology*, 123-143

Gil M.V., Oulego P., Casal M.D., et al. 2010. Mechanical durability and combustion characteristics of pellets from biomass blends. *Bioresource Technology*, 101, 8859-8867

Goh S.M., Alten S., van Dalen G., et al. 2008. The mechanical properties of model compacted tablets. *Journal of Materials Science*, 43, 7171-7178

Gray W.A. 1968. Compaction after deposition. *The Packing of Solid Particles*, 89-107

Greenspan L. 1977. Humidity fixed points of binary saturated aqueous solutions. *Journal of Research of the National Bureau of Standards – A Physics and Chemistry*, 81, 89-96

Grover P.D., Mishra S.K. 1996. *Biomass briquetting: technology and practices*. Regional wood energy development program in Asia, field document no. 46. Bangkok, Thailand: Food and Agriculture Organization of the United Nations

Gunnerman RW. 1977. *Fuel pellets and method for making them from organic fibrous materials*. US Patent 4015951

Hadzovic E., Betz G., Hadzidedic S, et al. 2011. Investigation of compressibility and compactibility parameters of roller compacted Theophylline and its binary mixtures. *International Journal of Pharmaceutics*, 416, 97– 103

Hall D. O. and Scrase J. I. 1998. Will biomass be the environmentally friendly fuel of the future? *Biomass and Bioenergy*, 15, 357-367

Hamel S., Krumm W. 2008. Near-wall porosity characteristics of fixed beds packed with wood chips. *Powder Technology*, 188, 55–63

Han J., Kim H. 2008. The reduction and control technology of tar during biomass gasification/pyrolysis: An overview. *Renewable and Sustainable Energy Reviews,* 12, 397–416

Hancock B.C., Colvin J.T., Mullarney M.P., Zinchuk, A.V. 2003. The relative densities of pharmaceutical powders, blends, dry granulations, and immediate-release tablets. *Pharmaceutical Technology,* 27, 64–80

Hann R.A., Black J.M., Blomquist R.F. 1963. How durable is particleboard? Part II. The effect of temperature and humidity. *Forest Products Journal XIII,* 169-174

Hartley P.A., Parfitt G.D., Pollack, L.B. 1985. The role of Van der Waals force in the agglomeration of powders containing submicron particles. *Powder Technology,* 42, 35-42

Hasler P., Nussbaumer T. 2000. Sampling and analysis of particles and tars from biomass gasifiers. *Biomass and Bioenergy,* 18, 61-66

Heckel R.W. 1961. An analysis of powder compaction phenomena. *Transactions of the Mettalurgical Society of AIME,* 221, 1001–1008

Hernandez J.J., Guadalupe A.A., Antonio B. 2010. Gasification of biomass wastes in an entrained flow gasifier: Effect of particle size and the residence time. *Fuel Processing Technology*, 91, 681-692

Hiestand E.N., Wells J.E., Peot C.B., et al. 1977. Physical processes of tableting. *Journal of Pharmaceutical Sciences*, 66, 510–519

Higman C, Burgt M.V. 2008. *Gasification Processes*. Gasification. Second ed. Burlington: Gulf Professional Publishing, 91-191

Hoag S.W., Dave S.V., Moolchandani V. 2008. Chapter 17: Compression and Compaction. *Pharmaceutical Dosage Forms: Tablets, Unit Operations and Mechanical Properties*. Third Edition, Informa Healthcare, 1, 555-619

Holman L.E. 1991. The Compaction Behaviour of Particulate Materials: An Elucidation based on Percolation Theory. *Powder Technology,* 66, 265

Horne P.A., Williams P.T. 1995. The effect of zeolite ZSM-5 catalyst deactivation during the upgrading of biomass-derived pyrolysis vapours. *Journal of Analytical and Applied Pyrolysis*, 34, 65-85

Husain Z., Zainac Z., Abdullah Z. 2002. Briquetting of palm fibre and shell from the processing of palm nuts to palm oil. *Biomass and Bioenergy*, 22, 505 – 509

Hwang I.H., Nakajima D., Matsuto T., et al. 2008. Improving the quality of waste-derived char by removing ash. *Waste Management,* 28, 424-434

Igathinathane C., Tumuluru J. S., Sokhansanj S., et al. 2010. Simple and inexpensive method of wood pellets macro-porosity measurement. *Bioresource Technology*, 101, 6528-6537

Islam M. N., Zailani R., Ani F. N. 1999. Pyrolytic oil from fluidised bed pyrolysis of oil palm shell and its characterisation. *Renewable Energy,* 17, 73-84

Jerabek M., Major Z., Lang R.W. 2010. Uniaxial compression testing of polymeric materials. *Polymer Testing*, 29, 302–309

Johansson B., Alderborn G. 2001. The effect of shape and porosity on the compression behaviour and tablet forming ability of granular materials formed from microcrystalline cellulose. *European Journal of Pharmaceutics and Biopharmaceutics*, 52, 347–357

Johnston I.F, Houseman J. 1985. *Fuel pellets*. US Patent 4529407

Jones T.M. 1981. Physicio-technical properties of starting materials used in tablet formulation. *International Journal of Pharmaceutical Technology and Product Manufacture*, 2, 17-24

Kaerger J.S., Edge S., Price R. 2004. Influence of particle size and shape on flowability and compactibility of binary mixtures of paracetamol and microcrystalline cellulose. *European Journal of Pharmaceutical Sciences*, 22, 173–179

Kaliyan N., Morey R.V. 2009. Factors affecting strength and durability of densified biomass products. *Biomass and Bioenergy*, 33, 337-359

Kasa P., Bajdik J., Zsigmond Z., et al. 2009. Study of the compaction behaviour and compressibility of binary mixtures of some pharmaceutical excipients during direct compression. *Chemical Engineering and Processing*, 48, 859-863

Kawakita K., Ludde K.H. 1971. Some considerations on powder compression equations. *Powder Technology*, 4, 61–68

Kim S.J., Jung S.H., Kim J.S. 2010. Fast pyrolysis of palm kernel shells: Influence of operation parameters on the bio-oil yield and the yield of phenol and phenolic compounds. *Bioresource Technology*, 101, 9294–9300

Kirubakaran V., Sivaramakrishnan V., Nalini R., et al. 2009. A review on gasification of biomass. *Renewable and Sustainable Energy Reviews*, 13, 179-186

Kolarik J. 1994. A model for the yield strength of binary blends of thermoplastics. *Polymer,* 35, 3631- 3637

Koningsveld H.V., Koegler J.H. 1997. Preparation and structure of crystals of zeolite H-ZSM-5 loaded with p-nitroaniline. *Microporous Materials*, 9, 71-81

Kunkeler P. J., Zuurdeeg B. J., van der Waal J. C. et al. 1998. Zeolite Beta: The Relationship between Calcination Procedure, Aluminum Configuration, and Lewis Acidity. *Journal of Catalysis*, 180, 234–244

Kutty T.R.G., Nair M.R., Sengupta P., et al. 2008. Characterization of (Th,U)O_2 fuel pellets made by impregnation technique. *Journal of Nuclear Materials*, 374, 9-19

Larsson S.H., Thyrel M., Geladi P., et al. 2008. High quality biofuel pellet production from pre-compacted low density raw materials. *Bioresource Technology*, 99, 7176-7182

Lee H.M., Huang C.Y., Wang C.J. 2009. Forming and sintering behaviors of commercial α-Al2O3 powders with different particle size distribution and agglomeration. *Journal of materials processing technology*, 209, 714-722

Lehtikangas P. 2000. Storage effects on pelletised sawdust, logging residues and bark. *Biomass and Bioenergy*, 19, 287-293

Leuenberger H., Jetzer W. 1984. The compactibility of powder systems. A novel approach. *Powder Technology*, 37, 209-218

Li Y., Liu H. 2000. High-pressure densification of wood residues to form an upgraded fuel. *Biomass and Bioenergy*, 19, 177–86

Li J., Yan R., Xiao B., et al. 2007. Influence of temperature on the formation of oil from pyrolyzing palm oil wastes in a fixed bed reactor. *Energy and Fuels,* 21, 2398-2407

Lordi N., Shiromani P. 1984. Mechanism of hardness of aged compacts. *Drug Development and Industrial Pharmacy,* 10, 729-752

Lu H., Ip E., Scott J., et al. 2010. Effects of particle shape and size on devolatilization of biomass particle. *Fuel*, 89, 1156-1168

Luangkiattikhun P., Tangsathitkulchai C., Tangsathitkulchai M. 2008. Non-isothermal thermogravimetric analysis of oil-palm solid wastes. *Bioresource Technology*, 99, 986-997

Lv P., Yuan Z., Ma L., et al. 2007. Hydrogen-rich gas production from biomass air and oxygen/steam gasification in a downdraft gasifier. *Renewable Energy*, 32, 2173-2185

Maarschalk K.V., Vromans H., Bolhuis G.K., et al. 1996a. The effect of viscoelasticity and tabletting speed on consolidation and relaxation of a viscoelastic material. *European Journal of Pharmaceutics and Biopharmaceutics* 42, 49–55.

Maarschalk K. V., Zuurman, K., Vromans H., et al. 1996b. Porosity expansion of tablets as a result of bonding and deformation of particulate solids. *International Journal of Pharmaceutics*, 140, 185-193

Maarschalk K.V., Vromans H., Groenendijk W., et al. 1997a. Effect of water on deformation and bonding of pregelatinized starch compacts. *European Journal of Pharmaceutics and Biopharmaceutics*, 44, 253-260

Maarschalk K.V., Zuurman K., Vromans H., et al. 1997b. Stress relaxation of compacts produced from viscoelastic materials. *International Journal of Pharmaceutics*, 151, 27-34

Maganti L. and Celik M. 1993. Compaction studies on pellets I. Uncoated pellets. *International Journal of Pharmaceutics*. 95, 29-42

Mahlia T.M.I., Abdulmuin M.Z., Alamsyah T.M.I, et al. 2001. An alternative source of palm wastes industry for Malaysia and Indonesia. *Energy Conversion and Management*, 42, 2109-2118

Malamataris S., Hatjichristos Th., Rees J.E. 1996. Apparent compressive elastic modulus and strength isotropy of compacts formed from binary powder mixes. *International Journal of Pharmaceutics*, 141, 101-108

Mani S., Tabil L.G., Sokhansanj S. 2006. Effects of compressive force, particle size and moisture content on mechanical properties of biomass pellets from grasses. *Biomass and Bioenergy*, 30, 648-654

Marshall P. V., York P., Maclaine J. Q. 1993. An investigation of the effect of the punch velocity on the compaction properties of ibuprofen. *Powder Technology*, 74, 171-177

Martinez A., Lopez C. 2005. The influence of ZSM-5 zeolite composition and crystal size on the in situ conversion of Fischer–Tropsch products over hybrid catalysts. *Applied Catalysis A: General*, 294, 251-259

Mattsson S., Nystrom C. 2001. Evaluation of critical binder properties affecting the compactibility of binary mixtures. *Drug Development and Industrial Pharmacy*, 27, 181-194

McKendry P. 2002. Energy production from biomass (part 3): gasification technologies. *Bioresource Technology*, 83, 55-63

Michrafy A., Dodds J.A., Kadiri M.S. 2004. Wall friction in the compaction of pharmaceutical powders: measurement and effect on the density distribution. *Powder Technology*, 148, 53-55

Michrafy A., Michrafy M., Kadiri M.S., et al. 2007. Predictions of tensile strength of binary tablets using linear and power law mixing rules. *International Journal of Pharmaceutics*, 333, 118-126

Milne T.A., Evans R.J., Abatzoglou N. 1998. *Biomass gasifier "tars": their nature, formation, and conversion*. Report no. NREL/TP-570-25357, NREL, Golden, Colorado, USA

Mohammed M.A.A., Salmiaton A., Wan Azlina W.A.K.G., et al. 2011a. Hydrogen rich gas from oil palm biomass as a potential source of renewable energy in Malaysia. *Renewable and Sustainable Energy Reviews*, 15, 1258-1270

Mohammed M.A.A., Salimiaton A., Wan Azlina W.A.K.G., et al. 2011b. Air gasification of empty fruit bunch for hydrogen-rich gas production in a fluidized-bed reactor. *Energy Conversion and Management*, 52, 1555-1561

Moghiman M., Hashemi T., Zahmatkesh I., et al. 2007. Effects of particle size and equivalence ratio on cyclone gasification of wood powder. *Journal of the Energy Institute*, 80, 29-34

Mohsenin N., Zaske J. 1976. Stress relaxation and energy requirements in compaction of unconsolidated materials. *Journal of Agricultural Engineering Research*, 21, 193-205

Mollan M.J., Celik M. 1995. The effects of humidity and storage time on the behaviour of maltodextrins for direct compression. *International Journal of Pharmaceutics*, 114, 23-32

Murcia P.R. 2007. *Organically clean biomass fuel*. US Patent 7241321

MPOB Economics & Industry Development Division. 2006. Malaysian Oil Palm Statistics 2005. *MPOB Publisher*, 25, 23-40

Nasrin A.B., Ma A.N., Choo Y.M., et al. 2008. Oil palm biomass as potential substitution raw materials for commercial biomass briquettes production. *American Journal of Applied Sciences*, 5, 179-183

Nayak V.S., Choudhary V.R. 1983. Acid Strength Distribution and Catalytic Properties of H-ZSM-5: Effect of Deammoniation Conditions of NH_4-ZSM-5. *Journal of Catalysis*, 81, 26-45

Newton J.M., Alderborn G., Nystrom C. 1992. A method of evaluating the mechanical characteristics of powders from the determination of the strength of compacts. *Powder Technology*, 72, 97-99

Newton J.M., Alderborn G., Nystrom C., et al., 1993. The compressive to tensile strength ratio of pharmaceutical compacts. *International Journal of Pharmaceutics*, 93, 249–251

Newton J.M., Haririanb I., Podczecka F. 2000. The determination of the mechanical properties of elongated tablets of varying cross section. *European Journal of Pharmaceutics and Biopharmaceutics*, 49, 59-64

Ng W.P.Q., Lam H.L., Ng F.Y., et al. 2012. Waste-to-wealth: green potential from palm biomass in Malaysia. *Journal of Cleaner Production*, 34, 57-65

Ni M., Leung D.Y.C., Leung M.K.H., et al. 2006. An overview of hydrogen production from biomass. *Fuel Processing Technology*, 87, 461-472

Nystrom C., Malmqvist K., Mazur J., et al. 1978. Measurement of axial and radial tensile strength of tablets and their relation to capping. *Acta Pharmaceutica Suecica*, 15, 226-232

Nystrom C., Karehill P.G. 1986. Studies on direct compression of tablets: XVI. The use of surface area measurements for the evaluation of bonding surface area in compressed powders. *Powder Technology*, 47, 201-209

Nystrom C., Alderborn G., Duberg M., et al. 1993. Bonding surface area and bonding mechanism - two important factors for the understanding of powder compactability. *Drug Development and Industrial Pharmacy*, 19, 2143-2196

Nystrom C., Karehill P.G. 1996. Chapter 2: The importance of Intermolecular Bonding Forces and the Concept of Bonding Surface Area. *Pharmaceutical Powder Compaction Technology, Informa Healthcare*, 1st Edition, ISBN-13:978-0824793760, 17-54

O'Dogherty M.J., Wheeler J.A. 1984. Compression of straw to high densities in closed cylindrical moulds. *Journal of Agricultural Engineering Research*, 29, 61-72

Olah G. A., Molnar A. 2003. *Hydrocarbon chemistry*. United States of America. John Wiley & Sons

Olazar M., Arabiourrutia M., Lopez G., et al. 2008. Effect of acid catalysts on scrap tyre pyrolysis under fast heating conditions. *Journal of Analytical and Applied Pyrolysis*, 82, 199-204

Onyekonwu M.O. 1988. The effects of relative permeability characteristics and thermal conductivity on in situ combustion performance. *Energy*, 13, 619-624

Pabst W., Gregorova E. 2007. A cross-property relation between the tensile modulus and the thermal conductivity of porous materials. *Ceramics International*, 33, 9-12

Paronen P., Ilkka J. 1996. Chapter 3: Porosity-Pressure Functions. *Pharmaceutical Powder Compaction Technology, Informa Healthcare*, 1st Edition, ISBN-13:978-0824793760, 55-76

Patel S., Bansal A.K. 2011. Prediction of mechanical properties of compacted binary mixtures containing high-dose poorly compressible drug. *International Journal of Pharmaceutics*, 403, 109-114

Patel S., Kaushal A.M., Bansal A.K. 2007. *Effect of particle size and compression force on compaction behavior and derived mathematical parameters on compressibility*. Parmaceutical Research, Vol. 24, No. 1

Perego C., Bosetti A. 2011. Biomass to fuels: The role of zeolite and mesoporous materials. *Microporous and Mesoporous Materials*, 144, 28-39

Perez P., Aznar M.P., Caballero M.A., et al. 1997. Hot gas cleaning and upgrading with a calcined dolomite located downstream a biomass fluidized bed gasifier operating with steam-oxygen mixtures. *Energy and Fuels*, 11, 1194-1197

Pietsch W. 1997. Size Enlargement by Agglomeration. *Handbook of Powder Science and Technology*, 2nd edition, eds. M.E. Fayed and L. Otten, International Thomson Publishing, Florence, 202-377

Quaak P., Knoef H., Stassen H.E. 1999. *Energy from biomass: a review of combustion and gasification technologies*. World Bank Technical Paper No. 422, The World Bank, Washington, DC

Radwan A.M., Kyotani T., Tomita A. 2000. Characterization of coke deposited from cracking of benzene over USY zeolite catalyst. *Applied Catalysis A: General*, 192, 43-50

Raghavan S., Wang H., Dinwiddie R.B., et al. 1998. The effect of grain size, porosity and yttria content on the thermal conductivity of nanocrystalline zirconia. *Scripta Materialia*, 39, 1119-1125

Rapagna S., Jand N., Kiennemann A., et al. 2000. Steam-gasification of biomass in a fluidised-bed of olivine particles. *Biomass and Bioenergy*, 19, 187-197

Razuan R., Finney K.N., Chen Q., et al. 2011. Pelletised fuel production from palm kernel cake. *Fuel Processing Technology*, 92, 609-615

Rees J.E., Rue P.J. 1978. Time-dependent deformation of some direct compression excipients. *Journal of Pharmacy and Pharmacology, 30, 601-607*

Rees J.E., Tsardaka K.D. 1994. Some effects of moisture on the viscoelastic behaviour of modified starch during powder compaction. *European Journal of Pharmaceutics and Biopharmaceutics*, 40, 193-197

Ren N., Yang Z.J., Lv X.C., et al. 2010. A seed surface crystallization approach for rapid synthesis of submicron ZSM-5 zeolite with controllable crystal size and morphology. *Microporous and Mesoporous Materials,* 131, 103-114

Rhen C., Gref R., Sjostrom M., et al. 2005. Effects of raw material moisture content, densification pressure and temperature on some properties of Norway spruce pellets. *Fuel Processing Technology*, 87, 11-16

Roopwani R., Buckner I.S. 2011. Understanding deformation mechanisms during powder compaction using principal component analysis of compression data. *International Journal of Pharmaceutics*, 418, 227-234

Ryshkewitch E., 1953. Compression strength of porous sintered alumina and zirconia. *Journal of the American Ceramic Society*, 36, 65–68

Sadeghbeigi R. 2000. *Fluid catalytic cracking handbook.* United States of America: Butterworth Heinemann

Schlichting K.W., Padture N.P., Klemens P.G. 2001. Thermal conductivity of dense and porous yttria-stabilized zirconia. *Journal of Materials Science,* 36, 3003-3010

Shi L.M., Feng Y.S., Sun C.C. 2011. Initial moisture content in raw material can profoundly influence high shear wet granulation process. *International Journal of Pharmaceutics*, 416, 43-48

Shuit S.H., Tan K.T., Lee K.T., et al. 2009. Oil palm biomass as a sustainable energy source: A Malaysian case study. *Energy*, 34, 1225–1235

Sixsmith D., McCluskey D. 1981. The effect of punch tip geometry on powder movement during the tableting process. *Journal of Pharmacy and Pharmacology,* 33, 79-81

Speight J.G. 2008. *Synthetic fuels handbook*. McGraw-Hill Professional

Spieker W.A., Regalbuto J.R. 2001. A fundamental model of platinum impregnation onto alumina. *Chemical Engineering Science*, 56, 3491-3504

Stasiak M., Tomas J., Molenda M., et al. 2010. Uniaxial compaction behaviour and elasticity of cohesive powders. *Powder Technology*, 203, 482-488

Stassen HEM, Prins W, van Swaaij WPM. 2002. *Thermal conversion of biomass into secondary products: the case of gasification and pyrolysis*. 12th European conference on biomass for energy, industry and climate protection, June 17-21, Amsterdam, Netherlands: ETA-Florence and WIP-Munich (Pub.), 38-44

Steendam R., Lerk C.F., 1998. Poly(DL-lactic acid) as a direct compression excipient in controlled release tablets: Part I. Compaction behaviour and release characteristics of poly(DL-lactic acid) matrix tablets. *International Journal of Pharmaceutics*, 175, 33–46

Stelte W., Holm J. K., Sanadi A.R., et al. 2011. A study of bonding and failure mechanisms in fuel pellets from different biomass resources. *Biomass and bioenergy*, 35, 910-918

Stevens C.A. 1987. *Starch gelatinization and the influence of particle size, steam pressure and die speed on the pelleting process*. Ph.D. dissertation. Manhattan, KS: Kansas State University

Sugawara A., Yoshizawa Y. 1961. An experimental investigation on the thermal conductivity of consolidated porous materials and its application to porous rock, *Australian Journal of Physics*, 14, 469-480

Sulaiman F., Abdullah N., Gerhauser H., et al. 2011. An outlook of Malaysian energy, oil palm industry and its utilization of wastes as useful resources. *Biomass and Bioenergy*, 35, 3775-3786

Sumathi S., Chai S.P., Mohamed A.R. 2008. Utilization of oil palm as a source of renewable energy in Malaysia. *Renewable and Sustainable Energy Reviews*, 12, 2404-2421

Sun C.C. 2008. Mechanism of moisture induced variations in true density and compaction properties of microcrystalline cellulose. *International Journal of Pharmaceutics*, 346, 93-101

Sutton D., Kelleher B., Ross J.R.H. 2001. Review of literature on catalysts for biomass gasification. *Fuel Processing Technology*, 73, 155-173

Tabil J.L., Sokhansanj S. 1996. Process conditions affecting the physical quality of alfalfa pellets. *Applied Engineering in Agriculture*, 12, 345–50

Tavman I.H. 1996. Effective thermal conductivity of granular porous materials. *Int. Commun. Heat Mass Transfer*, 23, 169-176

Tenth Malaysia Plan 2011-2015. 2010. http://www.epu.gov.my/html/themes/epu/html/RMKE10/rmke10_english.html (accessed 21 March 2011)

Tomishige K., Asadullah M. 2005. Catalyst development for the synthesis gas and hydrogen production from biomass by gasification, pyrogasification, and steam reforming. *In Progress in catalysis research*, Bevy LP (ed.), Nova Science, 1-39

Train D. 1956. An investigation into the compaction of powders, *Journal of Pharmacy and Pharmacology*, 8, 744–761

Tumuluru J.S., Wright C.T., Hess J.R., et al. 2011. A review of biomass densification systems to develop uniform feedstock commodities for bioenergy application. *Biofuels Bioproducts and Biorefining*, 5, 683-707

Tye C.K., Sun C. and Amindon G.E. 2005. Evaluation of the effects of tableting speed on the relationships between compaction pressure, tablet tensile strength, and tablet solid fraction. *Journal of Pharmaceutical Sciences*, 94, 465-472

Umikalsom M.S., Ariff A.B., Zulkifli H.S., et al. 1997. The treatment of oil palm empty fruit bunch fibre for subsequent use as substrate for cellulase production by Chaetomium globosum kunze. *Bioresource Technology*, 62, 1-9

Veen B.V., Maarschalk K.V., Bolhuis G.K., et al. 2000. Tensile strength of tablets containing two materials with a different compaction behavior. *International Journal of Pharmaceutics*, 203, 71-79

Veen B.V., Maarschalk K.V., Bolhuis G.K., et al. 2004. Predicting mechanical properties of compacts containing two components. *Powder Technology*, 139, 156-164

Velez J.F., Chejne F., Valdes C.F., et al. 2009. Co-gasification of Colombian coal and biomass in fluidized bed: An experimental study. *Fuel*, 88, 424-430

Vijaya S., Chow M.C., Ma A.N. 2004. Energy database of the oil palm. *MPOB Palm Oil Engineering Bulletin*, 70, 15-22

Vincent C., Silvain J.F., Heintz J.M., et al. 2012. Effect of porosity on the thermal conductivity of copper processed by powder metallurgy. *Journal of Physics and Chemistry of Solids*, 73, 499-504

Vitolo S., Bresci B., Seggiani M., et al. 2001. Catalytic upgrading of pyrolytic oils over HZSM-5 zeolite: behaviour of the catalyst when used in repeated upgrading-regenerating cycles. *Fuel*, 80, 17-26

Wang J., Wen H., Desai D. 2010. Lubrication in tablet formulations. *European Journal of Pharmaceutics and Biopharmaceutics*, 75, 1-15

Wang L.J., Weller C.L., Jones D.D., et al. 2008. Contemporary issues in thermal gasification of biomass and its application to electricity and fuel production. *Biomass and Bioenergy*, 32, 573-581

Weitkamp J. 2000. Zeolites and catalysis. *Solid State Ionics*, 131, 175-188

Wu C.Y., Best S.M., Bentham A.C., et al. 2005. A simple predictive model for the tensile strength of binary tablets. *European Journal of Pharmaceutical Sciences*, 25, 331-336

Wu C.Y., Best S.M., Bentham A.C., et al. 2006. Predicting the tensile strength of compacted multi-component mixtures of pharmaceutical powders. *Pharmaceutical Research*, 8, 1898-1905

Wu C.Y., Hancock B.C., Mills A., et al. 2008. Numerical and experimental investigation of capping mechanisms during pharmaceutical tablet compaction. *Powder Technology*, 181, 121-129

Wu C.Y., Seville J.P.K. 2009. A comparative study of compaction properties of binary and bilayer tablets. *Powder Technology*, 189, 285-294

Xu C., Donald J., Byambajav E., et al. 2010. Recent advances in catalysts for hot-gas removal of tar and NH_3 from biomass gasification. *Fuel*, 89, 1784-1795

Yasin S.M., Qureshi T.A. 1990. Cement bonded particleboard from eucalyptus camaldulensis wood. *Pakistan Journal of Forestry,* 40, 53-60

Yong T.L.K., Lee K.T., Mohamed A.R., et al. 2007. Potential of hydrogen from oil palm biomass as a source of renewable energy worldwide. *Energy Policy,* 35, 5692-5701

Yusoff, S. 2006. Renewable energy from palm oil - innovation on effective utilization of waste. *Journal of Cleaner Production*, 14, 87-93

Yusof Y.A., Ng S.K., Chin N.L., et al. 2010. Compaction pressure,wall friction and surface roughness upon compaction strength of Andrographis paniculata tablets. *Tribology International*, 43, 1168-1174

Zhang L., Xu C., Champagne P. 2010. Overview of recent advances in thermo-chemical conversion of biomass. *Energy Conversion and Management*, 51, 969-982

Zuurman K., Maarschalk K. V., Bolhuis, G.K. 1999. Effect of magnesium stearate on bonding and porosity expansion of tablets produced from materials with different consolidation properties. *International Journal of Pharmaceutics*, 179, 107-115